

ISSN 0973-8916

Current Trends in Biotechnology and Pharmacy

Volume 7

Issue 1

January 2013



www.abap.co.in

Current Trends in Biotechnology and Pharmacy

ISSN 0973-8916 (Print), 2230-7303 (Online)

Editors

Prof.K.R.S. Sambasiva Rao, India
krssrao@abap.co.in

Prof.Karnam S. Murthy, USA
skarnam@vcu.edu

Editorial Board

Prof. Anil Kumar, India
Prof. P.Appa Rao, India
Prof. Bhaskara R.Jasti, USA
Prof. Chellu S. Chetty, USA
Dr. S.J.S. Flora, India
Prof. H.M. Heise, Germany
Prof. Jian-Jiang Zhong, China
Prof. Kanyaratt Supaibulwatana, Thailand
Prof. Jamila K. Adam, South Africa
Prof. P.Kondaiah, India
Prof. Madhavan P.N. Nair, USA
Prof. Mohammed Alzoghaibi, Saudi Arabia
Prof. Milan Franek, Czech Republic
Prof. Nelson Duran, Brazil
Prof. Mulchand S. Patel, USA
Dr. R.K. Patel, India
Prof. G.Raja Rami Reddy, India
Dr. Ramanjulu Sunkar, USA
Prof. B.J. Rao, India
Prof. Roman R. Ganta, USA
Prof. Sham S. Kakar, USA
Dr. N.Sreenivasulu, Germany
Prof. Sung Soo Kim, Korea
Prof. N. Udupa, India
Dr.P. Ananda Kumar, India
Prof. Aswani Kumar, India
Prof. Carola Severi, Italy
Prof. K.P.R. Chowdary, India
Dr. Govinder S. Flora, USA
Prof. Huangxian Ju, China
Dr. K.S.Jagannatha Rao, Panama
Prof. Juergen Backhaus, Germany
Prof. P.B.Kavi Kishor, India
Prof. M.Krishnan, India
Prof. M.Lakshmi Narasu, India
Prof. Mahendra Rai, India
Prof. T.V.Narayana, India
Dr. Prasada Rao S.Kodavanti, USA
Prof. T.Ramana, India
Dr. C.N.Ramchand, India
Prof. P.Reddanna, India
Dr. Samuel J.K. Abraham, Japan
Dr. Shaji T. George, USA
Prof. Sehamuddin Galadari, UAE
Prof. B.Srinivasulu, India
Prof. B. Suresh, India
Prof. Swami Mruthinti, USA
Prof. Urmila Kodavanti, USA

Assistant Editors

Dr. Giridhar Mudduluru, Germany

Dr. Sridhar Kilaru, UK

Prof. Mohamed Ahmed El-Nabarawi, Egypt

Prof. Chitta Suresh Kumar, India

www.abap.co.in

ISSN 0973-8916

Current Trends in Biotechnology and Pharmacy

(An International Scientific Journal)

Volume 7

Issue 1

January 2013



www.abap.co.in

Indexed in Chemical Abstracts, EMBASE, ProQuest, Academic SearchTM, DOAJ, CAB Abstracts, Index Copernicus, Ulrich's Periodicals Directory, Open J-Gate Pharmoinfonet.in Indianjournals.com and Indian Science Abstracts.

Association of Biotechnology and Pharmacy (Regn. No. 28 OF 2007)

The *Association of Biotechnology and Pharmacy (ABAP)* was established for promoting the science of Biotechnology and Pharmacy. The objective of the Association is to advance and disseminate the knowledge and information in the areas of Biotechnology and Pharmacy by organising annual scientific meetings, seminars and symposia.

Members

The persons involved in research, teaching and work can become members of Association by paying membership fees to Association.

The members of the Association are allowed to write the title **MABAP** (Member of the Association of Biotechnology and Pharmacy) with their names.

Fellows

Every year, the Association will award Fellowships to the limited number of members of the Association with a distinguished academic and scientific career to be as Fellows of the Association during annual convention. The fellows can write the title **FABAP** (Fellow of the Association of Biotechnology and Pharmacy) with their names.

Membership details

(Membership and Journal)		India	SAARC	Others
Individuals	– 1 year	Rs. 600	Rs. 1000	\$100
	LifeMember	Rs. 4000	Rs. 6000	\$500
Institutions (Journal only)	– 1 year	Rs. 1500	Rs. 2000	\$200
	Life member	Rs.10000	Rs.12000	\$1200

Individuals can pay in two instalments, however the membership certificate will be issued on payment of full amount. All the members and Fellows will receive a copy of the journal free

Association of Biotechnology and Pharmacy
(Regn. No. 28 OF 2007)
#5-69-64; 6/19, Brodipet
Guntur – 522 002, Andhra Pradesh, India

Current Trends in Biotechnology and Pharmacy

ISSN 0973-8916

Volume 7 (1)	CONTENTS	January - 2013
Research papers		
	Evaluations of Haemostatic Alterations in Coronary Artery Bypass Graft Patients Before and After Angiography Using Thrombelastography <i>Sermin Tetik, Emre Ermengu, Koray Ak, Nilgün Tekkesin, Sarfraz Ahmad and K. Turay Yardimci</i>	492-498
	Raster Image Correlation Spectroscopy in Live cells Expressing Endothelin ET _A receptor <i>Damaris De La Torre, Elizabeth A. Gordon, Michelle A. Digman, Milka Stakic, Hanns Häberlein, Enrico Gratton and Catherina Caballero-George</i>	499-504
	Expression of C-terminal Prodomain Truncated <i>Petunia</i> Floral Defensins Inhibits the Growth of Transgenic Banana Plants <i>Siddhesh B. Ghag, Upendra K. Singh Shekhawat and Thumballi R. Ganapathi</i>	505-510
	Direct Organogenesis and Plant Regeneration from Cotyledons of a Multipurpose Tree, <i>Acacia mangium</i> Willd. <i>M. Shahinozzaman, M. O. Faruq, M. M. Ferdous, M. A. K. Azad and M. N. Amin</i>	511-517
	Production and Characterization of Extracellular L-asparaginase from Estuarine Actinomycetes Species by Submerged Fermentation Process <i>Koteswara Rao Chinta, J. Srinivasa Rao, Pulipati King, P. Jawahar Babu, M. V. V. Chandana Lakshmi and Ch. V. Ramachandra Murthy</i>	518-526
	Optimization of Culture Conditions for the Production of Polygalacturonase by <i>Phanerochaete chrysosporium</i> and <i>Aspergillus fumigatus</i> <i>S. Mrudula, Maheswari. V, Ashwitha Kodaparathi and Pavan Kumar Pindi</i>	527-534
	Development and Evaluation of Controlled Release Verapamil Hydrochloride Pellets by PAN Coating Process <i>S.Vidyadhara, M.Bhanu Prasad, R.L.C. Sasidhar and T. Bala Krishna</i>	535-543
	Identification and Validation of an Allele Specific Marker Associated with Pungency in <i>Capsicum</i> spp. <i>T. Chakradhar, B. Pradeep Reddy, N.Srinivas and P.Chandra Obul Reddy</i>	544-551
	Selection of Foot and Mouth Disease Virus Candidate Vaccine Strain for Serotype O <i>S. Yuvaraj, M. Madhanmohan, Ralla Kumar, Kankipati Manikumar, Jangam Anil Kumar, V. A. Srinivasan and Ramesh Matur</i>	552-557
Short Communications		
	<i>In Silico</i> Design of Inhibitors for β -Secretase: Implications for Alzheimer's Disease <i>S. Sai Madhukar, Anand Solomon, Viswanath Das, K. Anil Kumar and S. Krupanidhi</i>	558-566
	Biosorption Performance of <i>Adenantha pavonina</i> Leaf Powder for the Removal of Lead using Central Composite Design <i>J. Srinivasa Rao, C. Kesava Rao and G. Prabhakar</i>	567-578
	Age Dependent Lead Induced Perturbations in Serum Markers; Protective Effect of Nutrient Metal Mixture <i>V. Kavitha, K. Praveen Kumar and G. Rajarami Reddy</i>	579-591
	News Item	i - vii

Information to Authors

The *Current Trends in Biotechnology and Pharmacy* is an official international journal of *Association of Biotechnology and Pharmacy*. It is a peer reviewed quarterly journal dedicated to publish high quality original research articles in biotechnology and pharmacy. The journal will accept contributions from all areas of biotechnology and pharmacy including plant, animal, industrial, microbial, medical, pharmaceutical and analytical biotechnologies, immunology, proteomics, genomics, metabolomics, bioinformatics and different areas in pharmacy such as, pharmaceuticals, pharmacology, pharmaceutical chemistry, pharma analysis and pharmacognosy. In addition to the original research papers, review articles in the above mentioned fields will also be considered.

Call for papers

The Association is inviting original research or review papers and short communications in any of the above mentioned research areas for publication in *Current Trends in Biotechnology and Pharmacy*. The manuscripts should be concise, typed in double space in a general format containing a title page with a short running title and the names and addresses of the authors for correspondence followed by Abstract (350 words), 3 – 5 key words, Introduction, Materials and Methods, Results and Discussion, Conclusion, References, followed by the tables, figures and graphs on separate sheets. For quoting references in the text one has to follow the numbering of references in parentheses and full references with appropriate numbers at the end of the text in the same order. References have to be cited in the format below.

Mahavadi, S., Rao, R.S.S.K. and Murthy, K.S. (2007). Cross-regulation of VAPC2 receptor internalization by m2 receptors via c-Src-mediated phosphorylation of GRK2. *Regulatory Peptides*, 139: 109-114.

Lehninger, A.L., Nelson, D.L. and Cox, M.M. (2004). *Lehninger Principles of Biochemistry*, (4th edition), W.H. Freeman & Co., New York, USA, pp. 73-111.

Authors have to submit the figures, graphs and tables of the related research paper/article in Adobe Photoshop of the latest version for good illumination and alignment.

Authors can submit their papers and articles either to the editor or any of the editorial board members for onward transmission to the editorial office. Members of the editorial board are authorized to accept papers and can recommend for publication after the peer reviewing process. The email address of editorial board members are available in website www.abap.in. For submission of the articles directly, the authors are advised to submit by email to krssrao@abap.co.in or krssrao@yahoo.com.

Authors are solely responsible for the data, presentation and conclusions made in their articles/ research papers. It is the responsibility of the advertisers for the statements made in the advertisements. No part of the journal can be reproduced without the permission of the editorial office.

Evaluations of Haemostatic Alterations in Coronary Artery Bypass Graft Patients Before and After Angiography Using Thrombelastography

Sermin Tetik^{1,2*}, Emre Ermengu², Koray AK³, Nilgün Tekkesin⁴, Sarfraz Ahmad⁵ and K. Turay Yardimci¹

¹Department of Biochemistry & Molecular Biology, Faculty of Pharmacy, Cyprus International University, Mersin Yolu, Nicosia, Cyprus

²Department of Biochemistry, Faculty of Pharmacy, Marmara University, Istanbul

³Department of Heart Surgery, School of Medicine, Marmara University, Istanbul

⁴Department of Clinical Biochemistry, Memorial Hospital Group, Istanbul, Turkey

⁵Florida Hospital Medical Center, Orlando, FL 32804, USA

*For Correspondence - stetik@ciu.edu.tr

Abstract

The Thrombelastograph™ (TEG) provides a global assessment of blood coagulation. The study aim was to evaluate the dynamic haemostatic parameters utilizing TEG in blood specimens of hyperlipidemic patients (n=22) and healthy donors (n=15) before and 30 min after the angiography. Such TEG parameters as: reaction time (R, min), clot formation time (K, min), fibrinogen activity (Angle, degree), clotting maximum amplitude (MA, mm), and clotting index (CI) were quantitated. The patients' values before vs. after the angioplasty were: R = 4.74±1.59 vs. 3.36±0.89 min (5.48±1.39 min for control), K = 2.77±2.45 vs. 1.75±0.95 min (1.57±0.24 min for control), Angle = 64.38±11.21 vs. 69.72±8.22 degree (67.13±6.67 degree for control), MA = 52.2±16.94 vs. 57.84±9.46 mm (59.97±4.73 mm for control), and CI = 0.31±2.59 vs. 1.71±2.07 (0.22±2.14 for control). It is clear that the risk ratio was lowered in patients after the angiography where increased haemostatic defects were detected before the angiography.

Key words : Haemostatic system, Angiography, Thrombelastography, Coronary artery bypass graft.

Introduction

Peripheral artery disease, aside from heart and brain, represents all of the blood arterial

diseases (1); however, peripheral endothelial disease definition is used generally for expression of the peripheric artery disease. In contrast, atherosclerosis, which refers to the blood flow through the arms and legs (2,3). Generally, there is no sign of the disease among half of the individuals with peripheric (vein) damar disease. The most common signs of the disease are: intermittent claudication (the intermittent leg ache) with walking and the advanced cases legache when at rest. Angiography is the standard method used for the diagnosis of arterial disease (4), which shows the location and extent of the decrease in passage size or complete blockage of coronary arteries. By detecting the extent of shrinkage or blockage of the vein, the therapy protocol is directed (2).

Haemostasis is the process of dynamic continuous events in human body, which directs as to where and when fibrin formation is needed. It could be analyzed by dividing into two situations, viz., primary and secondary haemostasis. While the primary hemostasis impairment is dependent on platelets and vascular cases, the secondary haemostasis diseases causes coagulation system abnormalities (5). The history and physical examination occupy important places in patients' identification. For example, the primary haemostasis tests for platelet abnormalities are: platelet count, peripheric smear, and bleeding

time. For the examination of secondary peripheric impairment, the prothrombin time (PT), activated partial thromboplastin time (aPTT), thrombin time (TT), and fibrinogen analysis are commonly used. Of course, depending upon these primary tests, the other advanced tests could be performed accordingly (6).

The Thrombelastograph™ (TEG) provides a global assessment of blood coagulation, taking into account platelet number and function, coagulation factors and natural clotting inhibitors. It is a dynamic and essential test that provides specific results in which whole blood is used, where coagulation is evaluated as a whole and various (multitude) results could be quantitated (7,8). In this study, we sought to determine the stress effect of angiography in the secondary haemostasis system (the haemostatic alterations) in whole blood of coronary artery bypass graft (CABG) patients before and after the angiography utilizing the TEG system, and the data are compared with the normal healthy volunteers.

Materials and Methods

After the approval from the primary institution's Ethics Committee for human subjects use, the written informed consent from all participants of this study were obtained. Twentytwo patients (5 female, 17 male) between the age of 53-75 years, who enrolled to the Marmara University School of Medicine (Department of Heart & Vein Surgery), underwent peripheral arterial angiography procedure because of coronary arterial impairment, formed the basis of this study. Normal healthy volunteers (n=15) that had not taken any anticoagulant / aspirin for 10 days or before and were non-smokers, served as the control group.

Whole blood (10 mL) was drawn from the healthy volunteers as well as from the angioplasty patients (before and after the angiography) in sodium citrate as the anticoagulant (9:1) under vacuum. Blood analyses were performed within 1-2 h after the blood collection in the TEG Analyzer System (Haemostatics Corp., Niles, IL), located in the biochemistry laboratory of the Memorial

Hospital, Istanbul, Turkey. Such TEG parameters as reaction time (R, min), clot formation time (K, min), fibrinogen activity (Angle, degree), clotting maximum amplitude (MA, mm), and clotting index (CI) were quantitated for each subject.

The SPSS 11.5 program was used for the statistical analysis. For the data analyses, in addition to the standard statistical methods which give mean \pm standard error (SE), one-way ANOVA test was used for the comparisons between the groups with normal variations, and Tukey / standard deviation (SD) test was used for the detection of the group that causes variations. The Kruskal Wallis test was used for comparison of the groups sharing abnormal variations in parameters and Mann-Whitney U-test was used in detecting the groups causing differences. The results are evaluated in 95% dependence and $p < 0.05$ value was considered statistically significant.

Results

The demographics and baseline/clinical characteristics of the patients and the control groups are shown in Table 1. While a majority of subjects in this study were male, about a quarter of them were females in both groups. The mean value for patients' LDL was higher compared to the control group (168 ± 16.4 vs. 89 ± 6 mg/dL), the HDL level was 47 ± 4.3 mg/dL and triglyseride was 240 ± 25.7 mg/mL that were comparable to the control group. Also, the platelet counts were within the normal range for both group of subjects.

Fig. 1A show TEG results on Reaction Time (R), which was decreased after angiography (3.36 ± 0.89 min) as compared to the control group (5.48 ± 1.39 min, $p < 0.05$) and the value before angiography was 4.74 ± 1.59 min ($p > 0.05$). The R time of CABG patients on individual case basis before and after the angiography are presented in Fig. 1B.

The mean clot formation time (K) for the control group was determined to be 1.57 ± 0.24 min, which was not significantly different for the patients group [before angioplasty = 2.77 ± 2.45

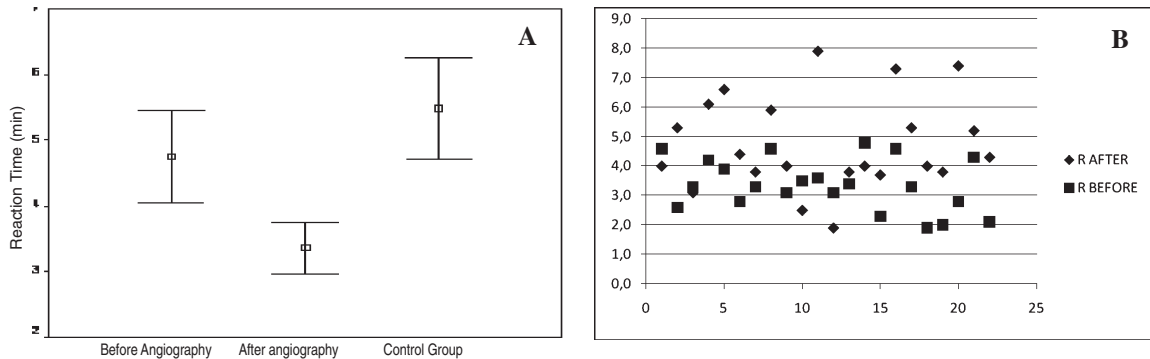


Fig. 1 (A) The Reaction Time (R) of controls and the GABG patient groups before and after the angiography as determined by TEG analyzer. **(B)** Data shows the individual R values determined for each patients before and after the angiography.

min, after angioplasty = 1.75 ± 0.95 min ($p > 0.05$)]. Wide variations in the values were noted throughout the experiment (Fig. 2A). Fig. 2B shows the data on individual patients' K values for before and after the angioplasty.

The results obtained on the TEG analyses for the fibrinogen activity (Angle) are shown in Fig. 3. Compared to the control group (67.13 ± 6.67 degree), the mean values for fibrinogen activity was not significantly different as compared to the

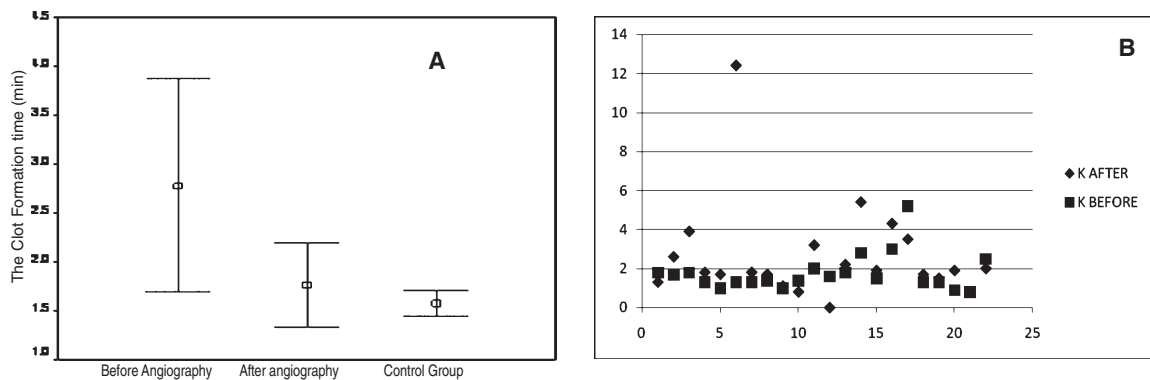


Fig. 2 (A) Clot formation time (K) of the control and the CABG patient groups before and after the angiography as determined by TEG analyzer. **(B)** Data shows the individual K values for each patients determined before and after the angiography.

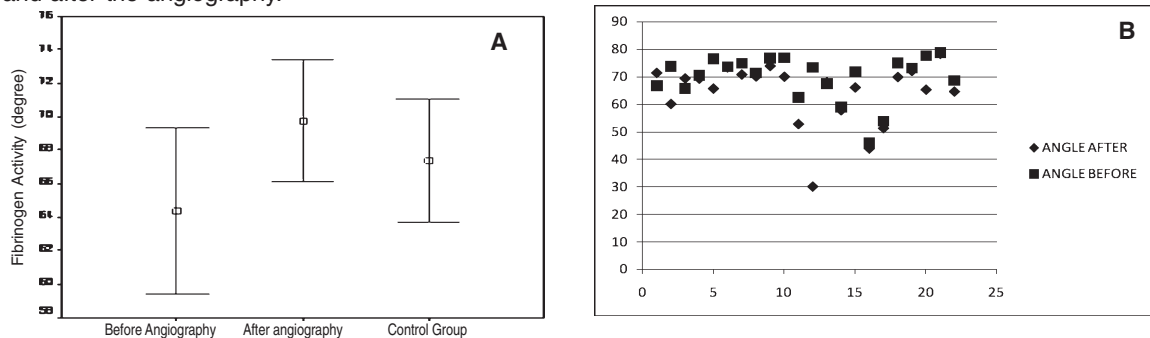


Fig. 3 (A) The fibrinogen activity (Angle) of the controls and the CABG patient groups before and after the angiography as determined by TEG analyzer. **(B)** Data on the fibrinogen activity (Angle) for individual patient as determined before and after the angiography.

patients group (before angioplasty 64.38 ± 11.21 vs. 69.72 ± 8.22 degree after angioplasty, $p > 0.05$) (Fig. 3A). Again, wide variations were noted. The actual data on the individual patient's fibrinogen activity before and after the angioplasty is shown in Fig. 3B.

Fig. 4 shows the TEG data obtained for the clot maximum amplitude (MA) values. As shown in Fig. 4A, increase in MA of the clot formation was detected before and after the angiography in CABG patients [before angioplasty = 52.20 ± 16.94 mm, and after angioplasty = 57.84 ± 9.46 (n=22)], which was not significantly different from the control group values [59.97 ± 4.73 mm (n=15)]. The MA values are

relative to the blood fibrinogen concentration in the patient group. The MA of clot values for individual patients before and after angiography are shown in Fig. 4B.

The results on the clot index (CI) determination by TEG analyzer are shown in Fig. 5. There was significant increase in the CI values, particularly after the angiography. As compared to the CI values for the control group [0.22 ± 2.14 (n=15)], the CABG patients CI values were 0.31 ± 2.59 (before angioplasty) and 1.71 ± 2.07 (after angioplasty; $p < 0.05$, n=22). The individual patients' results thus obtained in reference to angiography are presented in Fig. 5B.

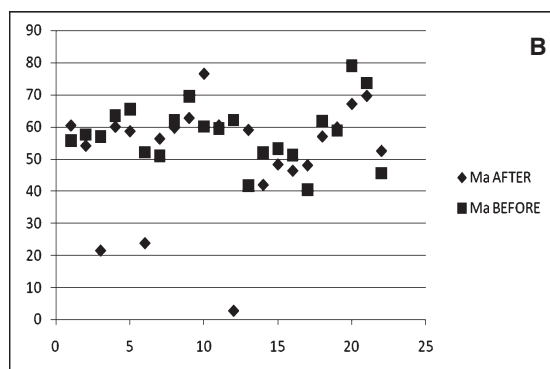
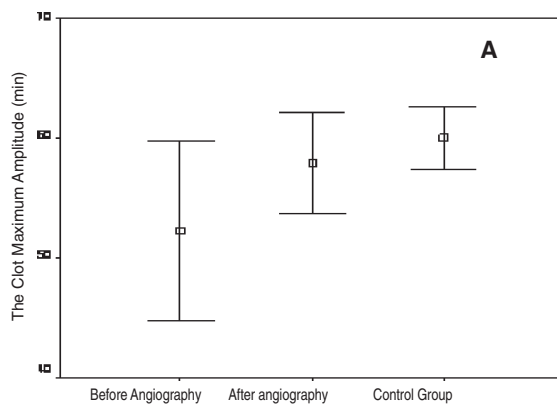


Fig. 4 (A) The TEG clot maximum amplitude (MA) values of the control and the CABG patient groups before and after the angiography. **(B)** Individual patient's MA values before and after angiography are shown.

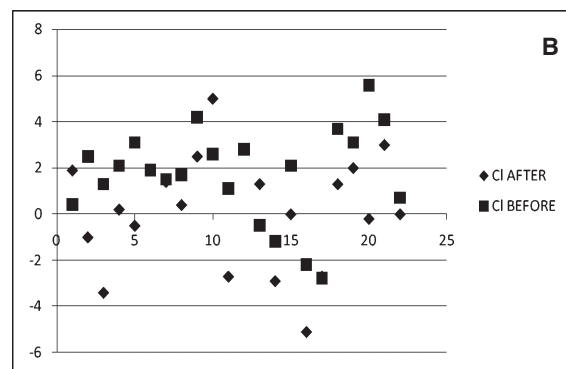
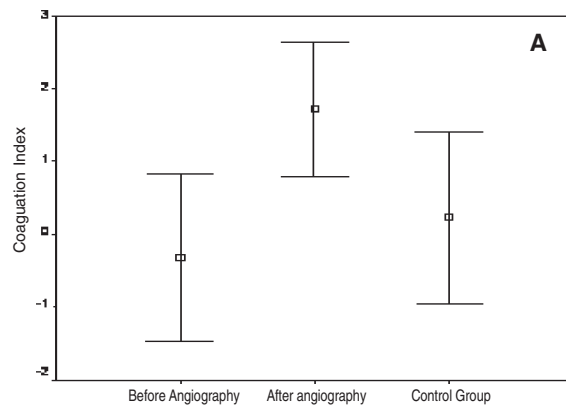


Fig. 5 (A) The clot index (CI) of the control group and patient group before and after angiography as analyzed by the TEG. **(B)** The differences in the CI values for individual patients evaluated by the TEG before and after angiography are shown.

Discussion

The haemostatic system can be altered in relation to impairment of the equilibrium between the activation of clot forming factors and the anticoagulant system. It is well known that the important parameters related to atherosclerosis, viz., high blood lipid profile, hypertension or diabetes are highly relevant where these patients have high myocardial infarction ratio (9). The haemostasis is governed by complex mechanisms where related systems are in interplay with each other, having synergistic effects, including the stimulation of the opposite mechanisms. Also, individual body's immune system and associated mechanisms as a whole play multifunctional roles (10-12). The haemostasis is analyzed according to its structural and functional entities, i.e., as primary and secondary systems. While the primary haemostasis is related to the platelet plug development in the damaged area of the vein, secondary haemostasis includes the plasma coagulation system reactions (13). Thus, haemostatic system works in relation with blood arteries, vein surfaces, endothelial system, platelets, coagulation factors, coagulation inhibitors, and fibrinolytic systems.

The TEG technique is an alternative method to conventional coagulation tests used in evaluation of the haemostatic system in general (9,14). The TEG is easily performed, with a relatively shorter turn-around-time and could evaluate the clot with its mechanical and visco-elastic specifications in the haemostatic system as a whole (15). The TEG generates several parameters during the clotting process. In patients where heart surgery is performed, the accurate evaluation of the serious haemostatic changes which play important role(s) in decreasing the transfusion quantity that causes the complications of the surgery is needed.

In this study, we demonstrate significant decrease in the reaction time after angiography utilizing TEG parameters analyses. In this patient group, the decrease in reaction time could have been one of the risk factors caused by angiography. While analyzing to angiography on the individual case basis for the increased reaction time (especially after the angiography), the decrease in reaction time becomes more significant/obvious. Notably, the clot formation time, fibrinogen activity, and maximum amplitude (before and after angiography) did not show much

Table 1. Demographics and baseline/clinical conditions of the patients and control groups

Factors	Patients (n=22)	Control (n=15)
Age (Years)	65 ± 12	52 ± 16
Gender (Female/Male)	5/17	4/11
Hypertension	13	N/A
Renal Pathology	5	N/A
On Statin, β-3-Blocker, ACE Inhibitor	6	N/A
LDL Cholesterol (mg/dL)	168.0 ± 16.4	89.0 ± 6.0
HDL Cholesterol (mg/dL)	47.0 ± 4.3	45.0 ± 8.7
Total Cholesterol (mg/dL)	N/A	175.0 ± 20.0
Triglyceride (mg/dL)	240.0 ± 25.7	210.0 ± 21.4
Platelet Count (x10 ⁹ /L)	248.4 ± 27.8	210.0 ± 14.6

Data are shown as mean ± standard deviation values
 Abbreviations: N/A = not applicable; ACE = angiotensin-converting enzyme; LDL = low-density lipoprotein; HDL = high-density lipoprotein;

variations. Also, the clot index in the patients (after angiography) was not significantly different as compared to the control group's index.

Based on the individual case for the CI analysis, four patients (before angioplasty) showed hypercoagulation, and three patients (after angioplasty) showed hypercoagulation tendency. The specific observations in clot formation time, fibrinogen activity, clot maximum amplitude showed in the patients with coagulation risk, their haemostatic balance is taken under control by angiographic performances (18). Literature suggests that in patients where heart surgery is performed, the TEG analysis is highly recommended as one of the blood protective methods (9).

In recent years, thrombolytic treatments have been widely used in the clinical situations where abnormal thrombosis is also present (16). These thrombolytic treatments, not only used in acute myocardial infarction, but also in pulmonary emboli, arterial emboli and deep-vein thrombosis cases, where morbidity and mortality is high and serves as superior treatment options. In such cases during angiography, the treatment method selection may cause decrease in systematic side effects (16,17). Hence, in decreasing the microvascular bleeding and selection of effective anti-fibrinolytic agent during the surgery/treatment regimen, the use of TEG serves as a quick directive method (15). For example, while evaluating the TEG parameters, elongation in R time and decrease in MA resulting regimens due to aprotinin treatment regimen may draw attention to clinicians (15).

Frequently seen defective haemostatic system should be followed in high number of heart surgery patients analyzed with conventional comparative analysis. In this work, increased coagulation in the patients at the end of angiography, the risk ratio was lowered. With the TEG method, the use of anticoagulant and antifibrinolytic agents were effective factors that could be appropriately evaluated in light of these TEG analyses. Thus, we demonstrate that the

risk ratio is lowered in the patients after angiography where increased coagulation were detected before the angiography.

References

1. Hershey, J.C., Baskin, E.P., Glass, J.D., Hartman, H.A., Gilberto, D.B., Rogers, I.T. and Cook, J.J. (2001). Revascularization in the rabbit hindlimb: Dissociation between capillary sprouting and arteriogenesis. *Cardiovasc. Res.*, 49: 618-625.
2. Norgren, L., Hiatt, W.R., Dormandy, J.A., Nehler, M.R., Harris, K.A. and Fowkes, F.G. (2007). TASC II Working Group. Inter-Society Consensus for the Management of Peripheral Arterial Disease (TASC II). *J. Vasc. Surg.*, 45: S5-S67.
3. Miller, N.E., Hammett, F., Saltissi, S., Rao, S., van Zeller, H., Coltart, J. and Lewis, B. (1981). Relation of angiographically defined coronary artery disease to plasma lipoprotein subfractions and apolipoproteins. *Br. Med. J. (Clin. Res. Ed.)*. 282: 1741-1744.
4. Vanhoenacker, P.K., Heijenbrok-Kal, M.H., van Heste, R., Decramer, I., van Hoe, L.R., Wijns, W. and Hunink, M.G. (2007). Diagnostic performance of multidetector CT angiography for assessment of coronary artery disease: Meta-analysis. *Radiology*. 244: 419-428.
5. Triplett, D.A. (2000). Coagulation and bleeding disorders: Review and update. *Clin. Chem.* 46: 1260-1269.
6. Haznedaroglu, I.C. (2005). Mechanisms of haemostasis. *Turkiye Klinik. J. Int. Med. Sci.*, 1: 1-5.
7. Glidden, P.F., Malaska, C. and Herring, S.W. (2000). Thromboelastograph assay for measuring the mechanical strength of fibrin sealant clots. *Clin. Appl. Thromb. Hemost.*, 6: 226-233.
8. Yee, D.M., Edwards, R.M., Mueller, B.U. and Teruya, J. (2009). Thromboelastographic and hemostatic characteristics in pediatric

- patients with sickle cell disease. *Arch. Pathol. Lab. Med.*, 129: 760-765.
9. Ak, K., Ýsbir, C.S., Tetik, S., Atalan, N., Tekeli, A., Aljodi, M., Civelek, A. and Arsan, S. (2009). Thromboelastography-based transfusion algorithm reduces blood product use after elective CABG: A prospective randomized study. *J. Card. Surg.*, 24: 404--410.
 10. Lopez, J.A., Armstrong, M.L., Piegors, D.J. and Heistad, D.D. (1990). Vascular responses to endothelin-1 in atherosclerotic primates. *Arteriosclerosis*. 10: 1113-1118.
 11. Khurl, S.F., Michelson, A.D., Valeri, C.R. (1997). Effects of cardiopulmonary bypass on hemostasis. *Boston Univ. MA Sch. Med.. Technical Rept.* 79: ADA360309.
 12. Linden, M.D. (2003). The hemostatic defect of cardiopulmonary bypass. *J. Thromb. Thrombolysis*. 16: 129-147.
 13. Colwell, C.W. Jr. and Hardwick, M.E. (2004). Natural history of venous thromboembolism. *Curr. Opin. Intern. Med.*, 19: 236-239.
 14. Hubson, A.R., Agarwala, R.A., Swallow, R.A., Dawkins, K.D. and Curzen, N.P. (2006). Thrombelastography: Current clinical applications and its potential role in interventional cardiology. *Platelets*. 17: 509-518.
 15. Ak, K., Atalan, N., Tekeli, A., Isbir, S., Civelek, A., Emekli, N., Arsan, S. (2008). Tromboelastografi ve kalp cerrahisinde kullanýmý. *Anadolu Kardiyol. Derg.*, 8: 154-162.
 16. Bayýr, A. and Ak, A. (2003). Acil olgularda trombolitik tedavi. *Genel. Týp. Derg.* 13: 81-88.
 17. Fried, R.E. (2002). Diagnosis and treatment of peripheral arterial disease. *JAMA*. 287: 315-316.

Raster Image Correlation Spectroscopy in Live cells Expressing Endothelin ET_A Receptor

Damaris De La Torre^{a,e}, Elizabeth A. Gordon^b, Michelle A. Digman^{b,c}, Milka Stakic^c, Hanns Häberlein^d, Enrico Gratton^{bc} and Catherina Caballero-George^a

^a Unit of Molecular Pharmacology and Pharmacognosy, Institute for Scientific Research and High Technology Services, Bld. 219, City of Knowledge, Clayton, Panama Republic

^b Department of Developmental and Cell Biology, University of California, Irvine, California, USA

^c Laboratory for Fluorescence Dynamics, Department of Biomedical Engineering, University of California, Irvine, California, USA

^d Institut für Biochemie und Molekularbiologie, Nussallee 11, 53115 Bonn, Germany

^e Department of Biotechnology, Acharya Nagarjuna University, Guntur, India

*For correspondence – c.caballeroGeorge@gmail.com

Abstract

Fluorescence spectroscopy is the most common non-radioactive technique used to study GPCR interactions with their ligands. Raster image correlation spectroscopy (RICS) exploits spatio-temporal correlation functions rather than the simple temporal correlations of conventional fluorescence correlation spectroscopy. In this paper we describe the use of RICS and the number and brightness method to determine the diffusion of a construct of endothelin ET_A receptor with EGFP and the aggregation state in the cytoplasm. Our construct seems to locate mainly in the cytoplasm where it undergoes diffusion and it appears to be monomeric. Although our construct could not fully represent the native protein, we believe that the methodology we describe in this paper could be used by anyone in this field.

Key words: Endothelin ET_A receptor, GPCR, live cell, imaging, RICS.

Introduction

Endothelins are a family of vasoconstrictive peptides expressed in different tissues (1), which maintain basal vascular tone and blood pressure (2). Endothelin 1 (ET-1), the most potent of these peptides, has been found as an etiologic or aggravating factor in a number of cardiovascular diseases, including essential hypertension, pulmonary hypertension, acute renal failure,

cerebral vasospasm after subarachnoid hemorrhage, vascular remodeling, cardiac hypertrophy, and congestive heart failure (3). ET-1 mediates its effects via two G-protein coupled receptors (GPCR) namely ET_A and ET_B, which are coupled to several subfamilies of the heterotrimeric G protein family (2). It has been shown that most of the apparently deleterious effects of ET-1 are mediated through the activation of ET_A receptors (4), thus this receptor has become an important target in drug discovery of cardioprotective drugs (5,6).

Fluorescence spectroscopy is the most common non-radioactive technique used to study GPCR interactions with their ligands. However, detailed biophysical data on these interactions is scarce (7). This is the case of the ET_A receptor, which in spite of its patho-physiological relevance, it has only been studied by fluorescence resonance energy transfer (FRET) (8,9) and more recently, fluorescence correlation spectroscopy (FCS) (10).

In classical single point FCS analysis, fluctuations are measured in one volume of illumination. This analysis has the drawback that it does not provide information regarding possible correlations between adjacent (or far) volumes of observation at different time, limiting the description of the full receptor dynamics.

In order to overcome these limitations, raster image correlation spectroscopy (RICS) exploits spatio-temporal correlation functions rather than the simple temporal correlations of conventional FCS (11). RICS provides spatial information on binding and diffusion coefficients in live cells using a conventional confocal microscope (12). With this methodology, the full extent of the probability of finding a particle at a different location and at a different time is introduced into the description of the correlation of the fluctuations to capture the time and spatial evolution of the particle.

In this paper we describe the use of RICS and the number and brightness method to determine the diffusion of a construct of ET_A with enhanced green fluorescent protein (EGFP) and the aggregation state in the cytoplasm.

Materials and Methods

Cell Culture: CHO-K1 cells were cultured in Dulbecco's Modified Eagle Medium: Nutrient Mixture F-12 media supplemented with 10 % Fetal Bovine Serum and 1 % Penicillin-

Streptomycin. They were plated on 8 well Nunc* Lab-Tek* II Chambered Coverglass overnight and transfected with eGFP ENDRA protein using the Lipofectamine 2000 transfection reagent. Experiments were also performed using NIH3T3 cells that were cultured in Dulbecco's Modified Eagle Medium (DMEM) supplemented with 10 % Fetal Bovine Serum, 1 % Penicillin-Streptomycin and 0.5 % 1 M HEPES solution.

Plasmid Construction- N-terminal HA C-Terminal eGFP ENDRA: cDNA for ENDRA (Endothelin receptor type A) [Catalog Number: #EDNBL0TN00] with 3xHA-tag (N-terminus) was obtained from Missouri S&T in pCDNA3.1+ from Invitrogen. The ENDRA coding sequence including the HA-tagged N-terminus to the last codon before the stop codon was amplified by PCR using *Pfu* Ultra DNA polymerase (Stratagene). The correct size PCR product (Insert size= 1926 bp.) was purified (Qiagen) and digested using restriction enzyme sites designed into the primers (Kpn1 and Age1) (Fig. 1). Product was run on a 1% agarose gel and

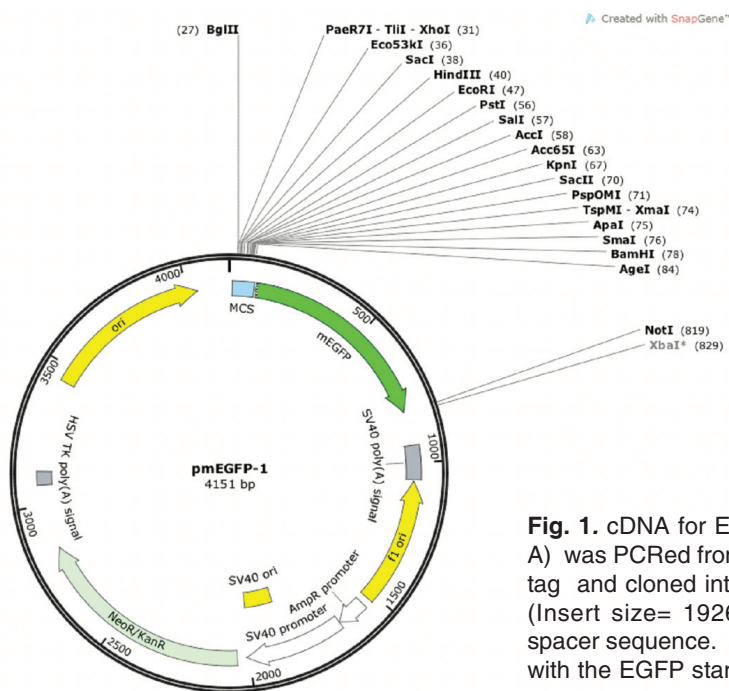


Fig. 1. cDNA for ENDRA (Endothelin receptor type A) was PCR'd from pCDNA3.1 template with 3xHA-tag and cloned into pmEGFP-1 using the Kpn1(5') (Insert size= 1926 bp) and stop codon removed spacer sequence. The Age1(3') site used is in frame with the EGFP start.

excised for gel extraction (Qiagen). Digestion of the vector pmEGFP-1 (Addgene 36409: - deposited by Benjamin S. Glick, PhD from the University of Chicago) with Kpn1 -HF™ and Age1-HF™ (NEB) was performed, followed by gel purification. The PCR product was ligated into the eGFP vector. The resulting plasmid (KAN resistant) were screened by restriction digest and then verified by DNA sequencing (Retrogen). The ENDRA and the eGFP were verified by using BLAST NCBI.

RICS measurements: An Olympus FV1000 confocal microscope was used for the RICS experiments. Excitation was at 488nm at a nominal power of 2%. Excitation/emission was split using the DM405/488. Emission was collected using BA505-525nm bandpass. The Objective was a UPLSAPO 60X W, NA 1.20 from Olympus. The frame size was set at 256x256 with a pixel dwell time of 10ms or 8 ms. The pixel size was 0.050mm or 0.072mm depending on the experiment, but always in the optimal range for the RICS experiments. Data were acquired using the pseudo-photon counting of the Olympus FV1000. For each experiment, 100 frames were acquired. RICS and brightness analysis was performed using the SimFCS software (www.lfd.uci.edu). For the brightness analysis the detrend option was used. This option compensate on a pixel basis for the bleaching.

RICS correlation functions: The RICS correlation function is defined in equation 1.

$$G_{RICS}(\xi, \psi) = \frac{\langle I(x, y)I(x + \xi, y + \psi) \rangle}{\langle I(x, y) \rangle^2} - 1$$

where I is the intensity at each pixel and the brackets indicate the average over all pixels x, y of an image. According to the definition of the correlation function, one image is sufficient to determine the RICS correlation function. However, in general, a stack of images must be collected to separate the mobile from the immobile fraction of molecules. The definition of the RICS correlation function is similar to the definition of the Image Correlation Spectroscopy

(ICS) given by Petersen et al (Petersen, 1986; Petersen, 1998; Petersen NO, 1993). The difference in the RICS approach with respect to ICS is in the particular way data are collected in the raster scan confocal microscope which results in a relationship between the position of the pixel in the image and the time a specific pixel is measured.

$$\begin{aligned} \text{time at pixel } n &= y \times \tau_l + x \times \tau_p \\ \xi &= x \times \tau_p \\ \psi &= y \times \tau_l \end{aligned}$$

The resulting correlation function can then be expressed in terms of the pixel time t_p and the line time t_l

Brightness analysis: The data set need for the Brightness analysis consists of a stack of images of the same field of view. These images generally are the same used for the RICS analysis. For each pixel of the stack of images we define

$$\begin{aligned} av &= \frac{\sum_k I(x, y)}{K} \\ var &= \frac{\sum_k (I(x, y) - av)^2}{K} \end{aligned}$$

Where the sum is over the same pixel in each frame of the stack, K is the number of frames and I is the intensity at one pixel of each frame. The brightness B is defined by the following relationship

$$B = \frac{var}{av}$$

For a pure Poisson distribution of counts, the brightness is equal to one. If there is an excess variance (with respect to the Poisson variance) the value of B will exceed 1. It was shown that this additional variance depends only on the molecular brightness of the particles that fluctuate in number in the volume of excitation. Brightness is generally expressed as counts/pixel-dwell-time/molecule. Since brightness depends on the laser intensity and system detection efficiency, the value of the brightness is calibrated

for a given substance. In this paper we use a monomeric EGFP construct expressed in the same type of cell to determine the “brightness of the monomer. Then the measurement of the brightness is expressed as a ratio to the brightness of the monomer. Generally a dimer will have a ration of 2 with respect to a monomer. Note that the brightness is a molecular property that cannot be derived from a simple intensity measurement since in general intensity is proportional to the product of the number of molecules in the volume of excitation times the brightness of each molecule.

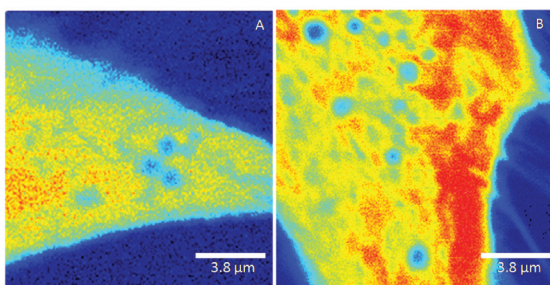


Fig. 2. A) CHO-K1 cell expressing the ET_A -EGFP construct. B) NIH 3T3 cell expressing the ET_A -EGFP construct. The focus is on the bottom part of the cell for both images.

Results and Discussion

The RICS method was applied to cells expressing the ET_A receptor. The plane of focus was set as close as possible to the bottom membrane plane. A typical image of a CHO-K1 cell expressing the ET_A -EGFP construct is shown in Fig. 2. Note that the border of the cells lack of the characteristic increase of intensity expected for a membrane bound receptor. The construct is well expressed in both cell lines.

The RICS correlation function and the fit using one component diffusion model for the CHO-K1 cell is shown in Fig. 3.

Analysis of three cells gives an average diffusion coefficient of $D=11.0\pm 0.3 \mu\text{m}^2/\text{s}$. The fits of the RICS correlation function are generally very good as judged by the relatively small residues as shown in the example of Fig. 3 (upper surface). On some of the cells, single point FCS measurements were done at selected points close to the membrane, giving comparable results for the diffusion coefficient. When the ligand was added to the cells, we found an increase in the diffusion coefficient giving $D=19.8\pm 2.8 \mu\text{m}^2/\text{s}$ after about 1 min and then

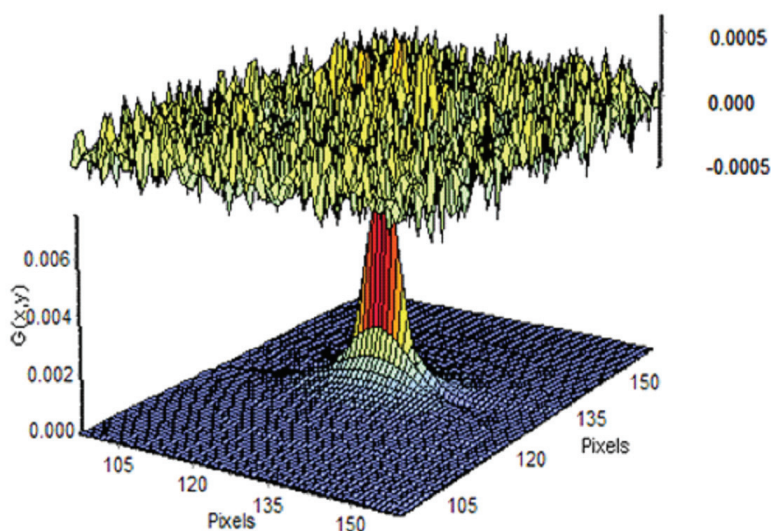


Fig. 3. Fit of the RICS correlation function. Bottom surface: RICS correlation for ET_A -EGFP in CHO-K1 cell. One component diffusion gives a value of $D=10.79\mu\text{m}^2/\text{s}$. The upper surface is the residues of the fit.

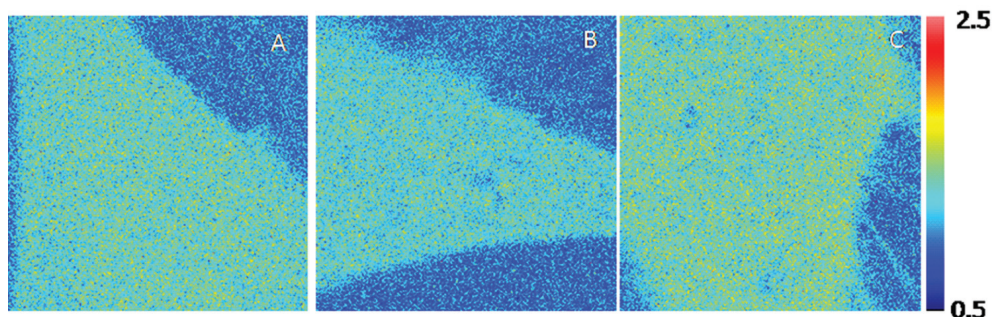


Fig. 4: Brightness map. A) CHO-K1 cell expressing monomeric EGFP; B) CHO-K1 cell expressing ET_A -EGFP, NIH 3T3 cell expressing ET_A -EGFP. The brightness is the same for all cells indicating that the protein is monomeric. In conclusion, our construct seems to locate mainly in the cytoplasm where it undergoes diffusion and it appears to be monomeric. We show that we can detect the cytoplasmic population of the ET_A receptor and accurately measure its brightness. Our specific protein seems to have lost the capability to reside at the membrane, so we were unable to study the interactions with ligand and the state of aggregation of the ET_A receptor at the membrane. Although our construct could not fully represent the native protein, we believe that the methodology we describe in this paper could be used by anyone in this field.

remained constant. Analysis of cells expressing EGFP only give a value of the diffusion coefficient of $D=21.1\pm 0.3 \mu m^2/s$, which is typical of free EGFP in the cytoplasm of cells. For the NIH3T3 cells we found a value of $D=16.3\pm 4.2 \mu m^2/s$.

Although we focused the plane of observation close to the bottom membrane, we believe that the ET_A molecules we observe are actually in the cytoplasm. The value of the diffusion coefficient is too large for molecules diffusing in the membrane. The prevalent localization of the mobile ET_A molecules in the cytoplasm rather than at the membrane could be due to the addition of the EGFP moiety to the receptor protein. Also the diffusion coefficient appears to be slightly smaller than the diffusion of EGFP alone, indicating that the protein is likely to be monomeric in the cytoplasm.

Brightness analysis shows that the protein is a monomer in the cytoplasm (Fig. 4). This is done by comparison with the brightness of the EGFP transfected cells (Figure 4A) with the ET_A -EGFP CHO-K1 (Fig. 4B) and NIH 3T3 (Fig. 4C) transfected cells. The ratio between the brightness of the ET_A -EGFP in both CHO-k1 and

NIH 3T3 cells and monomeric EGFP was 1.03 ± 0.11 .

Acknowledgments

Financial support by the Panamanian Secretariat of Science and Technology (SENACYT) through the incentive program of the National System of Innovation (SNI) and grant number COL10-070; and by a partnership program between the Organization for the Prohibition of Chemical Weapons (The Hague, Netherlands) and the International Foundation for Science (Stockholm, Sweden) is gratefully acknowledged. Thanks are also due to IFARHU from the Panamanian government, which jointly with SENACYT gave a scholarship to Ms. Damaris De La Torre. This work was supported in part by grant numbers: NIH-P41-RRO3155, P50-GM076516, and NIH-U54 GM064346, Cell Migration Consortium (to M.A.D. and E.G.).

References

1. Masaki, T. (2000). The endothelin family: an overview. *Journal of Cardiovascular Pharmacology*, 35: S3-S5.
2. Takigawa, M., Sakurai, T., Kasuya, Y., Abe, Y., Masaki, T., Goto, K. (1995). *Molecular*

- identification of guanine-nucleotide-binding regulatory proteins which couple to endothelin receptors. *Eur J Biochem*, 228: 102-108.
3. Goto, K. (1999). History of endothelin. In: Pulmonary actions of the endothelins. Goldie, R.G., Hay, D.W., editors. Kirkhäuser Verlag Basel, Switzerland, pp 1-20
 4. Haynes WG, Webb DJ. (1998). Endothelin as a regulator of cardiovascular function in health and disease. *Journal of Hypertension*, 16: 1081-1098
 5. Wainwright CL, McCabe C, Kane KA. (2005). Endothelin and the ischaemic heart. *Curr Vasc Pharmacol*, 3(4):333
 6. Caballero-George C.(2011). Does Nature has the Cure for Hypertension?: Endothelin Receptors as Drug Targets. *Current Trends in Biotechnology and Pharmacy*, 5(3): 1251-1272
 7. Langelaan D, Ngweniform P, Rainey J. (2011). Biophysical characterization of G-protein coupled receptorpeptide ligand binding. *Biochem Cell Biol*, 89(2): 98–105.
 8. Evans, N.J. and Walker, J.W. (2008). Sustained Ca²⁺ signaling and delayed internalization associated with endothelin receptor heterodimers linked through a PDZ finger. *Can J Physiol Pharmacol.*, 86(8): 526-35.
 9. Gregan, B., Schaefer, M., Rosenthal, W., Oksche, A. (2004). Fluorescence resonance energy transfer analysis reveals the existence of endothelin-A and endothelin-B receptor homodimers. *J Cardiovasc Pharmacol.*, 44 Suppl 1: S30-3.
 10. Caballero-George, C., Sorkalla, T., Jakobs, D., Bolaños, J., Raja, H., Shearer, C., Bermingham, E., Häberlein, H. (2012) Fluorescence correlation spectroscopy in drug discovery: study of Alexa532-endothelin 1 binding to the endothelin ET_A receptor to describe the pharmacological profile of natural products. *Scientific World Journal*, 2012: 524169.
 11. Digman, M.A., Stakic, M. and Gratton, E. (2013). Raster Image Correlation Spectroscopy and Number and Brightness Analysis. *Methods Enzymol.*, 518C: 121-144.
 12. Rossow, M.J., Sasaki, J.M., Digman, M.A. and Gratton, E. (2010). Raster image correlation spectroscopy in live cells. *Nat Protoc.*, 5(11): 1761-74.

Expression of C-terminal Prodomain Truncated *Petunia* Floral Defensins Inhibit the Growth of Transgenic Banana Plants

Siddhesh B Ghag, Upendra K Singh Shekhawat and Thumballi R Ganapathi*

Plant Cell Culture Technology Section, Nuclear Agriculture and Biotechnology Division, Bhabha Atomic Research Centre, Trombay, Mumbai-400 085, India.

*For Correspondence - trgana@barc.gov.in

Abstract

Plant defensins are basic proteins synthesized as part of innate immune response against the attack of fungal pathogens. These defensins show strong antimicrobial activity which is specifically directed towards the invading pathogen. Diverse defensins have been overexpressed in model transgenic plants to show their efficacy in heterologous systems. There are more than 350 plant defensins known today which have occurred due to convergent and divergent evolution over time. Although most of these peptides generally do not react with the host plant cells, some may have deleterious effect on plant organs. As a consequence plants build up advance strategy to nullify the effect by targeting the peptides to vacuoles, preventing its expression in sensitive organs and changing the amino acids composition. The C-terminal propeptide (CTPP) domains probably prevented any lethal effects of plant defensins while simultaneously enabling vacuolar sorting. In order to study the role of CTPP of two *Petunia* floral defensins (*PhDef1-T* and *PhDef2-T*), banana embryogenic cells were transformed with *PhDef1-T* and *PhDef2-T* without the CTPP domain region. The results obtained from this study clearly demonstrated that the absence of CTPP in *Petunia* floral defensins caused significant reduction in the number of embryos and its poor growth. Regenerated shoots were considerably slow in growth signifying the

relevance and the importance of the prodomain region in floral defensins.

Key words: Floral defensins, *Petunia*, banana, CTPP domains

Introduction

Plant defensins are low molecular weight antimicrobial peptides having 45-54 amino acid active domains. These cysteine-stabilized $\alpha\beta$ ($CS\alpha\beta$) structures mainly act as effective membrane destabilizers (1) and protein inhibitors (2). Potent activity of these defensins, derived mainly from seeds and floral tissues, against a wide array of fungal pathogens has been described in the past (3). Further, expression of some of these defensins in model transgenic plants has resulted in efficient resistance towards fungal infection. Although their potency against fungal pathogens is more or less established, their interactions with the target and the host organisms are not clear in most cases. Floral defensins from *Petunia* and *Nicotiana* possess strong antifungal activity and a highly stabilized structure having five intramolecular disulphide linkages (4). These defensins are synthesized as inactive proproteins having a 27-33 amino acids C-terminal prodomain which is postulated to be responsible for neutralizing the cationic defensin domain and possibly also for vacuolar targeting. The C-terminal prodomains of these defensins are rich in acidic and hydrophobic amino acids giving them a net negative charge

at neutral pH. This helps in avoiding any disturbance in the optimum plant cell milieu during synthesis and translocation of these defensins. Once the defensins reach their site of storage (intracellular vacuole), the C-terminal prodomain region is cleaved off by specific vacuolar proteases.

Recent report demonstrated that high level expression of full-length *Petunia* floral defensins (*PhDef1* and *PhDef2*) in banana cultivar *Rasthali* provides resistance to pathogenic Foc race 1 (5). Apart from having defined signal peptides and defensin domains, these defensins are unique in having C-terminal prodomain regions which probably also take part in intracellular sorting. Earlier reports demonstrated the role of plant defensins in growth and development of the host plant (6, 7). In the present study we demonstrated that transformed banana cells overexpressing *Petunia* floral defensins (*PhDef1-T* and *PhDef2-T*) showed reduced embryo formation and regeneration pointing towards the function in growth and development of plants. The shoots so obtained showed stunted growth and were unable to form roots. These results comprehend the role of CTPP in plant defensins that are produced in plants during pathogen attack.

Materials and Methods

Isolation and cloning of defensin genes: Total RNA was extracted from *Petunia hybrida* flowers using Concert Plant RNA Reagent (Invitrogen, USA) and was purified using RNeasy Plant Mini Kit (Qiagen, Germany). This RNA (approx. 5 µg) was then used to make first strand cDNA using Oligo (dT)₁₂₋₁₈ primer (Invitrogen, USA) and AccuScript Reverse Transcriptase (Stratagene, USA) according to manufacturer's instructions. The C-terminal truncated versions of the two defensins *PhDef1-T* and *PhDef2-T* were amplified from the flower derived cDNA using the following primers (from 5' to 3'): *PhDef1-T* Fw: GATCCTGCAGGATGGCTCGCTCCATCTGTTTC, Rv: ACTGGTACCCTAA CACTCTTTAGTGCA CAGACATCTTC; *PhDef2-T* Fw GATCCTG CAGG ATGGCTCGCTC CATCTGTTTC, Rv: ACTGG TACCTTAAC ACGGCTTAGTGC

ATAGGCA TCTTC. Thermal cycling conditions set for amplification were 94°C for 5 min followed by 30 cycles each with 94°C for 1min, 55°C for 1min and 72°C for 1min with a final extension of 72°C for 10min. The amplified products so obtained were gel purified and cloned into cloning vector pTZ57R/T (Invitrogen) and sequenced.

Construction of plant expression binary vectors : *PhDef1-T* and *PhDef2-T* coding sequence were digested from pTZ57R/T vector using *Pst*I and *Kpn*I and inserted into the multiple cloning site of pCAMBIA-1301 binary vector (digested with *Hind*III and *Kpn*I) having nos 3'UTR along with *Zea mays* polyubiquitin promoter (digested with *Hind*III and *Pst*I) in a three-way ligation reaction to form *pPhDef1-T-1301* and *pPhDef2-T-1301* respectively. These binary vectors were subsequently sequenced. *pPhDef1-T-1301* and *pPhDef2-T-1301* were mobilized into *Agrobacterium tumefaciens* strain EHA 105 by electroporation.

Generation of transgenic banana plants:

Banana cv. *Rasthali* embryogenic cell suspension cultures were transformed by the newly constructed binary vectors as described earlier (8). The transformed cells were cocultured in M2 medium for 3 days and later on banana embryogenic medium for 9 weeks with repeated subculture after every 3 weeks in presence of hygromycin (5mg/L) as selective agent. Putatively transformed embryos were germinated in presence of low concentration of BAP (0.5 mg/L).

Histochemical GUS assay: Putatively transformed *in vitro* leaves were injured with forcep and incubated in GUS buffer overnight at 37°C. The leaves were transferred to 70% ethanol to remove the chlorophyll for easy visualization of GUS staining.

Detection of transgenic nature by PCR:

Genomic DNA was isolated from *in vitro* developed banana leaves using GenElute Plant Genomic DNA Miniprep Kit (Sigma, USA). Polymerase chain reaction was carried out using above mentioned primers and amplification

protocol. The amplified products were visualized in 1% TAE gel with ethidium bromide.

Results

Petunia hybrida defensins namely *PhDef1-T* and *PhDef2-T* were successfully amplified from the cDNA of floral tissues. After cloning *PhDef1-T* and *PhDef2-T* into pTZ57R/T vector it was sequenced. The sequence of both the amplified products were translated into the protein sequence using online ExpASY translate tool (<http://au.expasy.org/tools/dna.html>). 24 amino acids signal peptide was identified in both the defensins using online SignalP software (<http://www.cbs.dtu.dk/services/SignalP>). Active defensin domain in *PhDef1-T* is of 47 amino acids whereas in *PhDef2-T* it is 49 amino acids long which undergo characteristic folding to form the CS $\alpha\beta$ structure. These PCR amplified products were cloned into pCAMBIA 1301 binary vector as an expression cassette driven by *Zea mays* polyubiquitin promoter and again sequenced to determine the orientation of the insert between the promoter and the nos 3'UTR. Fresh embryogenic cell suspension cultures were used for *Agrobacterium*-mediated transformation. Embryogenic cells transformed with p*PhDef1-T*-1301 and p*PhDef2-T*-1301 binary vectors (Fig. 1 A) were significantly slow in their growth in the embryo induction and development medium (Fig. 1 B, C). Additionally, the number of putatively transformed embryos which grew on selection medium was less than 20 % of p*PhDef1*-1301 and p*PhDef2*-1301 derived embryos (full length defensin constructs described earlier in 5). Owing to their stunted and slower growth, very few transformed shoots could be obtained for these two truncated defensin constructs (Fig. 1D, E). These shoots further failed to produce profuse root system on medium supplemented with NAA. As a result the shoots obtained could not be hardened in the green house. This observation reveals the lethality of overexpressing floral defensins without the CTPP domains. The total number of embryos and shoots which could be recovered after selection in hygromycin medium was less. To confirm the transgenic nature of

these shoots, genomic DNA PCR was carried out using primers specific for *PhDef1-T* and *PhDef2-T*. Single amplified product derived from *PhDef1-T* and *PhDef2-T* coding sequence (~250bp) was obtained in transgenic banana plants overexpressing *PhDef1-T* and *PhDef2-T* (Fig.1F). These products were absent in untransformed control plants. The leaf tissue from *in vitro* shoots was incubated in GUS buffer at 37°C overnight in order to determine the expression of T-DNA in banana leaves. Transformed leaf tissues showed intense blue coloration indicating stable integration and expression of the T-DNA in the transgenic banana shoots (Fig. 1 G, H). Two predicted roles such as vacuolar sorting and transportation of the unique C-terminal prodomains of these defensins can be directly correlated with the observed growth inhibition.

Discussion

Plant floral defensins are stable, cationic peptides produced in flowers to prevent the possibility of fungal attack (9). Plant defensins are secreted during stress conditions such as salt, drought or cold and pathogen attack describing its role in growth, development and defense (10). Several defensin genes have been used to transform economically important crops such as rice (11), banana (5), and potato (12) to provide broad spectrum resistance against phytopathogens. Full length *Petunia* floral defensins (*PhDef1* and *PhDef2*) when constitutively expressed in banana plants cv. *Rasthali* it imparted resistance to pathogenic strain of *Fusarium oxysporum* f. sp. *cubense* race 1 without affecting the morphology of the transgenic banana plants (5). Interestingly when we constitutively overexpressed the same floral defensins (*PhDef1-T* and *PhDef2-T*) without the CTPP in banana cv. *Rasthali* driven by same *Zea mays* polyubiquitin promoter there was drastic reduction in number of embryos formed (data not shown) and the ones that were formed showed reduced capability of regeneration. The shoots obtained by germinating the embryo did not undergo profuse multiple shoot development in

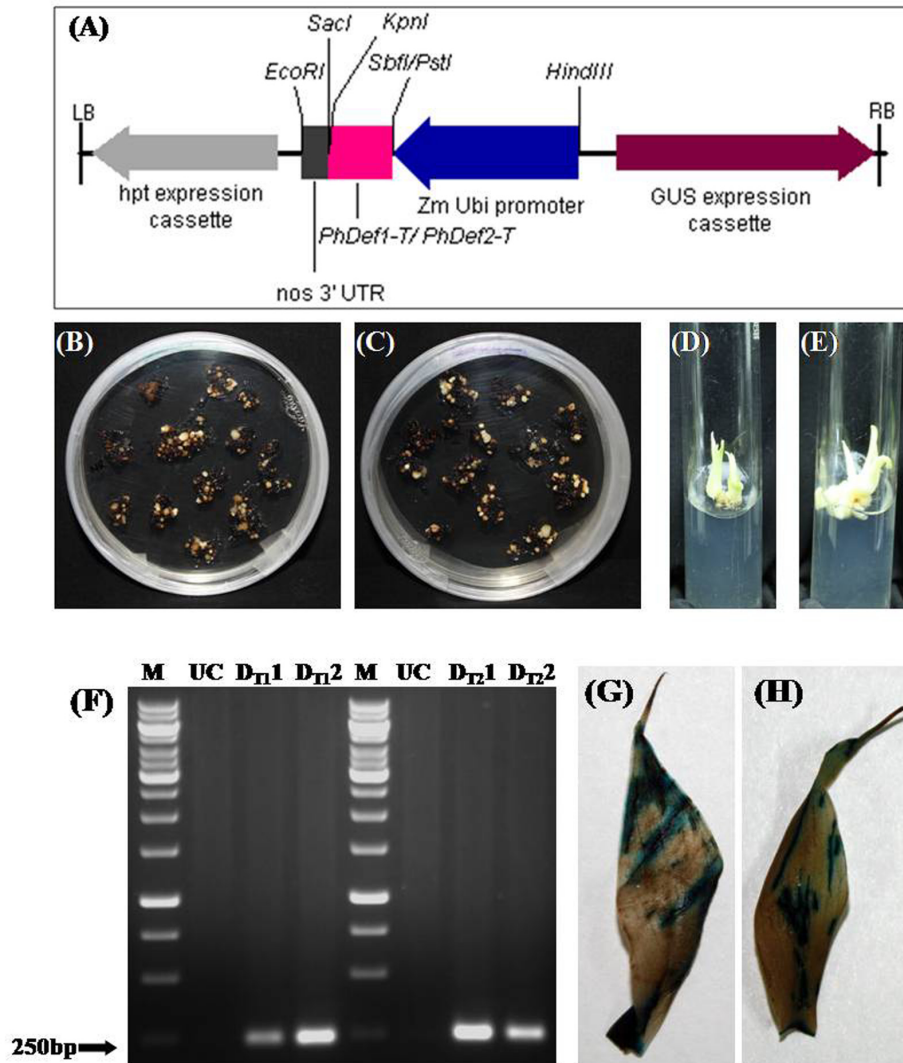


Fig. 1. Genetic transformation of banana cv. *Rasthali* with truncated *Petunia* defensin constructs and analysis of transformants. (A) T- DNA region of p*PhDef1-T-1301*/ p*PhDef2-T-1301* binary vector wherein C-terminal truncated *PhDef1* and *PhDef2* coding sequences (without the prodomain) were cloned downstream of *Zea mays* polyubiquitin promoter and upstream of nos (nopaline synthase) 3' UTR in MCS of pCAMBIA-1301 vector. (B) and (C) Somatic embryos derived from p*PhDef1-T-1301*/ p*PhDef2-T-1301* transformed cells on embryo induction medium 10 weeks post cocultivation. Note the significant browning as well as reduction in number of fresh embryos. (D) and (E) Multiple shoots derived from p*PhDef1-T-1301*/ p*PhDef2-T-1301* transformed cells on shoot induction medium 20 weeks post cocultivation. Growth and multiplication of shoots was significantly slower than those derived from untransformed controls or from p*PhDef1-1301* and p*PhDef2-1301* transformed cells. (F) Genomic DNA PCR of two selected lines each derived from p*PhDef1-T-1301*(D_{T1}1, D_{T1}2), p*PhDef2-T-1301*(D_{T2}1, D_{T2}2) and untransformed control (UC) plants (Lane1and 5: 1 kb DNA ladder). (G) and (H) histochemical GUS staining of p*PhDef1-T-1301*/ p*PhDef2-T-1301* transformed banana leaves.

medium supplemented with BAP (2 mg/L). In order to know whether these shoots showed root development we transferred them onto the rooting medium. These shoots were unable to form the root system. This study finds that the absence of CTPP domains in both the defensins may have caused severe retardation in growth and development. To further confirm the transgenic nature of the putatively transformed banana shoots genomic DNA PCR was carried out using primers specific to *PhDef1-T* and *PhDef2-T* coding sequence. Transformed leaves overexpressing *PhDef1-T* and *PhDef2-T* showed positive GUS staining demonstrating that the T-DNA has been successfully integrated in the euchromatin region of banana genome and is expressing the GUS transcript to show the characteristic blue coloration. This clearly indicates that the coding sequence of *PhDef1-T* and *PhDef2-T* without the CTPP domain is also expressed in the transgenic banana shoots. Since the transgenic banana shoots overexpressing *PhDef1-T* and *PhDef2-T* without CTPP showed abnormal phenotype and poor growth and development explains the importance of CTPP in such potent defense molecules. Even though there are reports where high level expression of defense molecules provided durable resistance to phytopathogens but some of them may have toxic effect on plant growth. A potent defensin NaD1 isolated from tobacco when transformed into cotton lacking CTPP resulted in plants with distorted leaves and short internodes (13). The neutralization of the positively charged defensin domain by the negatively charged C-terminal domain helps prevent any deleterious effects on the plant cells. Also the prodomains are involved in vacuolar sorting and transportation (14). Our results could be very well correlated wherein there was abnormal shoot proliferation in transgenic banana shoots *in vitro*. The truncated versions of the two *Petunia* floral defensins probably failed to get translocated in the vacuoles resulting in their accumulation in the cytosol leading to charge imbalances and growth retardation. Stotz and co-workers (9) proposed the role of tomato defensin

DEF2 in both defense and development. Ectopic expression of this DEF2 peptide in tomato resulted in growth retardation. Overexpression or antisense repression of DEF2 in tomato plants resulted in smaller leaves and reduction in pollen viability. This explains the fact that plant defensin expression is prudently regulated in plants in particular organs and for specific time period. Certain plant defensins are not expressed in some organs at all owing to its organ specific lethality. For example *Medicago* defensins MsDef1 and MtDef2 are not present in the roots of this plant (7, 15). Plants mostly fall prey to fungal diseases than bacterial ones; thus during the course of evolution it developed defense molecules targeting specifically the fungal pathogens. Many of the plant defensins inhibit fungal hyphal tip growth by disrupting the cytosolic calcium gradients. Root hair development in plants and hyphal tip growth in fungus is thought to be similar phenomenon involving calcium channels; as a result those defensins which target the fungal hyphal tip may attack the growing root hairs of the host plants explaining its absence in *Medicago* roots. *Arabidopsis* seeds when treated with MsDef1, MtDef2, RsAFP2 and KP4 showed root growth inhibition at lower concentrations but later on removal of these peptides resulted in reversal of the phenotype (7). The results presented here clearly demonstrate that plant defensins not only help in antimicrobiosis but also play role in plant growth and signalling. Detailed investigation is needed so as to understand the interactions of these floral defensins with fungal counterparts. There remains much scope to study the mechanism of action, molecular interactions and regulation of these prodomains in plant defensins. Further these prodomains can be tagged to potent broad spectrum antimicrobials to obtain sustainable resistance for wide array of phytopathogens.

Acknowledgement

Authors wish to thank Dr. S F D'Souza, Head, Nuclear Agriculture and Biotechnology Division, BARC for his constant support.

References

1. Thevissen, K., Terras, F.R. and Broekaert WF (1999). Permeabilization of fungal membranes by plant defensins inhibits fungal growth. *Appl Environ Microbiol.*, 65:5451–5458.
2. Bloch, C. Jr. and Richardson, M. (1991). A new family of small (5 kDa) protein inhibitors of insect alpha-amylases from seeds of sorghum (*Sorghum bicolor* (L) Moench) have sequence homologies with wheat gamma-purothionins. *FEBS Lett.*, 279:101–104.
3. Broekaert, W.F., Cammue, B.P.A., De Bolle, M.F.C., Thevissen, K., De Samblanx, G.W. and Osborn, R.W. (1997). Antimicrobial Peptides from Plants. *Crit. Rev. Plant Sci.*, 16: 297-323.
4. Lay, F.T., Brugliera, F. and Anderson, M.A. (2003). Isolation and properties of floral defensins from ornamental tobacco and petunia. *Plant Physiol.*, 131: 1283-1293.
5. Ghag, S.B., Shekhawat, U.K.S. and Ganapathi, T.R. (2012). *Petunia* floral defensins with unique prodomains as novel candidates for development of *Fusarium* wilt resistance in transgenic banana plants. *PLoS ONE* 7(6): e39557. doi:10.1371/journal.pone.0039557.
6. Stotz, H.U., Spence, B. and Wang, Y. (2009). A defensin from tomato with dual function in defense and development. *Plant mol. Biol.*, 71: 131-43.
7. Allen, A., Synder, A.K., Preuss, M., Nieslsen, E.E., Shah, D.M. and Smith, T.J. (2008). Plant defensins and virally encoded fungal toxin KP4 inhibit plant root growth. *Planta*, 227: 331-9.
8. Ganapathi, T.R., Higgs, N.S., Balint-Kurti, P.J., Arntzen, C.J., May, G.D., and Van Eck, J.M. (2001). *Agrobacterium* -mediated transformation of the embryogenic cell suspensions of the banana cultivar Rasthali (AAB). *Plant Cell Rep.*, 20: 157-162.
9. Tavares, L.S., Santos, Mde. O., Viccini, L.F., Moreira, J.S. and Miller, R.N. (2008). Biotechnological potential of antimicrobial peptides from flowers. *Peptides*, 29: 1842-1851.
10. Lay, F.T. and Anderson, M.A. (2005). Defensins- Components of the innate immune system in plants. *Curr Prot Pept Sci.*, 6: 85-101.
11. Jha, S., Chattoo, B.B. (2010). Expression of a plant defensin in rice confers resistance to fungal phytopathogens. *Transgenic Res.*, 19:373-384.
12. Gao, A.G., Hakimi, S.M., Mittanck, C.A., Wu, Y., Woerner, B.M. Stark, D.M., Shah, D.M., Liang, J. and Rommens C.M.T. (2000) Fungal pathogen protection in potato by expression of a plant defensin peptide. *Nat Biotechnol.*, 18: 1307-1310.
13. Anderson, M.A., Heath, R.L., Lay, F.T. and Poon, S. (2009). Modified plant defensin. US patent application 2009, Application 20090083880.
14. Nielson, K.J., Hill, J.M., Anderson, M.A. and Craik, D.J. (1996). Synthesis and structure determination by NMR of a putative vacuolar targeting peptide and model of a proteinase inhibitor from *Nicotiana glauca*. *Biochem.*, 35: 369–378.
15. Hanks, J.N., Snyder, A.K., Graham, M.A., Shah, R.K., Blaylock, L.A., Harrison, M.J. and Shah, D.M. (2005). Defensin gene family in *Medicago truncatula*: structure, expression and induction by signal molecules. *Plant Mol Biol.*, 58: 385-99.

Direct Organogenesis and Plant Regeneration from Cotyledons of a Multipurpose Tree, *Acacia mangium* Willd.

M. Shahinozzaman*, M. O. Faruq, M. M. Ferdous, M. A. K. Azad and M. N. Amin
Plant Tissue Culture Laboratory, Department of Botany, University of Rajshahi, Bangladesh
*For Correspondence – mshahin81@gmail.com

Abstract

Using cotyledons of 2-week old *in vitro* germinated seedlings, a rapid and efficient regeneration protocol was established for *A. mangium* on Murashige and Skoog (MS) basal medium. Cotyledons showed better direct shoot organogenesis producing maximum 10.88 ± 0.35 shoots per explant when cultured on MS medium supplemented with 2.0 μM BA and 1.0 μM NAA. Full strength of MS medium supplemented with IBA (8.0 μM) was found best for rooting of *in vitro* shoots. The rooted plantlets were then transferred to small pots containing a sterilized mixture of sand, garden soil and compost (1:1:1) for acclimatization where plantlets grew well with 65% survival rate.

Key words: Direct organogenesis, cotyledon, multipurpose tree.

Introduction

Tissue culture propagation is a common technique, which has been applied extensively to many important forest tree species (1, 2). This technique exploits the regeneration capacity of the selected tissues, however, it is difficult to achieve in materials beyond the juvenile stage (3). Most of the investigations, on the development of protocols for tissue culture propagation of forest tree species, are concentrated on juvenile materials like seedling derived explants. Tissue culture propagation is said to be a viable method for producing numerous plants for reforestation, conventional breeding and mass propagation (4) and it has been practiced in many tree legumes such as,

Acacia albida (5), *A. auriculiformis* (6), *A. mangium* (7, 8, 9), *A. nilotica* (10), *A. sinuata* (11) and *A. tortilis* (12) etc. using different seedling derived explants.

A. mangium is one of the important leguminous trees having multipurpose uses in several fields, like furniture making, paper and pulp industries and cosmetics industries etc. As conventional methods have limited scope for large scale propagation of *A. mangium*, *in vitro* techniques are the crucial need for large scale propagation of this plant (13). Adventitious shoot regeneration from suitable explants is one of the desired *in vitro* techniques applied for large scale propagation of target plant species, which can be achieved through two different processes—direct and indirect. Indirect shoot regeneration implies regeneration of shoots via callus formation while direct shoot regeneration can occur directly from the explants without intermediate proliferation of undifferentiated tissues. In addition, indirect process for adventitious shoot regeneration may produce variation in next generation, which is the major drawback for clonal propagation. That is why direct shoot organogenesis is preferred over indirect process in case of several plant species. A few reports on direct adventitious shoot regeneration have been found in *Dalbergia sisso* (14), *Tamarindus indica* (15), *Leucaena leucocephala* (16) using seedling derived explants like hypocotyl, cotyledon, leaflet and petiole etc. But no such reports have been found in case of *A. mangium* yet. The present investigation elucidates rapid plant regeneration

in *A. mangium* through direct shoot organogenesis from cotyledon explants and successful establishment of plantlets under natural soil condition.

Materials and Methods

Establishment of in vitro seedlings and procurement of explants: Mature pods of *A. mangium* were collected from an elite tree grown in Rajshahi University campus, Bangladesh and seeds were removed carefully from pods. Seeds were then washed with continuous agitation in a few drops savlon (Chlorhexidine gluconate 0.3% w/v + cetrimide 3% w/v solution) containing water for 15 minutes. Washed seeds were pre-treated by immersing them in boiling water for 2-5 minutes followed by soaking in cold water for 20 minutes. The pre-treated seeds were then treated with 0.1 % HgCl₂ for 5 minutes under laminar air flow cabinet to disinfect them. Finally, seeds were washed 3 to 5 times with sterile distilled water to remove any trace of the sterilizing agent and were placed in culture tubes (25 × 150 mm) containing hormone free MS medium (17). Seedlings were categorized into four different groups viz. 10_≥, 14-15, 18-20 and 22_≤ days old depending on the age of seedlings after seed germination. Cotyledons were excised from four seedlings group separately.

Media and culture condition: MS medium was used in all experiments. The media were prepared with 3 % (w/v) sucrose and 0.8 % (w/v) agar (Sigma Chemical Co. USA). The pH of the medium was adjusted 5.7 ± 0.1 before autoclaving at 121 °C for 20 minutes at 1.2 kg/cm² pressure. All the cultures were maintained at 25 ± 2 °C under a 16h light and 8h dark cycle with the light intensity of 2000 – 3000 lux provided by cool-white fluorescent tubes (36W).

Induction of adventitious shoot organogenesis: Cotyledons excised from 10_≥ days old seedling group were delicate in nature while 22_≤ days old seedlings' derived cotyledons were mature and spontaneously detached from embryonal axis. Cotyledons excised from of all seedling groups were placed in adaxial (upper

surface facing down) orientation on MS medium containing different concentrations (1.0-8.0 μM) of 6-benzyl adenine (BA) alone or in combination with either 0.5-2.0 μM α-naphthalene acetic acid (NAA) or indole-3-butyric acid (IBA) to determine the optimum culture condition for direct shoot organogenesis. Cotyledons were placed on slanted medium surface in 25 × 150 mm culture tubes. After 4 weeks of incubation the explants were transferred to 200 ml conical flasks for multiplication and elongation of adventitious shoots. The percentage of shoot formation, total number of shoots and average length of shoots were recorded after 8 weeks of culture.

Root induction and acclimatization: Shoots having 2-3 leaves were isolated from multiple shoot clumps and transferred to two different strengths (full and half) of MS basal medium supplemented with 4.0, 6.0 and 8.0 μM IBA for root induction. The cultures were carefully examined in every week and the morphological changes were recorded on the basis of observations. Data were recorded on percentage of rooting, number of roots per culture and average length of roots after 4 weeks of incubation. Rooted plantlets were acclimatized in sterilized soil mix (sand, garden soil and compost in 1: 1: 1 ratio) and healthy plantlets were established in potting soils and transferred to the field condition.

Statistical analysis: One explant was implanted per culture and all experiments were repeated thrice with 10-15 replications per treatment. Data were submitted to ANOVA and the difference between the means was compared using Duncan's multiple range test (DMRT) at 5% probability level.

Results and Discussion

The seedling age, from which cotyledons were excised, showed a remarkable effect on direct shoot organogenesis. Among four different age categories of seedlings used as explant source, 14-15 days seedling derived cotyledons showed 100% response (Fig. 1a) producing

8.08 ± 0.81 shoot buds with average 2.71 ± 0.32 cm lengths (Table 1) followed by 18-20 days old seedling derived cotyledons. In addition, cotyledons procured from 14-15 days old seedlings formed adventitious shoot buds early. Cotyledons of 10_≥ days old seedlings were too juvenile to form shoot buds and it is likely that the cotyledons may absorb nutrients and growth regulators from the medium and then form a few shoot buds at late. On the other hand, cotyledons of 20_≤ days old seedlings were somehow beyond of juvenility and produced few shoots. This study revealed that cotyledons excised from 14-15 days old seedlings were suitable for direct adventitious shoot organogenesis in *A. mangium*. In *Dalbergia sissoo*, 8-10 days old *in vitro* seedling derived cotyledons produced adventitious shoots directly on MS medium (14).

Cotyledon explants lacking of the embryonal axis showed varied responses in terms of direct organogenesis, depending upon the concentration and combination of growth regulators (Table. 2). When BA was used as sole growth regulator, maximum number of shoots (3.87 ± 0.67) as well as longest shoots (2.32 ± 0.96) was found at 2.0 μM BA containing medium. Incorporation of auxin along with BA to the medium enhanced the frequency of shoot bud differentiation considerably. NAA was found to be more appropriate auxin in combination with

BA for direct shoot proliferation from cotyledons while IBA showed less activity. In this experiment 2.0 μM BA + 1.0 μM NAA was found as optimum growth regulator combination for direct shoot organogenesis, where 10.88 ± 0.35 shoots with 3.90 ± 0.23 cm length were produced at a faster rate (Fig. 1b and c). In all the cases, adventitious shoot buds were developed only from the proximal end of cotyledons and no bud was formed at the distal part as this part was also wounded during culture. Findings of this experiment are supported by a previous report on *Dalbergia sissoo* (14), where 0.26 μM NAA along with 4.44 μM BA enhanced shoot bud differentiation directly from the proximal region of cotyledons. In another reports on *Leucaena leucocephala* (16), it has been demonstrated that cotyledons produce adventitious shoots directly from the proximal end with forming callus at the base of cotyledons when transfer them from a pre-induction medium having high BA concentration to low BA containing medium. In addition, no shoot bud formation was found from the distal part of cotyledons of *L. leucocephala*. During this experiment, when cotyledons placed in adaxial (upper surface facing down) orientation on medium surface more adventitious shoot buds were produced from the cut margin of cotyledons (Data not shown). In tomato (18), cotyledons produced greater number as well as longest shoots when placed in abaxial (lower surface

Table 1. Effect of seedling age on direct shoot development from cotyledon explants cultured on MS medium supplemented with 2.0 μM BA + 1.0 μM NAA.

Age of seedlings (days)	% of explant produced shoots	Days to sprout adventitious shoot bud	Average No. of shoots/ culture	Average length of shoots/ culture (cm)
10 _≥	41.66 ± 4.48 ^c	15.29 ± 0.58 ^{ab}	1.66 ± 0.65 ^c	1.10 ± 0.40 ^b
14-15	100.00 ± 0.00 ^a	10.71 ± 0.92 ^c	8.08 ± 0.81 ^a	2.71 ± 0.32 ^a
18-20	98.33 ± 1.66 ^a	12.18 ± 0.39 ^{bc}	5.75 ± 0.59 ^b	1.55 ± 0.14 ^b
22 _≤	83.33 ± 3.76 ^b	16.12 ± 0.37 ^a	4.66 ± 0.82 ^b	1.25 ± 0.20 ^b

Values represent means ± standard error of 12 explants per treatment in three repeated experiments. The different letters within column show significant differences by ANOVA and Duncan's multiple range tests at p_≤0.05.

facing down) orientation on the medium surface, which is not in agreement to the present study.

The *in vitro* developed shoots from the cotyledon culture were separated carefully and transferred to full strength and half strength MS medium containing IBA at three different concentrations (4.0, 6.0 and 8.0 μM). Maximum number of roots (3.01 ± 1.37) were observed when micro-shoots were cultured on full strength medium having 8.0 μM IBA. In addition, longest shoots were also found on full strength MS medium augmented with 6.0 μM IBA. Full strength MS medium was found to be best for root induction in *A. mangium*. Out of three concentrations of IBA tested, best rooting was recorded at 8.0 μM (Fig. 1d). In another report

(13), we suggested 8.0 μM IBA as better auxin concentration for *in vitro* rooting of *A. mangium*. The present studies corroborate the findings of several previous works where full strength MS medium containing different concentrations of auxins was found appropriate for rooting in *Acacia mangium* (9, 19, 20, 21, 22); *Acacia auriculiformis* (23); *Acacia koa* (24); *Acacia saligna* (25); *Acacia mearnsii* (26); *Acacia sinuata* (27); *Acacia chundra* (28) and *Acacia catechu* (29). The *in vitro* regenerated rooted plantlets were washed with sterile water and transferred to small plastic pots containing sand, garden soil and compost (1: 1: 1) mixture. Then the plants were maintained under culture room conditions (Fig. 1e) for three weeks. The regenerated plants were transferred to the soil with 65% survival rate.

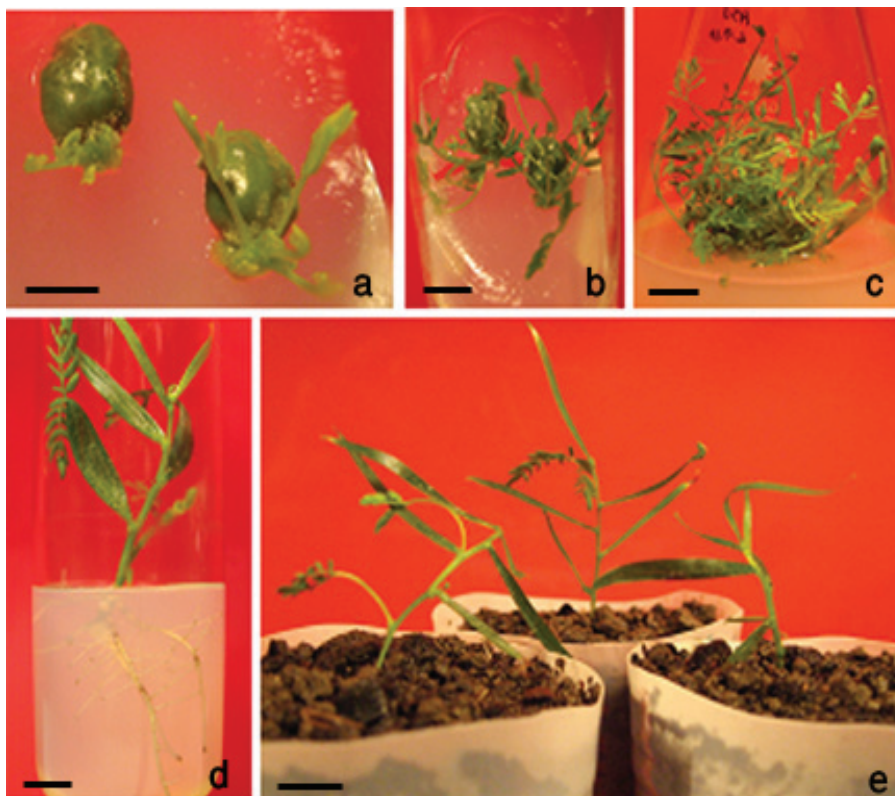


Fig. 1. *In vitro* regeneration of *A. mangium* Willd. from cotyledon explants. a-b. Adventitious shoot formation from the cut margin of cotyledons after 2 weeks and 4 weeks of culture respectively. c. Development and multiplication of shoots after 8 weeks of culture. d. Rooting of *in vitro* regenerated shoots in four weeks. e. Plantlets growing on the soil mixture under culture room conditions after 10 days of transfer. (bar = 5 mm)

Table 2. Effect of plant growth regulators on direct adventitious shoot formation from cotyledon explants of *A. mangium*.

Plant growth regulators (μm)	Mean no. of shoots per explant	Mean length of shoots (cm)
BA		
1.0	1.20 \pm 0.80 ^f	0.99 \pm 0.41 ^{cd}
2.0	3.87 \pm 0.67 ^{cde}	2.32 \pm 0.96 ^{abcd}
4.0	2.20 \pm 0.96 ^{ef}	2.16 \pm 0.91 ^{abcd}
6.0	1.20 \pm 0.29 ^f	0.78 \pm 0.29 ^d
8.0	0.80 \pm 0.80 ^f	0.84 \pm 0.31 ^{cd}
BA + NAA		
1.0 + 0.5	4.12 \pm 0.51 ^{cde}	2.69 \pm 0.26 ^{abc}
1.0 + 1.0	3.25 \pm 0.36 ^{cde}	1.65 \pm 0.18 ^{bcd}
1.0 + 2.0	1.37 \pm 0.32 ^f	1.21 \pm 0.22 ^{cd}
2.0 + 0.5	7.25 \pm 0.65 ^{bc}	3.25 \pm 0.47 ^{ab}
2.0 + 1.0	10.88 \pm 0.35 ^a	3.90 \pm 0.23 ^a
2.0 + 2.0	3.08 \pm 0.81 ^{de}	1.78 \pm 0.56 ^{bcd}
4.0 + 0.5	6.75 \pm 0.61 ^{bcd}	2.16 \pm 0.32 ^{abcd}
4.0 + 1.0	8.37 \pm 0.73 ^{ab}	1.72 \pm 0.16 ^{bcd}
4.0 + 2.0	2.56 \pm 0.75 ^f	1.52 \pm 0.45 ^{bcd}
BA + IBA		
1.0 + 0.5	3.12 \pm 0.51 ^{de}	2.05 \pm 0.64 ^{bcd}
1.0 + 1.0	2.37 \pm 0.80 ^{ef}	1.60 \pm 0.53 ^{bcd}
1.0 + 2.0	1.37 \pm 0.67 ^f	1.20 \pm 0.61 ^{cd}
2.0 + 0.5	3.62 \pm 0.53 ^{cde}	2.14 \pm 0.52 ^{abcd}
2.0 + 1.0	6.12 \pm 0.81 ^{bcd}	2.16 \pm 0.52 ^{abcd}
2.0 + 2.0	1.62 \pm 0.44 ^f	1.14 \pm 0.57 ^{cd}
4.0 + 0.5	3.87 \pm 0.61 ^{cde}	2.13 \pm 0.71 ^{abcd}
4.0 + 1.0	3.50 \pm 0.73 ^{cde}	1.93 \pm 0.73 ^{bcd}
4.0 + 2.0	1.12 \pm 0.34 ^f	0.69 \pm 0.46 ^d

Values represent means \pm standard error of 15 explants per treatment in three repeated experiments. The different letters within column show significant differences by ANOVA and Duncan's multiple range tests at $p \leq 0.05$.

Table 3. Effect of IBA along with two different nutrient formulations (MS & MMS₁) on rooting of *in vitro* regenerated micro-shoots of *A. mangium*.

Auxin (IBA) concentration (µM)	Nutrient formulations ^a	Mean no. of roots/culture	Mean length of roots/culture (cm)
4.0	MS	2.48 ± 1.01 ^{bc}	1.89 ± 0.97 ^a
6.0	MS	2.51 ± 1.18 ^{ab}	2.11 ± 1.03 ^a
8.0	MS	3.01 ± 1.37 ^a	1.79 ± 0.87 ^a
4.0	MMS ₁	2.19 ± 1.39 ^{bc}	1.15 ± 0.95 ^b
6.0	MMS ₁	2.08 ± 0.89 ^{bc}	1.02 ± 0.92 ^b
8.0	MMS ₁	1.73 ± 0.63 ^{cd}	0.89 ± 0.28 ^{bc}

Values represent means ± standard error of 15 explants per treatment in three repeated experiments. The different letters within column show significant differences by ANOVA and Duncan's multiple range tests at p≤0.05.

^aMS = Full strength MS medium; MMS₁ = MS with ½ strength of major salts only

Thus it is concluded that cotyledons of 2-week old *A. mangium* seedlings is appropriate for direct shoot organogenesis, which produce maximum number of shoots via direct organogenesis on MS medium having 2.0 µM BA and 1.0 µM NAA. Hence, *A. mangium* can successfully be multiplied or conserved *in vitro* by using MS medium augmented with a combination of BA (2.0 µM) - NAA (1.0 µM) for acquiring the highest level of direct shoot multiplication, while 8.0 µM IBA in the same medium found precise for root induction.

References

- Bonga, J.M. and von Aderkas, P. (1992). *In vitro* culture of trees. Kluwer Academic Publ, Dordrecht, The Netherlands, pp 236.
- Ahuja, M.R. (1993). Micropropagation of woody plants. Kluwer Academic Publ., Dordrecht. The Netherlands, pp 507.
- Yasodha, R., Sumathi, R. and Gurumurthi, K. (2004). Micropropagation for quality propagule production in plantation forestry. Indian J. Biotech. 3: 159-170.
- Ortiz, B.O.C., Reyes, M.E.P. and Balch, E.P.M. (2000). Somatic embryogenesis and plant regeneration in *Acacia farnesiana* and *Acacia schaffneri*. *In Vitro Cell. Dev. Biol.-Plant*. 36: 268-272.
- Duhoux, E. and Davies, D. (1985). Shoot Production from cotyledonary buds of *Acacia albida* and influence of sucrose on rhizogenesis. *J. Plant Physiol*. 125: 175-180.
- Mittal, A., Agarwal, R. and Gupta, S.C. (1989). *In vitro* development of plantlets from axillary buds of *Acacia auriculiformis*- a leguminous tree. *Plant Cell Tiss. Org. Cult*. 19: 65-70.
- Ahmad, D.H. (1991). Micropropagation of *Acacia mangium* from aseptically germinated seedlings. *J. Trop. Forest Sci*. 3 (3): 204-208.
- Douglas, G.C. and McNamara, J. (2000). Shoot regeneration from seedling explants of *Acacia mangium* Willd. *In Vitro Cell. Dev. Biol*. 36 (5): 412-415.
- Galiana, A., Tibok, A. and Duhoux, E. (1991). *In vitro* propagation of the nitrogen fixing tree- legume *Acacia mangium* Willd. *Plant and Soil* 135: 151-159.
- Dewan, A., Nanda, K. and Gupta, S.C. (1992). *In vitro* micropropagation of *Acacia nilotica* subsp. *indica* Bernan via Cotyledonary nodes. *Plant Cell Rep*. 12: 18-21.

11. Vengadesan, G., Ganapathi, A., Prem, R. and Anbazhagan, V.R. (2002). *In vitro* propagation of *Acaica sinuata* (Lour.) Merr. via cotyledonary nodes. *Agroforestry systems* 55: 9-15.
12. Nangia, S. and Singh, R. (1996). Micropropagation of *Acacia tortilis* Hayne (Umbrella thorn) through cotyledonary node culture. *Indian J. Exp. Physiol.* 1(2): 77-79.
13. Shahinozzaman, M., Azad, M.A.K. and Amin, M.N. (2012). *In vitro* clonal propagation of fast growing legume tree-*Acacia mangium* Willd. Employing cotyledonary node explants. *Not Sci Biol.* 4 (2): 79-85.
14. Singh, A.K., Chand, S., Pattanaik, S. and Chand, P.K. (2002). Adventitious shoot organogenesis and plant regeneration from cotyledons of *Dalbergia sissoo* Roxb., a timber yielding tree legume. *Plant Cell Tiss. Org. Cult.* 68: 203-209.
15. Sonia, Jaiwal, P.K., Gulati, A. and Dahiya, S. (1998). Direct organogenesis in hypocotyl cultures of *Tamarindus indica*. *Biol. Plant.* 41 (3): 331-337.
16. Saafi, H. and Borthakur, D. (2002). *In vitro* plantlet regeneration from cotyledons of the tree-legume *Leucaena leucocephala*. *Plant Growth Reg.* 38: 279-285.
17. Murashige, T. and Skoog, F. (1962). A revised medium for rapid growth and bioassay with tobacco tissue culture. *Physiol. Plant.* 15: 473-497.
18. Poonam, B., Ashwath, N. and Minmore, D.J. (2005). Effects of genotype, explant orientation and wounding on shoot regeneration in tomato. *In Vitro Cell. Dev. Biol.-Plant* 41: 457-464.
19. Darus, H.A., Thompson, S. and Pirre, A. (1991). Vegetative propagation of *Acacia mangium* by stem cuttings, the effect of seedling age and phyllode number on rooting. *Journal of Tropical Science, Forest Research Institute, Malaysia.* 2 (4): 224-279.
20. Bhaskar, P. and Subhash, K. (1996). Micropropagation of *Acacia mangium* Willd. through nodal bud culture. *Ind. J. Exp. Biol.* 34: 590-591.
21. Toda, T., Tajima, M. and Brini, P.B. (1995). Tissue culture of *Acacia mangium*, *A. auriculiformis* and their hybrid. *Bull. Nation. For. Tree. Breed. Centre* 13: 157-165.
22. Nanda, R., Das, P. and Rout, G.R. (2004). *In vitro* clonal propagation of *Acacia mangium* Willd. and its evaluation of genetic stability through RAPD marker. *Ann. For. Sci.* 61: 381-386.
23. Das, P.K., Chakravarti, V. and Maity, S. (1993). Plantlets formation in tissue culture from cotyledon of *Acacia auriculiformis* A. Cunn. ex Benth. *Indian Journal of Forestry.* 16: 189-192.
24. Skolmen, R.G. and Mapes O.M. (1976). *Acacia koa* gray plantlets from somatic callus tissue. *Journal of Heredity.* 67: 114-115.
25. Barakat, M.N. and El-Lakany, M.H. (1992). Clonal propagation *Acacia saligna* by shoot tip culture. *Euphytica.* 59: 103-107.
26. Huang, F.H., Al-Khayri J.M. and Gbur, E.E. (1994). Micropropagation of *Acacia mearnsii*. *In Vitro Cellular Developmental Biology-Plant.* 30: 70-74.
27. Vengadesan, G., Ganapathi, A., Anand R.P. and Anbazhagan, V. R. (2002). *In vitro* propagation of *Acacia sinuata* (Lour.) Merr. via cotyledonary nodes. *Agroforestry Systems.* 55: 9-15.
28. Rout, G.R., Senapati and Aparajeta, S.K.S. (2008). Micropropagation of *Acacia chundra* (Roxb.) DC. *Horticultural Science.* 35(1): 22-26.
29. Kaur, K., Verma, B. and Kant, U. (1998). Plants obtained from the khair tree (*Acacia catechu* Willd.) using mature nodal explants. *Plant Cell Rep.* 17: 421-429.

Production and Characterization of Extracellular L-asparaginase from Estuarine Actinomycetes Species by Submerged Fermentation Process

Koteswara Rao Chinta¹, J. Srinivasa Rao^{2*}, Pulipati King³, P. Jawahar Babu²,
M. V. V. Chandana Lakshmi¹ and Ch. V. Ramachandra Murthy³

¹Centre for Biotechnology, Department of Chemical Engineering, A. U. College of Engineering (A),
Andhra University, Visakhapatnam-530003.

²Department of Biotechnology, Bapatla Engineering College, Bapatla-522 101

³Department of Chemical Engineering, A. U. College of Engineering (A),
Andhra University, Visakhapatnam-530003.

*For correspondence - jsrbec@gmail.com

Abstract

Actinomycetes were isolated from different estuarine sediments in the regions of Bay of Bengal off shores from Parawada to Visakhapatnam, India for extracellular L-asparaginase production. 5 different samples, 20 Actinomycetes strains were isolated. Among them 5 strains showing pink colour zones with high intensity were selected for the production of L-asparaginase. Out of 5 Actinomycetes, Strain PW-A12 shows maximum L-asparaginase activity with a yield of 3.933 IU/ml for 24 hrs Submerged Fermentation time. Further, optimizations of parameters were conducted with the strain PW-A12, by consecutive evaluation method. Maximum enzyme production with a yield of 5.73 IU/ml was observed with 4% peptone at pH 7.5. Reduced enzyme production was observed (5.6 IU/ml) while using on Yeast extract concentration of 1.2 gm /100 ml (w/v) and at a pH of 7.0 found to be optimal culture condition by the strain *Streptomyces* species PW-A12 by submerged fermentation Process. Hence the present study indicated a scope for exploring estuarine Actinomycetes as a source for extracellular L-asparaginase production.

Key words: Estuarine Actinomycetes, estuarine sediments, L-asparaginase, *Streptomyces* species.

Introduction

Actinomycetes are Gram-positive bacteria which grow typically in the form of branched elongated cells or branched filaments. Most genera form is an extensive mycelium which in some cases fragments into coccoid or rod shaped elements. Certain genera occur as individual branched cells and seldom produce a mycelium (1). Actinomycetes have been shown to be a good source for L-asparaginase too. L-asparaginase (L-asparagine amido hydrolase, E.C.3.5.1.1) has been widely used as a therapeutic agent in the treatment of certain human cancers, mainly in acute lymphoblastic leukemia (2). There are some basic differences between normal and malignant cells e.g. tumour cells have lost the capability to synthesize L-asparagine, as a result they depend on its supply from the blood. L-asparaginase is an enzyme that hydrolyzes asparagine and if administered into the blood stream, it converts blood asparagines into aspartic acid. Normal cell circumvents this problem since they synthesize asparagines required for their growth and maintenance. The cancerous cells exhaust all external asparagines rapidly and ultimately die due to starvation (3). The production of L-asparaginase has been studied in *Streptomyces griseus* (4), *Streptomyces* strains (PDK2, PDK7) (5), *Streptomyces aurantiacus* (6), *Streptomyces*

albidoflavus (7), *Streptomyces* strains S3, S4 and K8 (8), *Streptomyces gulbargensis* (9), *Streptomyces noursei* MTCC 10469 (10), *Streptomyces* ABR2 (11). Among the various sources of L-asparaginase, actinomycetes are the least studied organisms. In the present study an attempt was made for the first time on the production and characterization of an extra-cellular L-asparaginase, under submerged fermentation from estuarine Actinomycetes species.

Materials and Methods

Sample collection: A total of five estuarine sediments samples were collected for the isolation of marine Actinomycetes. The five sediment samples were collected at a depth of 1 to 10 centimetres at 2.5 to 9 km off shores Parawada coast of Bay of Bengal. The texture of the samples colour was sandy with brown to blackish in colour. The estuarine sediment samples were collected and stored in sterilized bags.

Media: The media used to isolate Actinomycetes from the estuarine samples are; Potassium tellurite agar medium: Potassium tellurite: 0.1gm, Peptone: 5.0gm, Yeast extract: 2.5gm, Agar: 20gm, D.W: 1lit, pH: 6.4 and Starch- casein agar medium: Soluble starch: 10gm, Casein: 0.3gm, KNO₃: 2gm, NaCl: 10gm, K₂HPO₄: 2gm, MgSO₄.7H₂O: 0.05gm, CaCO₃: 0.02gm, FeSO₄.7H₂O: 0.01gm, Agar: 20gm, D.W: 1.0lit, pH: 7.0.

Isolation and screening: Different Estuarine sediments samples were serially diluted in sterile distilled water under aseptic conditions. Actinomycetes were isolated from estuarine sediments by plating them on Starch casein agar media with different dilutions and Incubated at 30°C for 5th day and up to three weeks. Rifampicin (12) (2.5 µg/ml) and Cyclohexamide (50 µg/ml) added to medium to inhibit bacterial and fungal contamination. After 5th day to three weeks, suspected Actinomycete colonies were identified based on their morphological characteristics. The selected Actinomycetes are

shown in Table 1. The isolated Actinomycetes were maintained as slant culture on yeast extract malt extract agar medium.

Table 1. Distribution of Actinomycetes from estuarine sediments samples.

Sample No.	No. of colonies	No. of Actinomycetes isolated	No. of active isolates	Batch
PW-01	22	7	6	Batch PW-A
PW-02	14	5	2	
PW-03	66	3	1	Batch PW-B
PW-04	6	5	2	

(PW-Parawada, PW-A, PW-F- Batch number)

Screening of estuarine isolates for L-asparaginase production by rapid plate assay:

The estuarine isolates were screened for L-asparaginase activity using the method of Gulati *et al.*, (13). The medium used were modified M-9 (composition in g/l: KH₂PO₄ - 2.0, L-asparagine -6.0, MgSO₄.7H₂O - 1.0, CaCl₂.2H₂O - 1.0, glucose - 3.0, and agar - 20.0) supplemented with phenol red as a pH indicator. L-asparaginase activity was identified by formation of a pink zone around colonies.

L-asparaginase production by submerged fermentation:

Different mediums (Table 2) were used for the production of L-asparaginase from Positive estuarine Actinomycetes was carried out by submerged fermentation.

Determination of enzyme activity: The crude enzyme was prepared by cooling centrifuge at 14,000 rpm for 20 min. The supernatant was taken as the crude enzyme. The enzyme activity was determined according to the method of Imada *et al.* (14), where the liberated ammonia to the action of enzyme was estimated using Nessler's reagent. A reaction mixture containing 0.5 ml of 0.04 M L-asparagine, 0.5 ml of 0.5 M buffer, 0.5 ml of an enzyme preparation, and distilled water to a total volume of 2.0 ml incubated at 37°C for 30 min. The reaction stopped by adding 0.5 ml of 1.5 M trichloroacetic

acid. Blank tubes were run by without enzyme and control tubes were run by adding the enzyme preparation after the addition of trichloroacetic acid. 3.7 ml of distilled water, 0.1 ml of the above mixtures and 0.2 ml of Nessler's reagent were added and after keeping the mixture at 15 to 20°C for 20 min, extinction at 450 nm measured with a Spectrophotometer and the amount of released ammonia determined. One international unit (i.u.) of L-asparaginase is the amount of enzyme which liberates 1 μmol of ammonia in 1 min at 37°C.

Table 2. Different medium Composition for production of L-asparaginase

Medium	Composition
Tryptone Glucose Yeast extract (TGY) broth (100ml)	Glucose, 0.1g; K ₂ HPO ₄ , 0.1 g; Yeast extract, 0.5 g; Tryptone, 0.5 g; pH 7.0.
Tryptone Fructose Yeast extract (TFY) broth (100ml)	Tryptone, 0.5 g; yeast extract, 0.5 g; fructose, 0.1 g; potassium dihydrogen phosphate, 0.1g; pH 7.0
Yeast malt glucose (YMG) broth (100ml)	glucose, 0.4; yeast extract, 0.4 g; malt extract, 1g; pH 7.0
Yeast malt (YM) broth (100ml)	Yeast extract, 0.4 g; Malt extract, 1 g; pH 7.0
4% peptone broth(100ml)	yeast extract, 1g; Bactopeptone, 4g; pH 7.0

Strain identification of selected organism

Morphological and physiological characterization: The selected isolate *Streptomyces* species was inoculated on Starch Casein Agar and incubated at 30°C for 7-10 days to get maximum sporulation. The colours of aerial mycelium, substrate mycelium and soluble pigment when grown on different media were observed and recorded. The macro and micro-

morphological features of the colonies and the colour determinations of the aerial mycelium; substrate mycelium and soluble pigment were examined after 14 days of incubation. Macro morphology was noted by the naked eye and by observation with magnifying lens. The morphological studies and colour determinations of the selected isolates were studied by following the International *Streptomyces* Project (ISP) procedure (15). The following media as recommended by ISP were used for the morphological studies and colour determinations. Yeast extract malt extract agar (ISP-2), Oat meal agar (ISP-3), Inorganic salts starch agar medium (ISP-4), Glycerol asparagines agar medium (ISP-5)

Biochemical characterization: Various biochemical reactions were performed for the identification of the select isolate (*Streptomyces* species) determined employing the prescribed media: melanin formation (15), H₂S production (15), tyrosine reaction (15), carbon source utilization (15), gelatine hydrolysis (16), coagulation and peptonization of milk (17), casein hydrolysis (17), starch hydrolysis (17), nitrate reduction (17), ability to produce antibiotic factors (18), sodium chloride tolerance (19), effect of various nitrogen sources on growth (18), growth temperature range (18) and chemical tolerance (18) by inoculating the isolate in ISP broth supplemented respective sugars and incubated for 7 day at 30°C.

Optimization of process parameters for production of L-asparaginase: Various fermentation parameters that influence the enzyme production during submerged fermentation were optimized over a wide range. The strategy adopted for standardization of fermentation parameter to evaluate the effect of an individual parameter and incorporate it at standard level before standardizing. Incubation time: The production medium flasks were inoculated with 3 ml of 24 hrs seed culture and incubated for 6, 12, 18, 24, 30, 36, 42, 48 and 54 hrs at 37°C; Incubation temperature: The

production medium flasks were inoculated with 3ml of 24 hrs seed culture and incubated at 32, 35, 36, 37 and 39°C; pH: To find out optimum pH for production of L-asparaginase, the pH of the production medium varies as 5.0, 5.5, 6.0, 6.5, 7.0, 7.5, 8 and 8.5, sterilized and incubated with the seed culture (3 ml) followed by incubation at 37°C for 36 hrs; Inoculum volume: To determine the optimum amount of inoculum required to utilize the maximum amount of substrate for the production of maximum amount of L-asparaginase. The seed culture added to production medium in 1, 2, 3, 4, 5 and 6 ml and incubated at 37°C for 36 hrs; Concentration of yeast extract: To determine the effect of yeast extract concentration on L-asparaginase production, the production medium prepared with concentrations of 0.4, 0.6, 0.8, 1.0, 1.2, 1.4, 1.6

and 1.8 gm/100 ml. The flasks were sterilized, inoculated with 3ml of the seed culture and incubated at 37°C and analyzed.

Results and Discussion

Characterization of the isolate PW-A12

Micro-morphology: The sporophores occurred as short open spirals with 2 to 4 turns. The sporophores are arranged in groups formed open spiral spore chains, which belongs to section “spira (S)”.

Physiological and biochemical properties: The cultural characteristics, physiological and biochemical properties, carbon source utilization pattern, antimicrobial spectrum, growth in the presence of various nitrogen sources, resistance or sensitivity of the isolate PW-A12 are shown in Tables 3 and 4.

Table 3. Cultural characteristics of isolate PW-A12.

Medium	Cultural characteristics
Yeast extract- malt extract agar (ISP-2)	G*: good, wrinkled colonies AM*: white to gray R*: thick yellowish brown SP*: none
Oat meal agar (ISP-3)	G: moderate, convex colonies AM: white to gray R: _____ SP: none
Inorganic salt-starch agar (ISP-4)	G: moderate, convex colonies AM: white to gray R: _____ SP: none
Glycerol- asparagines agar (ISP-5)	G: good, very compact colonies AM: white to gray R: light sand dunes SP: blackish brown.
Starch-casein agar	G: good AM: white to gray R: light brown (light sand dunes) SP: None

G* = Growth, AM* = aerial mycelium, R* = reverse colour, SP*: soluble pigment

Table 4. Physiological and Biochemical properties of isolate PW-A12.

Reaction	Response	Result
1) Melanin reaction on Medium ISP-1 Medium ISP-6 Medium ISP-7	No growth in the medium Light almond sand colour (light brownish colour)Light bottled olives colour (light brownish colour)	Negative Positive Positive
2) H ₂ S production Medium ISP-6	4 th day 15 th day Light brownish colour Light brownish colour	Positive
3) Tyrosine reaction Medium ISP-7	Light brownish colour Light brownish colour	Positive
4) Starch hydrolysis	HZ/GZ=16mm/8mm	Positive
5) Casein hydrolysis	HZ/GZ=32mm/14mm	Positive
6) Gelatin hydrolysis	HZ/GZ=0.0mm/8mm	Negative
7) Milk-coagulation and peptonization	Coagulation followed by peptonization	Positive
8) Nitrate reduction	Pink colour Formation	Positive
9) Growth temperature range a) 10°C b) 20°C c) 28°C d) 30°C e) 32°C f) 37°C g) 40°C	- - + + ++ +++ ++	Growth from 28-40°C Good Growth at 37°C
10) Chemical tolerance (pH range)	6.0 to 8.0	good growth at 6.5

(- No growth, + poor growth, ++ moderate growth, +++ good growth)

Screening programme for L-asparaginase producing isolates:

A total of 20 colonies were isolated from all the samples eliminating those that appear close to each other and 10 isolates showing pink colour zones were chosen. The isolate which is showing the highest pink colour zone has been chosen as the best isolate (Fig. 5) for the production and optimization of L-asparaginase by submerged fermentation.



Fig. 5. A rapid plate assay for screening L-asparaginase producing Actinomycetes (Batch PW-A: Strains 10-12).

Media screening: The selected one was isolated and used for L-asparaginase production in five different mediums i.e. Tryptone Glucose Yeast extract (TGY) broth, Tryptone Fructose east extract (TFY), Yeast malt glucose (YMG) broth, Yeast malt (YM) broth and 4% peptone broth in 37°C and at 200 rpm. They are analyzed for the L-asparaginase production potentiality for 24 hrs incubation period. After incubation period they are transferred to 2 ml centrifuged tubes & centrifuged and supernatant liquid was taken, L-asparaginase assay was prepared from the supernatant liquid (14). The obtained results noted in the Fig. 6.

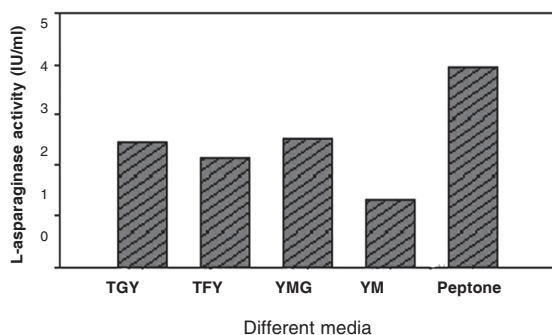


Fig. 6. Media screening for L-asparaginase activity

Optimization of parameters

Effect of incubation time on production of L-asparaginase: Experiments were conducted with the selected media viz. 4% peptone for a period of 54 hrs at regular intervals of 6 hrs to evaluate the optimum time of fermentation for the enzyme production and the results were shown in Fig. 7. It can be concluded that the accumulation of maximal L-asparaginase production (4.8 IU/ml) is observed at 36 hrs. Fermentation beyond 36 hrs showed a decrease in enzyme production, which could be either due to the inactivation of the enzyme because of the presence of some kind of proteolytic activity or the growth of the organism might have reached a stage from which it could no longer balances its steady growth with the availability of nutrient resources.

Effect of temperature on L-asparaginase production: Fermentation carried out at various temperatures such as 32, 35, 36, 37 and 39°C to study their effect on enzyme production. Results were presented in Fig.7 indicating that maximum enzyme production (4.833 IU/ml) was obtained when SMF was carried out at 36°C. However, the enzyme production reduced gradually with further incubation temperature above 37°C. This may be due to the denaturation of microbial strain at high temperatures.

Effect of inoculum volume on production of L-asparaginase: Fermentation carried out with different inoculum volumes (1-6 ml) for a period of 48 hrs to study its effect on L-asparaginase production. The maximum enzyme production (5.366 IU/ml) was obtained with 2 ml of 1 day seed culture of *Streptomyces* species. as shown in Fig. 7. If inoculum volume is further increased then gradually there is a decrease in the production of enzyme and microbial activity which might be attributed to the nutrient limitations necessary for product formation or accumulation of some non-volatile self inhibiting substances.

Effect of pH on L-asparaginase production: Experiments were performed to optimize pH in order to maintain the favourable conditions for the increase in the production of L-asparaginase. This is established by carrying out the fermentation by varying the pH from 5-8.5. The profound effect of initial pH of the fermentation on L-asparaginase production was shown in Fig. 7 and the maximum L-asparaginase activity (5.73 IU/ml) was recorded at pH 7.5. A further increase in pH results the gradual decrease of L-asparaginase activity due to denaturation or inactivation of the microbial strain.

Effects of yeast extract concentration on production of L-asparaginase: Since Yeast extract is the substrate of L-asparaginase, the addition to fermentation medium might stimulate enzyme production. Hence, fermentation was carried out with different concentrations of yeast extract ranging from 0.4-1.8 (% w/v) for a period

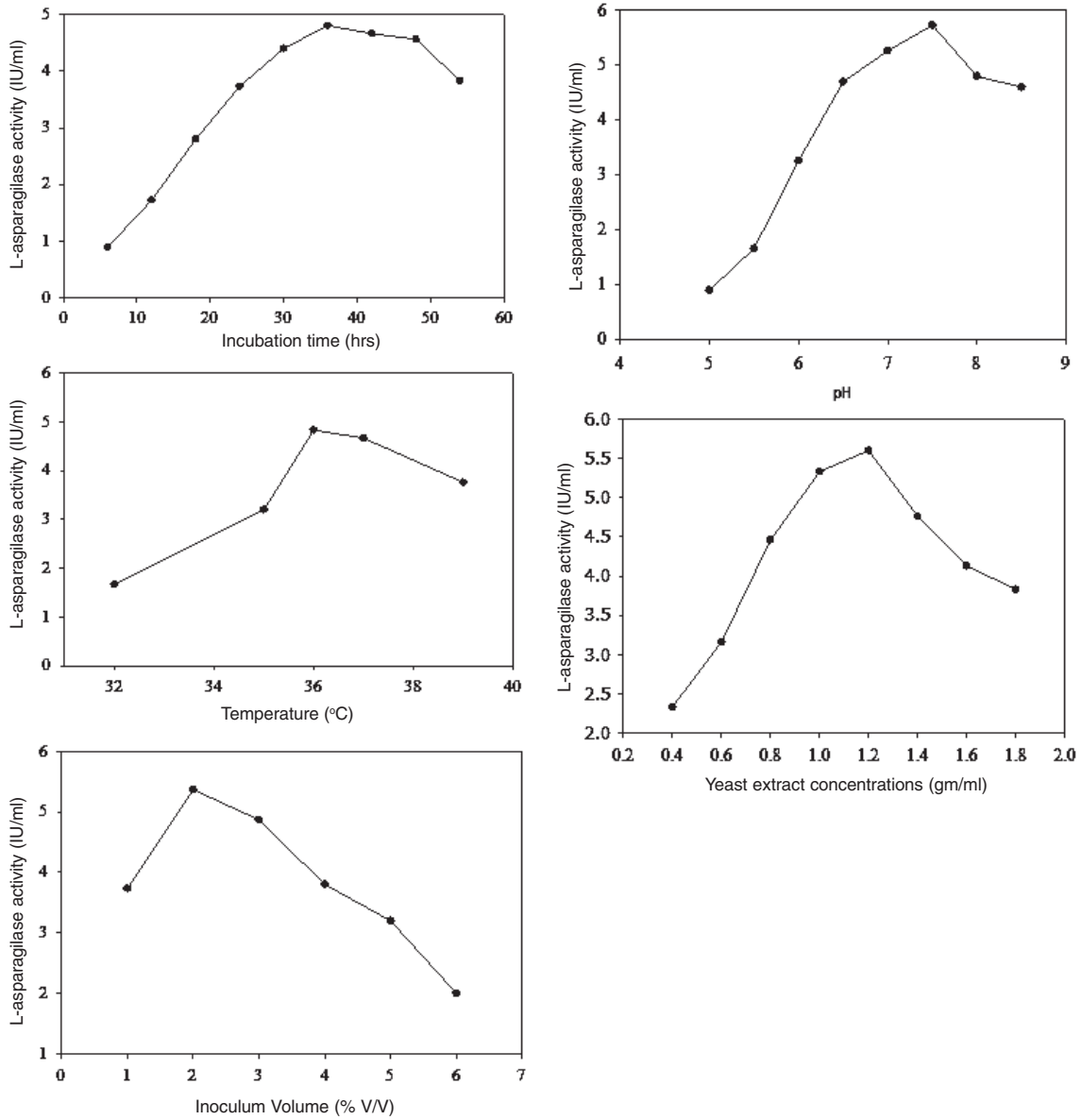


Fig. 7. Effect of Incubation time, Temperature, Inoculum volume, pH and Yeast extract concentration on L-asparaginase production

of 48 h to study its effect on L-asparaginase production. The maximum enzyme production (5.6 U/ml) was observed with 1.2 (% w/v) as shown in Fig. 7. Further increase in L-asparaginase concentration resulted in the decrement of enzyme production.

Discussions for isolation of *Streptomyces species strain*:

The strain grows well on most of the media. The sporophores occurred as spiral spore chains. The aerial mycelium developed moderately to good on most of the media and is gray in colour. The vegetative of the mycelium white to gray is almost dependent on media. The strain is non-chromogenic without any characteristic diffusible pigment and it produces soluble pigment. The strain H₂S and Tyrosinase reactions are positive. It showed moderate diastatic activity and showed a good proteolytic activity by hydrolyzing casein and starch. This strain PW-A12 is capable of coagulating and peptonizing the milk. It exhibits positive nitrate reduction. It grows well at 37°C. It tolerated the pH levels 6.5-7.5 good growth. It exhibited good growth on glucose, sucrose, Inositol, D-mannitol, D-fructose, lactose, maltose and Galactose. It showed poor to moderate growth on L-arabinose, D-xylose and cellulose. It exhibited good antibacterial activity. It exhibited good growth on L-arginine, L-cysteine and potassium nitrate. Moderate growth is on L-asparagine, L-histidine, and L-valine containing medium. Poor growth is on tyrosine containing medium.

Summary and Conclusion

Enzymes used for therapeutic purposes, cover a wide range of disease and conditions viz. inborn errors of metabolism, cancer, blood clotting deficiency etc. L-Asparaginase (E.C.3.5.1.1, L-Asparagin Amido hydrolase) used alone or in combination with other drugs is finding increased success in the management of childhood lymphoblastic leukaemia. Keeping the potential of this particular enzyme in cancer treatment, the present work is planned with 5 different estuarine sediment samples, 20 Actinomycetes strains were isolated. Among

them 5 strains showing pink colour zones with high intensity were selected for the production of L-asparaginase. Out of 5 Actinomycetes strains PW-A12, 4th strain exhibited maximum L-asparaginase activity with a yield of 3.933 IU/ml for 24 hrs Submerged Fermentation time. Further, optimizations of parameters were conducted with the strain PW-A12, by consecutive evaluation method. Maximum enzyme production with a yield of 5.73 IU/ml was observed with 4% peptone at pH 7.5. Reduced enzyme production was observed (5.6 IU/ml) while using on Yeast extract concentration of 1.2 gm / 100 ml and at a pH of 7.0. After optimization, the production of L-asparaginase increased by 1.45 times. The results of the present study indicated a scope for exploring estuarine Actinomycetes as a source for extracellular L-asparaginase, an enzyme that has gained industrial and pharmaceutical significance.

References

1. Goodfellow, M. and Cross, J. (1973). Taxonomy and classification of the actinomycetes. In: G. Sykes and FA Skinner (eds.), Actinomycetes, Characteristics and practical Importance. Academic Press, London and New York. 11-112.
2. Verma, N., Kumar, K., Kaur, G. and Anand S. (2007). L-asparaginase: a promising chemotherapeutic agent. Crit. Rev. Biotechnol., 27(1): 45-62.
3. Tek, C.B., Monica, S. and Nitya, N.S. (2007) "Microbial production of Flavours and fragrances; Fats and oils; Dyes; Bioplastics (PHAs); Polysaccharides; Pharmacologically active substances from marine microbes; Anti-cancer agents and Microbial biotransformation", Applied Microbiology.
4. Peter, J.D. (1972) L-Asparaginase production by *Streptomyces griseus*, Appl Microbiol, 23: 1163-1164.
5. Dhevagi, P. and Poorani, E. (2006). Isolation and characterization of L-

- asparaginase from marine actinomycetes. *Ind J Biotech*, 5:514-520.
6. Gupta, N., Mishra, S. and Basak, U.C. (2007). Occurrence of *Streptomyces aurantiacus* in mangroves of Bhitarkanika. *Malaysian J Microbiol*, 3:7-14.
 7. Narayana, K.J.P., Kumar, K.G. and Vijayalakshmi, M. (2008). L-asparaginase production by *Streptomyces albidoflavus*. *I J Microbiol*, 48(3):331-336.
 8. Basha, N.S., Rekha, R., Komala, M. and Ruby S. (2009). Production of extracellular antileukaemic enzyme L-asparaginase from marine actinomycetes by solid state and submerged fermentation: purification and characterisation. *Trop J Pharm Res* 8:353-360.
 9. Amena, S., Vishalakshi, N., Prabhakar, M., Dayanand, A. And Lingappa, K. (2010). Production, Purification and Characterization of L-asparaginase from *Streptomyces gulbargensis*. *Brazilian Journal of Microbiology*, 41: 173-178.
 10. Dharmaraj Selvakumar (2011). Study of L-asparaginase production by *Streptomyces noursei* MTCC 10469, isolated from marine sponge *Callyspongia diffusa*. *Iranian Journal of Biotechnology*, 9(2):102-108.
 11. Ankit, P.S., Bhaumik, R.D., Kalkal, A.T. and Ramalingam B. S. (2012). Production and amplification of an l-asparaginase gene from actinomycete isolate *Streptomyces ABR2*, *Annals of Microbiology*, DOI: 10.1007/s13213-011-0417-0.
 12. Pisano, M.A., Sommer, M.J. and Brancaccio, L. (1989). Isolation of bioactive actinomycetes from marine sediments using rifampicin. *Appl Microbiol Biotech* 31: 609-612.
 13. Gulati, R., Saxena, R.K. and Gupta, R. (1997). A rapid plate assay for screening L-asparaginase producing micro-organisms. *Lett Appl Microbiol*, 24: 23-26.
 14. Imada, A., Igarasi, S., Nakahama, K. and Isono, M. (1973). Asparaginase and Glutaminase Activities of Micro-organisms. *J Gen Microbiol*, 76: 85-99.
 15. Shirling, E.B. and Gottlieb, D. (1966). Methods for characterization of *Streptomyces* species. *Inter J Syst Bacteriol*, 16: 313-340.
 16. Gordon, R.E. and Milim J.M. (1957). *J Bacteriol*, 73: 15.
 17. Salle, A.J. (1948). *Laboratory manual on fundamental principles of Bacteriology* (3rd ed), Mc Graw-Hill Book Co.
 18. Williams, S.T., Sharp, M.E. and Holt, J.G. (1989). *Bergey's manual of systematic bacteriology*, Vol. 4, The Williams and Wilkins Co, Tokyo.
 19. Pridham, J.G., Anderson, P., Foley, C., Lindenfesler, L.A., Hesseltine, C.W. and Benedict, R.G. (1957). A selection of media for maintenance and taxonomic study of *Streptomyces*. *Antibiot Ann*, 57: 947-953.

Optimization of Culture Conditions for the Production of Polygalacturonase by *Phanerochaete chrysosporium* and *Aspergillus fumigatus*

S. Mrudula, Maheswari. V, Ashwitha Kodaparthi and Pavan Kumar Pindi*

Department of Microbiology, Palamuru University, Mahabubnagar, A.P, India- 509001

*For correspondence - pavankumarpindi@gmail.com

Abstract

In the present study *Phanerochaete chrysosporium* and *Aspergillus fumigatus* were screened for polygalacturonase production. The strains were grown in submerged fermentation and the most important physical parameters such as temperature and pH were optimized. The optimum temperature for maximum enzyme production was found to be 50 and 40 °C for *P. chrysosporium* and *A. fumigatus*, respectively. An optimum pH of 4.5 and 5.0 was recorded for *P. chrysosporium* and *A. fumigatus*, respectively. Under optimum condition the strain *P. chrysosporium* and *A. fumigatus* produced 1850 and 3218 units of enzyme per litre of culture broth, respectively. The polygalacturonase enzyme from the culture filtrates of both *P. chrysosporium* and *A. fumigatus* was purified to homogeneity. The purified fraction of polygalacturonase from *P. chrysosporium* and *A. fumigatus* was observed as single band. The molecular weights of purified enzyme from *P. chrysosporium* and *A. fumigatus* were 53 and 63 KDa, respectively. Overall the specific activities of polygalacturonases from *P. chrysosporium* and *A. fumigatus* were increased to 23.49 and 20.94 with a yield of 24.34 and 25.35, respectively.

Key words: *Aspergillus fumigatus*, *Phanerochaete chrysosporium*, polygalacturo-nase, optimization, purification.

Introduction

Polygalacturonases are one among the most important hydrolytic enzymes. Currently

Polygalacturonases find application in industrial processes such as food, textile, paper and waste water treatment. In food industries, they are used for the extraction, filterations and clarification of fruit juices (1) and they are also used to stabilize the cloud of citrus juices, purees and nectars. Pectinases are used to remove fibers containing gum in textile making. Bio technological degumming using pectinases in combination with xylanases present an ecofriendly and economic alternative to the chemical degumming treatment (2). In paper making, pectinases are employed in depolymerizing polymers of galacturonic acids, which subsequently lower the cationic demand of pectin solutions and the filtrate from peroxide bleaching (3). In the treatment of pectic waste water, pectinolytic enzymes, facilitates removal of pectinaceous material and renders it suitable for decomposition by activated sludge treatment (2). Though polygalacturonase originate from different sources including plants, animals and microorganisms, industrially, they are mainly produced by employing microorganisms (4). The advantage of using micro-organism is due to their increased yield and stability. Though pectinases are produced from a wide variety of microbial source such as bacteria, fungi, yeast and actinomycetes (5, 6), among them the major producer is fungi. There are many reports available on polygalacturonase production from fungi belonging to genus *Phanerochaete* and *Aspergillus* (7, 8).

In view of the above, the present investigation is aimed for the production and purification of polygalacturonase using *P. chrysosporium* and *A. fumigatus*.

Materials and Methods

Microorganism and culture maintenance: *Phanerochaete chrysosporium* and *Aspergillus fumigatus* used in the present study were obtained from Mycology unit, Dept. of Botany, CAS (Centre for Advanced Studies), University of Madras. Both the strains were maintained at room temperature. The *P. chrysosporium* culture was grown on 2% (w/v) malt agar slants, whereas *A. fumigatus* was grown in yeast soluble starch agar medium containing (g/l): starch, 1.5; yeast extract, 0.4; K_2HPO_4 , 0.23; KH_2PO_4 , 0.2; $MgSO_4 \cdot 7H_2O$, 0.05; citric acid, 0.052 at pH 5.6.

Inoculum preparation: The fungal cultures were stored on potato dextrose agar (PDA) slants and incubated at 30 °C for 5 days. The sporulated slants were stored at 4 °C. The spores were harvested by adding 2 ml sterile saline containing 0.01% (w/v) Tween 20 to the sporulated slant and the spores were dislodged using the inoculation needle under aseptic condition. This suspension was then collected in a sterile container and used as inoculum source.

Cultivation of the strains: The *P. chrysosporium* and *A. fumigatus* strains were grown individually in 500 ml Erlenmeyer flasks containing 100 ml of sterile Hankins medium composed of (g/l): mineral salt solution, 1000 ml; yeast extract, 2; pectin, 10; agar agar, 30. Mineral salt solution contains (g/l): $(NH_4)_2SO_4$, 4; KH_2PO_4 , 8; Na_2HPO_4 , 12; $FeSO_4 \cdot 7H_2O$, 0.4; $CaCl_2$, 0.02; H_3BO_3 , 0.2; $MnSO_4$, 0.2; $ZnSO_4$, 0.14; MoO_3 , 0.2; 0.5% (v/v) of respective spore suspensions were used as a source of inoculum. The strains were incubated at 30 °C for 5 days.

Screening of fungi for polygalacturonase production: The organisms which produce polygalacturonase enzyme were screened by growing them on pectin (1.5 % w/v) containing

agar plates. At the end of incubation (5 days at 28 °C), the plates were flooded with 1 % (w/v) cetrimide solution. Colonies producing polygalacturonase were exhibited with a clear zone around them.

Submerged fermentation: The submerged fermentation was carried out in 250 ml Erlenmeyer flasks containing fermentation medium (Hankin's medium). The medium was sterilized by autoclaving at 121 °C for 15 min. The fermentation medium was inoculated with 0.5% (v/v) of respective spore suspension. The strains were incubated at 30 °C on rotatory shaker at 240 rpm for 10 days.

Enzyme preparation: At the end of incubation period, the broth was centrifuged at 10,000 rpm for 20 min in cooling centrifuge. The supernatant was used as a source of extra cellular enzyme.

Enzyme activity: Polygalacturonase activity was determined by measuring the release of reducing groups in the reaction mixture. The reaction mixture (3ml) consists of 0.8 ml of citrus pectin (1.0 % w/v) and 0.2 ml of appropriately diluted enzyme source in 2 ml of sodium acetate buffer (0.1M, pH 5). The reaction mixture was incubated at 40 °C for 10 min (9), followed by addition of 1 ml of 1N NaOH and 1 ml of DNS to the tubes and the reaction was stopped by boiling the tubes in boiling water bath for 10 min, the reducing sugars released by enzymatic hydrolysis were determined (10). A separate blank was set up to correct the non-enzymatic release of sugar. One unit of polygalacturonase activity was defined as the amount of enzyme required to release one micromole of galacturonic acid per minute under the standard assay conditions.

Protein estimation: Protein content was determined by the method of Lowry *et al.*, (11) using bovine serum albumin (BSA) as standard.

Effect of temperature: Broth was inoculated and incubated at different temperatures ranging from 20 to 60 °C for *P. chrysosporium* and 30 to 70 °C for *A. fumigatus*.

Effect of pH: The effect of initial pH of the medium and polygalacturonase production was studied by growing the culture at different pH range from 3.5 to 5.5 for *P. chrysosporium* and 4.0 to 6.0 for *A. fumigatus*. The pH of the medium was adjusted by using 0.1N H₂SO₄ or NaOH.

Purification of enzymes: The organisms were grown separately in culture medium at 30 °C for 5 days. At the end of incubation, the broths from 2 different strains were centrifuged at 6000 rpm for 15 min at 4 °C to obtain cell free filtrates. The cell free filtrate containing polygalacturonase from two strains were collected and their activities and protein content were determined as described above. 1000 ml of each of the above prepared cell free filtrate from the strains were transferred into two different flasks. Analytical grade solid ammonium sulphate was then added to the flasks at a saturation level of 40%. The flasks were incubated at 4 °C overnight. The precipitations formed from the two different flasks were collected by centrifugation (15,000 rpm, 20 min at 4 °C) dissolved in acetate buffer (50 mM, pH 5.0). The suspension was dialyzed overnight against the same buffer. The dialyzed enzyme was applied onto DEAE cellulose column (24x7 cm), previously equilibrated with acetate buffer (50 mM, pH 5.0) and eluted with gradient salt solution (0 to 0.5 M NaCl). The concentrations of protein in the fractions were measured by the absorbance at 280 nm and enzyme assay was carried out. The active fractions were pooled, and subjected to SDS-PAGE to determine the number of bands.

Results

Screening of polygalacturonase production: Cultivation of *P. chrysosporium* and *A. fumigatus* strains on pectin agar plates supplemented with 1.5 % (w/v) pectin showed clear cut halo forming zone confirms the pectinase production after flooding with cetrimide solution.

Optimization of process parameters

Temperature: *P. chrysosporium* and *A. fumigatus* produced enzyme at all temperature

ranges (i.e. 20 to 60 °C for *P. chrysosporium* and 30 to 70 °C for *A. fumigatus*) and the optimum temperature for maximum enzyme production was found to be 50 and 40 °C, respectively (Fig. 1 and 2).

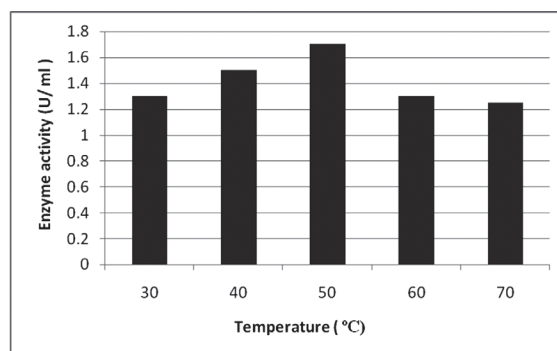


Fig. 1. Effect of temperature on polygalacturonase production by *P. chrysosporium*

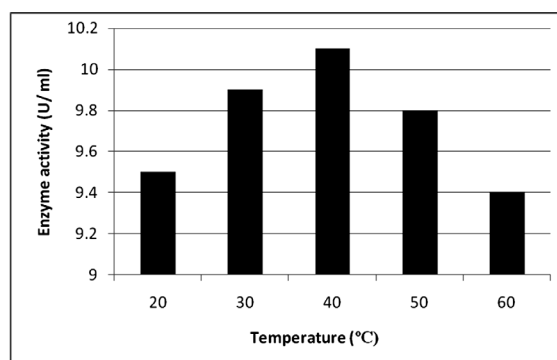


Fig. 2. Effect of temperature on polygalacturonase production by *A. fumigatus*

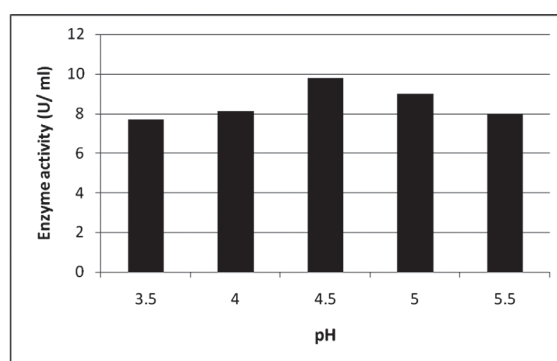


Fig. 3. Effect of pH on polygalacturonase production by *P. chrysosporium*

pH. The effect of initial pH on polygalacturonase production is shown in Fig. 3 and 4. The optimum pH for maximum production of enzyme from *P. chrysosporium* and *A. fumigatus* was found to be 4.5 and 5, respectively (Fig. 3 and 4).

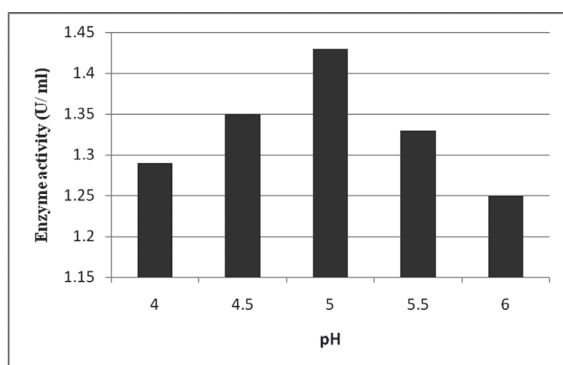


Fig. 4. Effect of pH on polygalacturonase production by *A. fumigatus*

Purification: When the organisms were grown individually in Hankin's broth supplemented with 1.5 % (w/v) pectin the strain *P. chrysosporium* and *A. fumigatus* produced 1850 and 3218 units of enzyme per litre culture broth, respectively. After salting out the enzymes with ammonium sulphate, the centrifuged culture supernatant showed approximately 918 and 2109 units of polygalacturonase from *P. chrysosporium* and *A.*

fumigatus per liter, respectively. There was an increase of specific activities from 5.92 to 21.29 and 7.64 to 37.39, respectively for enzymes from *P. chrysosporium* and *A. fumigatus*.

The enzyme from *P. chrysosporium* was purified about 23.49 fold with a specific activity of 139.09 IU/mg giving a yield of 24.34% after ion exchange chromatography which resulted in almost a single peak when absorbance was recorded at 280 nm. (Table 1 and Fig. 5). The purified polygalacturonase showed a single band on 12 % SDS-PAGE (Fig. 6). The molecular weight was found to be 53 kDa which indicated that it was novel enzyme from *P. chrysosporium*.

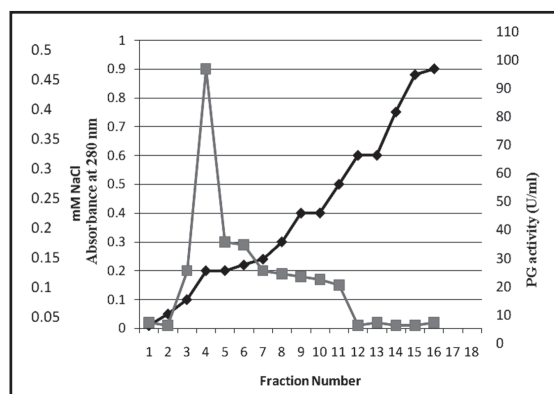


Fig. 5. Elution profile of polygalacturonase produced by *P. chrysosporium*.

Table 1. Purification of polygalacturonase produced extracellularly by *P. chrysosporium*

Step	Volume (ml)	Total Activity	Total Protein (mg)	Specific activity (IU/mg)	Fold (IU)	% Yield Purification
Crude	1000	1850	312	5.92	1	100
Ammonium sulphate precipitation	56	918	43.1	21.29	3.59	49.62
Ion chromatography	32	459	3.3	139.09	23.49	24.34

The enzyme from *A. fumigatus* was purified about 20.94 fold with a specific activity of 160 IU/mg giving a yield of 25.35% after the chromatography which resulted in almost a single peak when absorbance was recorded at 280 nm (Table 2 and Fig. 6). The purified polygalacturonase showed a single band on 12% SDS PAGE

(Fig. 7). The molecular weight was found to be 63kDa.

Lane 1 indicates Standard marker, Lane 2 and 3 indicates Crude extract, Lane 4 and 5 indicates partially purified enzyme by salt fractionation, Lane 6 and 7 indicates Purified

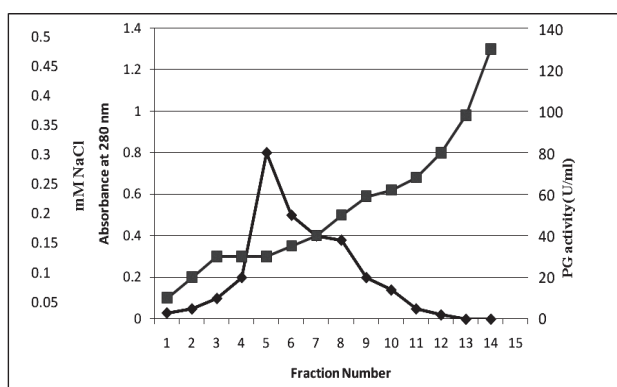


Fig. 6. Elution profile of polygalacturonase produced by *A.fumigatus*.

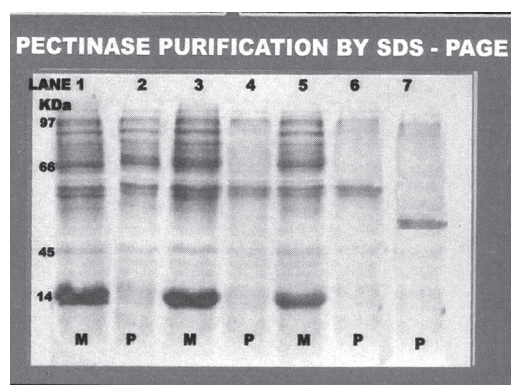


Fig. 7. Analysis of purified polygalacturonase enzyme on SDS PAGE

Table 2. Purification of polygalacturonase produced extracellularly by *A. fumigatus*

Step	Volume (ml)	Total Activity	Total Protein (mg)	Specific activity (IU/mg)	Fold (IU)	% Yield Purification
Crude	1000	3218	421	7.64	1	100
Ammonium sulphate precipitation	56	2109	56.4	37.39	4.8	69.53
Ion chromatography	32	816	5.1	160	20.94	25.35

polygalacturonase enzyme by ion exchange chromatography.

Discussion

The influence of temperature on polygalacturonase production is related to the growth of the organism. Most polygalacturonase production studies have been carried out with

fungi. Optimum yields of polygalacturonase were achieved at 42 °C for *Mucor circinelloides* (12), 50 °C for *Penicillium chrysogenum* (13) and 37 °C for *Penicillium expansum* (14). In this study, the enzyme synthesis of *P. chrysosporium* and *A. fumigatus* occurred at a temperature range between 20 and 60 °C and 30 and 70 °C with an optimum of 40 and 50 °C, respectively. Fevela-

Tores *et al.*, (15) described about the optimum temperature of polygalacturonase from *A. niger* has been established in the range of 36 to 45 °C which is close to our finding.

Among the physical parameters tested the pH of the growth medium plays an important role by inducing morphological change observed during the growth of the organism and also affects product stability in the medium. Most of the *Aspergillus* and *Phanerochaete* strains used commercially for the production of polygalacturonase by SmF have an optimum pH of 4.0-5.0. Maximum enzyme production was achieved at pH 4.5 and 5 by *P. chrysosporium* and *A. fumigatus*, respectively in this study. The results are in accordance with polygalacturonase production by *A. niger*, SA6 (16), *P. griseoroseum* (17) and *P. viridicatum* (18). Piccoli-Valee *et al.*, (17) observed high polygalacturonase activity by *P. griseoroseum* at acidic pH of 4.5 and 5. Same result has been given by Silva *et al.*, (9) using *P. viridicatum* for polygalacturonase. In another study the optimum pH for polygalacturonase production by *Penicillium chrysogenum* was found to be 6.5 (13). In the present study, the enzyme from *P. chrysosporium* and *A. fumigatus* was precipitated up to 40 % saturation. Baumann (18) and Berger *et al.*, (19) reported that polygalacturonase can be precipitated up to 90 % of ammonium sulphate depending on the source of the enzyme. Nithin Kumar and Bhushan (20) saturated the cell supernatant with 60 % ammonium sulphate. The purification of enzyme in this study was carried out with ion exchange chromatography. This purification method is similar to Alana *et al.*, (21) who purified the enzyme from *P. italicum* on DEAE cellulose of ion exchange chromatography.

In the present study, the molecular weight of *P. chrysosporium* and *A. fumigatus* was found to be 63 and 53 KDa with 23.49 and 20.94 fold higher than crude respectively. Akhilesh Thakur *et al.*, (12) purified polygalacturonase on Sephacryl S-100 gel filtration chromatography and obtained the molecular weight of 66 kDa on

SDS-PAGE. (24) purified the enzyme from *Penicillium* sp. by ion exchange chromatography and obtained the molecular weight of 35 kDa. Jurick *et al.*, (23) reported molecular weight of polygalacturonase from *Penicillium expansum* as 45 kDa.

In the present study, two strains *P. chrysosporium* and *A. fumigatus* were selected and screened for polygalacturonase production. The strains were grown in submerged fermentation and the most important physical parameters such as temperature and pH were optimized. Under optimum conditions, the strain *P. chrysosporium* and *A. fumigatus* produced 1850 and 3218 units of enzyme per litre of culture broth, respectively. The enzyme was purified by ammonium salt precipitation and ion exchange chromatography. The purified enzyme obtained from this study has a wide range of industrial applications including extraction and clarification of fruit juices, processing of cotton fabric in textile industries etc.

Acknowledgement

Authors would like thank Prof. G. Bhagyanarayana Vice-Chancellor and Prof. K. Venkata Chalam, Registrar, PU for their kind support and encouragement. One of the authors (Maheswari.V) wishes to acknowledge the Management of M.G.R. College, Hosur for their kind support.

Conflict of interest : The authors declare that they are no competing interests.

References

1. Fernandez-Gonzalez, M., Ubeda, J.F., Vasudevan, T.G., Cordero, Otera, R.R. and Briones, A.J., (2004). Evaluation of polygalacturonase activity in *Saccharomyces cerevisiae* wine strains. FEMS Microbiol. Lett. 38: 987-996.
2. Jayani, Ranveer, Singh, Saxena, Shivalika and Gupta, Reena, (2005). Microbial pectinolytic enzymes: A review. Process Biochem. 40: 2931-2944.

3. Kashyap, D.R., Vohra, P.K., Chopra. S. and Tewari, R. (2001). Application of pectinases in the commercial sector : A review. *Biores Technol.* 77: 215-227.
4. Bayoumi, R.A., Yassin, H.M., Swelim, M.A. and Abdel-All, E.Z. (2008). Production of bacterial pectinase(s) from agro-industrial wastes under solid state fermentation conditions. *J. Appl. Sci. Res.* 4 (12): 1708-172. .
5. Ahmed, R., Ahmad, S., Iqbal, J. and Baig, M.A. (1997). Shake flask studies for preliminaries by *Aspergillus foetidus*. *Pak J. Sci. Res.* 49: 36-39.
6. Solis-pereyra, S., Favela-Torres, E., Gutierrez-Rojas, M., Rousses, S., Saucedo Castaneda, Gunasekaran, P. and Viniegra-Gonzalez, G. (1996). Production of pectinases by *Aspergillus niger* in solid state fermentation at high initial glucose concentration *World J. Microbiol. Biotechnol.* 12:257-260.
7. Denning, D. and Brass, A. (2007). *Aspergillus fumigatus* Genome project, Wellcome trust Genome campus. 1-2.
8. Shanley, N.A., Vanden, Brock, L.A.M., Voragen, A.G.J. and Coughlas (1993). Isolation and characterization of endopolygalacturonase from *Phanerochaete chrysosporium* *J. Biotechnol* 28: 030-38.
9. Silva, R., Soares, M.M.C.N. and Gomes, E. (2002). Pectinase production by *Penicillium viridicatum* RFC3 by solid state fermentation using agricultural wastes and agro-industrial by-products. *Braz. J. Microbiol.* 33: 318-324
10. Miller, G.L., (1959). Use of dinitrosalicylic acid reagent for determination of reducing sugar. *Anal. Chem.* 31: 426-428.
11. Lowry, Oliver, H., Nira, J., Rosebrough, A., Lewis Farr, and Rose, J., Randall, (1951). Protein measurement with the Follin phenol reagent. *J. Biol. Chem.* 193: 265-275.
12. Akhilesh Thakur, Roma Pahwa, Smarika Singh, and Reena Gupta, (2010). Production, purification and characterization of polygalacturonase from *Mucor circinelloides* ITCC6025. *Enzyme Research.* 1: 1-7.
13. Banu, R.A., Kalpana, Devi, M., Ganaprabhal, G.R., Pradeep, B.V. and Palaniswamy (2010). Production and characterization of pectinase enzyme from *penicillium chrysogenum*. *I.J.Sci.Technol.* 3: 377-381.
14. Wayne, M., Ivana, Vico, Jurick, II, Mary, J., Camp, Wojciech, J., Janisiewicz and William, S. Conway (2010). Temperature Suppresses Decay on Apple Fruit by Affecting *Penicillium solitum* Conidial Germination, Mycelial Growth and Polygalacturonase Activity. *Plant Pathology Journal*, 9: 144-148.
15. Favela-Torres, E., Volke-Sepulveda, T. and Viniegra-Gonzalez, G. (2006). Production of hydrolytic depolymerising pectinases. *Food Technol. Biotechnol.* 44: 221-227.
16. Mohammed, L., Buga, Sani, Ibrahim, and Andrew, J., Nok, (2010). Physico-chemical characteristics of immobilized polygalacturonase form *Aspergillus niger* (SA6). *Afr. J. Biotechnol.* 9: 8934-8943.
17. Piccoli-Valle, R.H., Passos, F.J.V., and Silva, D.O., (2001). Purification of pectin lyase by *Penicillium griseoroseum* in bioreactor in the absence of inducer. *Braz. J. Microbiol.* 32: 135-140.
18. Baumann, J.W. (1981). Application of enzymes in fruit juice technology. In G.G. Birch, N. Blakebrough, and K.J. Parker (ed). London. Appl. Sci. Publisher Ltd. 129-147.

19. Berger, D.K., Oelofse, D., Arendse, M.S., Duplessis, E. and Dubery, I.A. (2000). Bean polygalacturonase inhibitor protein-1 (PGIP-1) inhibits polygalacturonase from , *Stenocarpella maydis*. *Physiol. Mol. Plant pathol.* 57: 5-14.
20. Nitinkumar, P.P. and Bhushan, L.C. (2010). Production and purification of pectinase by soil isolate *Penicillium* sp and search for better agro-residue for its SSF. *Research in Science and Technology.* 2: 36-42.
21. Alana, A., Gabilondo, A., Hernando, F., Moragues, M.D., Dominquez, J.B., Liama, M.J. and Sessa, J.L. (1989). Pectin lyase production by a *Penicillium italicum* strain. *Appl. Environ. Microbiol.* 55: 1612-1616.
22. Jacob, and Parukuttyamma, Prema (2006). Influence of mode of fermentation on production of polygalacturonase by a novel strain of *Streptomyces indicus*. *Food Technol. Bio Technol.* 44(2): 263-267. .
23. Jurick, W.M., Vico, I., McEvoy, J.L., Whitaker, B.D., Janisiewicz, Wand, Conway, W.S., (2010). Isolation, purification and characterization of a polygalacturonase produced in *penicillium solitum* decayed golden delicious apple fruit. *Phyto Pathol.* 93: 636-64.

Development and Evaluation of Controlled Release Verapamil Hydrochloride Pellets by PAN Coating Process

S.Vidyadhara^{1*}, M.Bhanu Prasad², R.L.C. Sasidhar¹ and T. Bala Krishna¹

¹Chebrolu Hanumaiah Institute of Pharmaceutical Sciences. Guntur. A.P.

²Department of Biotechnology, Acharya Nagarjuna University, Guntur. A.P.

*For Correspondence - svidyadhara@gmail.com

Abstract

The present investigation was mainly focused on the development of controlled release pellets of verapamil HCl with ethyl cellulose and hydroxypropyl methyl cellulose phthalate (HPMCP) by employing pan coating technique. Ethyl cellulose 7cps a high viscosity grade controlled release polymer was mainly used as coating agent for regulating the drug release from pellets. HPMCP, an enteric coating polymer was used in the present study to regulate the drug release at varied G.I pH conditions. An attempt was made to optimize the composition of these two polymers to achieve the controlled release of drugs from the pellets. Low viscosity hydroxypropyl methylcellulose (HPMC E5) was used a film former in the present investigation. Croscaremellose sodium was used as disintegrant to create channels in the coating for drug release. Povidone was used as binder to achieve uniform drug layering in the present investigation. It was observed that increase in the concentration of polymers ethyl cellulose and resulted in delay in the drug release. The increase in the hydroxypropyl methylcellulose phthalate polymeric concentration in formulations showed initial delay in drug release and has no effect on further drug release.

Key words: Verapamil hydrochloride, controlled release, pellets, pan coating.

Introduction

Multiparticulate dosage forms (MPDF) are receiving a immense attention as alternative drug

delivery system for oral drug delivery even though single unit dosage forms have been widely used for decades. The most commonly used pharmaceutical solid dosage forms today include granules, pellets, tablets and capsules, out of which tablets being the most popular dosage form, accounting for 70% of all ethical pharmaceutical preparations produced. The most increasingly interesting area in the development of MPDF'S is incorporation into tablets instead of hard gelatin capsules in order to make it more economical to the consumers and gaining more attention currently. The present research work focuses on the pelletized form of multiple units, they are prepared by process called Pelletization which is referred to as a size enlargement process and the final product obtained is called pellets. Pellets provide a reduction in the dosage regimen and gastrointestinal irritation moreover controlling the drug release and increasing the absorption of the active ingredient. Also one of the advantageous properties of the pellet formulations is being good candidates for the delivery of the drug substances due to minimizing the dose dumping effect. The reproducibility of the release characteristics from pellet formulations is also much better with respect to the single-unit dosage forms. They are suitable systems for film coating with respect to the low surface area-volume ratios. Also, resistance to external factors such as moisture, air and light are the most advantageous properties of these dosage forms (1-4).

In the present investigation pan coating is employed for the preparation of verapamil HCl

pellets. In pan coating method, a core material is coated with the drug substance following a secondary coating process in which the release controlling polymer material is introduced (5-6). The coating process for pellets is carried out primarily in order to modify the release of the drug from the pelletized drug delivery systems. The some of the Coating equipments used for the pan coating processes are standard coating pan and the perforated coating pan.

Verapamil hydrochloride is a calcium channel blocker and a class IV antiarrhythmic drug. It is a white crystalline powder, soluble in water; sparingly soluble in alcohol, freely soluble in methyl alcohol. A 5% solution in water has a pH of 4.5 to 6.5. Verapamil is approximately 90% absorbed from the GI tract but the bioavailability is only about 20% due to first-pass metabolism in the liver. It has terminal elimination half-life of 2 to 8 hours and prolonged after repeated oral doses. its plasma protein binding is up to 90% (7).

The present investigation was mainly focused on the development of controlled release pellets of verapamil HCl with ethyl cellulose and hydroxypropyl methyl cellulose phthalate by employing pan coating technique. Ethyl cellulose 7cps a high viscosity grade controlled release polymer was mainly used as coating agent for regulating the drug release from pellets. HPMCP, an enteric coating polymer was used in the present study to prevent burst effect of the drug from pellets during the first two hours of the dissolution. An attempt was made to optimize the composition of these two polymers to achieve the controlled release of drugs from the pellets. HPMC E5 was used a film former in the present investigation. Croscaremellose sodium was used as disintegrant to create channels in the coating for drug release. Povidone was used as binder to achieve uniform drug layering in the present investigation (8-9).

Experimental Section

Materials: Verapamil HCl was obtained as a gift sample from Pellet Pharma Ltd. The excipients

povidone k-30 and ethyl cellulose(EC) 7cps were obtained as gift samples from pellet Pharma Ltd., HPMC E₅ was obtained as gift sample from Dow Chemicals Asia pvt., Ltd., Mumbai. hydroxypropyl methyl cellulose phthalate (HPMCP), talc, isopropyl alcohol, propylene glycol were obtained as gift samples from Loba chemi pvt ltd., Mumbai.

Preparation of verapamil HCl controlled release pellets by pan coating technique:

Equal quantities of verapamil HCl and croscarmellose sodium were taken in to bowl and mixed manually. To the mixer another equivalent quantity of verapamil HCl was added and mixed with the help of gloved hand and remaining quantity of drug was loaded in to the blender and mixed with the powder for 10 mins.

Preparation of povidone solution: Isopropyl alcohol, PVP K-30 and Tween 80 were taken into stainless steel the tank and switched on the propeller type stirrer and mixed for 10mins. The solution was filtered through nylon cloth in to SS tank.

Drug loading: Sugar pellets were loaded into the pan. On to the sugar pellets verapamil HCl and croscarmallose blends prepared, earlier were loaded while spraying the povidone solution by using 1.2 mm spray gun nozzle. Pan was allowed to rotate for about 10 mins until uniform drug loading occurs. The coating pan was operated at an rpm of 15-20. The pellets bed was agitated to avoid sticking to coating pan. The pellets were kept under rotation for 30 minutes to avoid sticking. The drug loaded pellets from the pan were spread on to the trays uniformly and dried at 60°C temperature for about 3hrs. After drying the pellets were sifted by using vibro sifter to remove fines and collected the uniform sized pellets.

Preparation of HPMCE₅ solution: HPMC- E₅ and water were taken into the stainless steel tank and mixed for 10mins with propeller type stirrer. The solution was filtered through nylon cloth into SS tank.

Sub coating: The drug loaded pellets were loaded in to the pan and coated with HPMCE₅ polymer solution by using 1.2 mm spray gun nozzle. Coating of the pellets was done under specified conditions like inlet temperature of 40°C and outlet temperature of 35°C. Flow rate rpm was adjusted to 15-20 rpm. Coating pan was allowed to rotate for 10 mins until uniform coating was applied. The drug loaded pellets from the pan were spread on to the trays uniformly and dried at 60°C temperature for about 3hrs. After drying the pellets were sifted by using vibro sifter to remove fines and collected the uniform sized pellets.

Preparation of HPMCP solution: HPMCP, cetyl alcohol, acetone and isopropyl alcohol were taken in to the tank and mixed for 10 mins at 1300 rpm by using propeller type stirrer and filtered through nylon cloth in to SS tank.

Polymer loading: HPMC coated pellets were loaded in to the pan and coated with HPMCP by using 1.2 mm spray gun nozzle. Coating of the pellets was done under specified conditions like inlet temperature of 40°C and outlet temperature of 35°C. Coating pan was allowed to rotate for 10 mins until uniform coating was applied. The drug loaded pellets from the pan were spread on to the trays uniformly and dried at 60°C temperature for about 3hrs. After drying the pellets were sifted by using vibro sifter to remove fines and collected the uniform sized pellets.

Preparation of EC solution: Ethyl cellulose, Diethyl phthalate, talc, IPA and acetone were taken in to the SS tank. They were mixed in homogenizer for 15 mins and filtered through nylon cloth into SS tank.

Polymer loading: HPMCP coated pellets were loaded in to the pan and coated with ethyl cellulose solution by using 1.2 mm spray gun nozzle. After coating with EC solution coating pan was allowed to rotate for 10 mins until uniform coating was applied. The finally coated pellets were dried at ambient conditions for 2hrs and sifted through vibro sifter to collect uniform sized

pellets. The composition of various verapamil hydrochloride controlled release pellets were given in tables 2.

Evaluation of Physical parameters

Percentage yield: All the batches of controlled release Verapamil pellets prepared by pan coating were evaluated for percentage yield of the pellets. The actual percentage yields of pellets were calculated by using the following formula. The %yields of various batches of pellets were given in table 3.

$$\text{Percentage yield of pellets} = \frac{\text{Practical yield of pellets}}{\text{Theoretical yield of pellets}} \times 100$$

Particle Size determination: The average particle size of the pellet formulations of verapamil hydrochloride were analyzed by simple sieve analysis method (10). The particle size of various batches of pellets was given in table 3.

Friability: The friability of the core pellets of verapamil hydrochloride (11) was determined as % weight loss after 100 revolutions of 10 g of pellets in a friabilator. The friability values of various pellets formulations were given in table 3.

Drug content: One gram of verapamil hydrochloride pellets from each batch were taken at random and were crushed to a fine powder. The powdered material was transferred into a 100ml volumetric flask and 70ml of distilled water was added to it. It was shaken occasionally for about 30 minutes and the volume was made up to 100ml by adding distilled water. About 10ml of the solution from the volumetric flask was taken and centrifuged. The supernatant solution from the centrifuge tube was collected and again filtered by using Millipore filter. Then the filtrate was subsequently diluted and the absorbance was measured at 278 nm for verapamil hydrochloride respectively. Verapamil hydrochloride obeys Beer's law in the concentration range of 0-50 µg/ml. This test was repeated six times (N=6) for each batch of pellets. The drug content of various batches of pellets was given in table 3.

In vitro dissolution studies: 120 mg equivalent weight of verapamil hydrochloride containing pellets were collected and weighed at random from each batch of pellet formulation and dissolution studies were performed in a calibrated 8 station dissolution test apparatus (Disso 2000), equipped with paddles (USP apparatus II method) (12) employing 900ml of 0.1 N HCl for first 2 hrs and pH 7.4 phosphate buffer for remaining period of time as dissolution medium. The paddles were operated at 50 rpm and the temperature was maintained at $37 \pm 1^\circ\text{C}$ through out the experiment. 5ml of samples were withdrawn at regular intervals up to 24 hours and replaced with equal volume of fresh dissolution medium to maintain a constant volume of dissolution medium through out the experiment. Samples withdrawn at various time intervals were suitably diluted with same dissolution medium and the amount of drug released was estimated by ELICO double beam spectrophotometer at 278nm. The dissolution studies on each formulation were conducted in three times. Necessary corrections were made for the loss of drug due to each sampling.

The dissolution profiles of all the pellet formulations for verapamil hydrochloride were compared with the marketed extended release pellet formulation of verapamil hydrochloride by using a model independent approach of similarity factor, f_2 , with all time points included in the *in vitro* dissolution studies (13-14). The equation for calculating similarity factor is

$$f_2 = 50 \times \log \left\{ \left[1 + \frac{1}{n} \sum_{j=1}^n |R_j - T_j|^2 \right]^{-0.5} \times 100 \right\}$$

Where 'n' is the number of dissolution time and R_j and T_j are the reference (theoretical) and test dissolution values at time 't'. Dissolution profile was considered satisfactory if f_2 value lies more than 50. Two dissolution profiles are considered similar when the f_2 value is 50 to 100.

Characterization of pellets: Selected formulations were subjected to IR studies to identify any possible interaction between drug and polymers during coating process. The

surface characteristics of the pellets were characterized by SEM analysis.

Accelerated stability studies: The formulations which showed good *in vitro* performance were subjected to accelerated stability studies. These studies were carried out by investigating the effect of temperature on the physical properties of pellets and drug release of verapamil HCl from the pellets.

Results and Discussion

Verapamil HCl pellets were prepared by pan coating process. Non pariel sugar spheres were used to coat the verapamil HCl. The drug layer was further coated HPMCP as sub coating and finally the spheres were coated with ethyl cellulose. Ethyl cellulose 7cps a high viscosity grade controlled release polymer was mainly used as coating agent for regulating the drug release from pellets. HPMCP, an enteric coating polymer was used in the present study to prevent burst effect of the drug from pellets during the first two hours of the dissolution. An attempt was made to optimize the composition of these two polymers to achieve the controlled release of drugs from the pellets. HPMC E5 was used a film former in the present investigation. Croscaremellose sodium was used as disintegrant to create channels in the coating for drug release. Povidone was used as binder to achieve uniform drug layering in the present investigation. All batches of pellet formulations were formulated manufactured under identical conditions by maintaining specific process parameters which were given in the table 1. The compositions of EC and HPMCP were varied in different pellet formulations. The compositions of various pellet formulations were given in table 2.

All the pellet formulations were evaluated for physical parameters such as % yield, particle size, friability and drug content. The percent yields of various coated pellets were in the range of 90 to 95 % and particle size of all the batches of pellets were in the range of 700 to 800 microns determined by sieve analysis. The friability loss

Table 1. Pan coating process variables

No	Process Controls	Specifications
1	Batch Size	500 G
2	Inlet Air temperature	40°C
3	Product Temperature	36°C
4	Air Flow	200 - 300 cfm
5	No. of Spray Guns	1
6	Nozzle Aperture	1.2 mm
7	Atomization Air Pressure	20 psi
8	Spray time	10 min
9	Secondary drying	60 °C

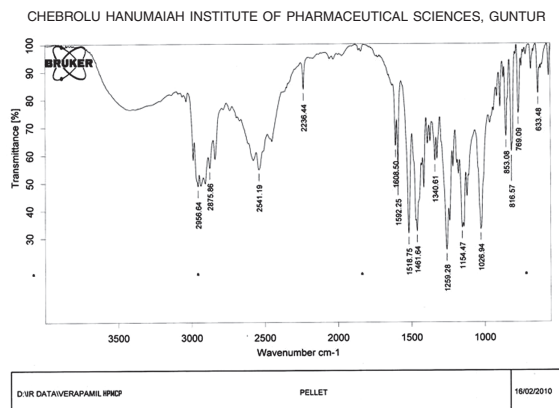


Fig. 1. FT IR Spectra of verapamil hydrochloride pure drug

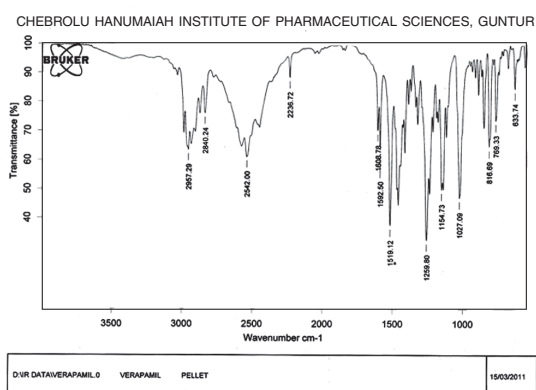


Fig. 2. FT IR spectra of verapamil hydrochloride pellet (FVL5)

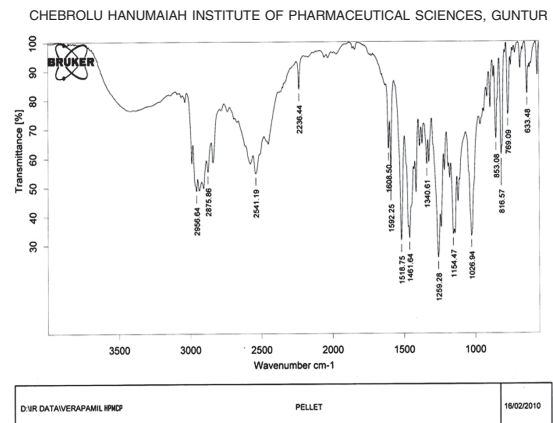


Fig. 3. FT IR spectra of verapamil hydrochloride pellet (FVL11)

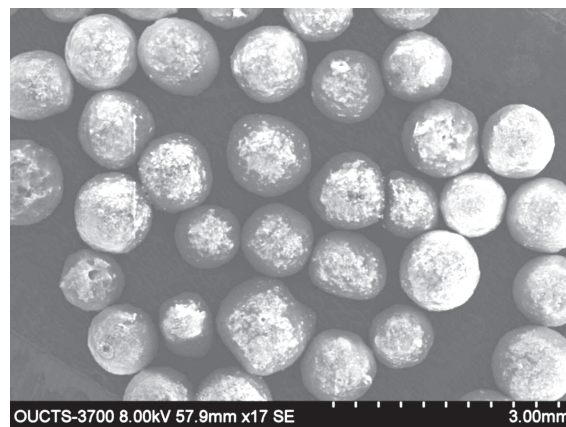


Fig. 4. SEM Images of verapamil HCl pellets

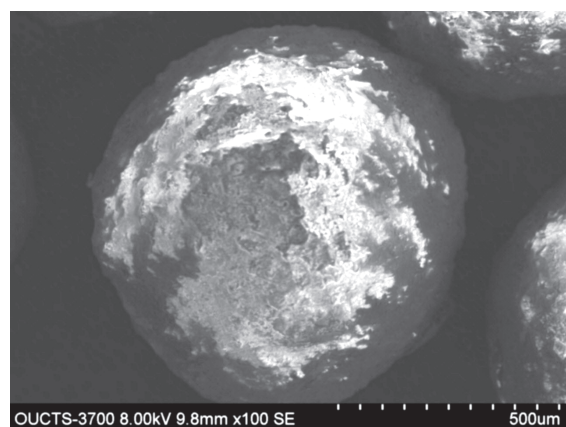


Fig. 5. SEM Images of verapamil HCl pellets studies

Table 2. Composition of various verapamil HCl pellets prepared by pan coating

Ingredients for 10gms	FVL1	FVL2	FVL3	FVL4	FVL5	FVL6	FVL7	FVL8	FVL9	FVL10	FVL11
VerapamilHCl	5.728	5.728	5.728	5.728	5.728	5.728	5.728	5.728	5.728	5.728	5.728
Povidone K 30	0.376	0.376	0.376	0.376	0.376	0.376	0.276	0.276	0.276	0.276	0.276
Ethyl Cellulose	0.010	0.012	0.014	0.016	0.018	0.020	0.020	0.020	0.020	0.020	0.020
HPMC E _s	0.240	0.240	0.240	0.240	0.240	0.240	0.240	0.240	0.240	0.240	0.240
HPMC Phthalate	0.020	0.020	0.020	0.020	0.020	0.010	0.012	0.014	0.016	0.018	0.020
Cetyl Alcohol	0.015	0.015	0.015	0.015	0.015	0.015	0.015	0.015	0.015	0.015	0.015
Diethyl Phthalate	0.016	0.016	0.016	0.016	0.016	0.016	0.016	0.016	0.016	0.016	0.016
Acetone	2.308	2.308	2.308	2.308	2.308	2.308	2.308	2.308	2.308	2.308	2.308
IPA	5.543	5.543	5.543	5.543	5.543	5.543	5.543	5.543	5.543	5.543	5.543
Talc	0.037	0.037	0.037	0.037	0.037	0.037	0.037	0.037	0.037	0.037	0.037
Croscarmellose sodium	0.055	0.055	0.055	0.055	0.055	0.055	0.056	0.056	0.056	0.056	0.056
Sugar Spheres	3.518	3.518	3.518	3.518	3.518	3.518	3.518	3.518	3.518	3.518	3.518
Purified Water	1.847	1.847	1.847	1.847	1.847	1.847	1.847	1.847	1.847	1.847	1.847
Tween-80	0.027	0.027	0.027	0.027	0.027	0.027	0.027	0.027	0.027	0.027	0.027

Table 3. Physical parameters of verapamil HCl pellets by pan coating

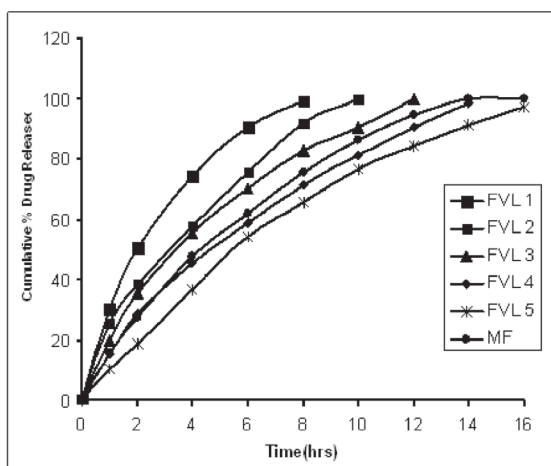
Formulations	%Yield	Particle Size (µm)	Friability%	Drug content
FVL 1	90.5 ± 0.2	752 ± 15	0.125	96.2 ± 0.3
FVL 2	91.4 ± 0.6	732 ± 15	0.093	97.6 ± 0.6
FVL 3	91.5 ± 0.5	736 ± 10	0.192	98.5 ± 0.4
FVL 4	94.5 ± 0.2	745 ± 15	0.117	98.2 ± 0.4
FVL 5	93.4 ± 0.2	741 ± 14	0.132	98.2 ± 0.5
FVL 6	93.5 ± 0.3	746 ± 15	0.124	97.8 ± 0.4
FVL 7	91.7 ± 0.4	756 ± 10	0.198	98.7 ± 0.4
FVL 8	94.4 ± 0.3	756 ± 10	0.092	96.4 ± 0.5
FVL 9	93.6 ± 0.5	758 ± 15	0.126	98.8 ± 0.5
FVL 10	93.4 ± 0.2	751 ± 20	0.134	98.6 ± 0.5
FVL 11	95.8 ± 0.3	754 ± 15	0.094	98.9 ± 0.5

of the coated pellets were less than 0.1 % and the percent of drug present in various pellet formulations were found to be in range of 96 to 99 %. All the physical parameters evaluated for the various batches of pellet formulations were

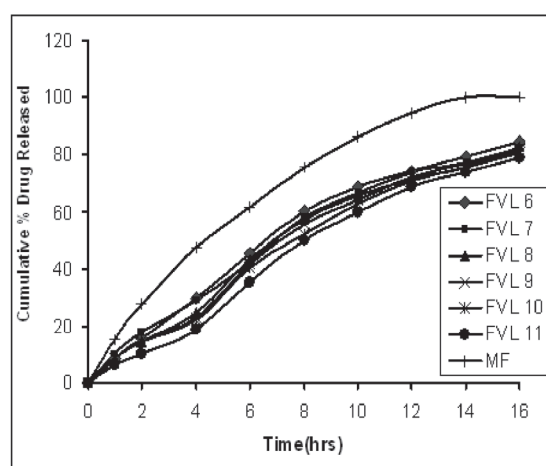
given in table 3. Dissolution studies were performed on all the controlled release pellets by using U.S.P paddle method (apparatus II). The drug release from the pellet formulations were extended up to 18hrs in majority of the

Table 4. *In vitro* dissolution parameters of verapamil hydrochloride pellets by pan coating

Formulation	First Order Constant		Higuchi Constants		Peppas Constant	
	K(hr ⁻¹)	R ²	K(mg ^{1/2})	R ²	n	R ²
FVL-1	0.272	0.999	30.34	0.987	0.52	0.998
FVL-2	0.127	0.994	28.24	0.978	0.66	0.987
FVL-3	0.146	0.991	27.95	0.981	0.59	0.984
FVL-4	0.161	0.994	26.27	0.993	0.71	0.991
FVL-5	0.157	0.991	24.34	0.985	0.76	0.996
FVL-6	0.168	0.988	27.16	0.969	0.81	0.997
FVL-7	0.204	0.996	26.77	0.986	0.85	0.999
FVL-8	0.222	0.990	25.12	0.978	0.82	0.995
FVL-9	0.198	0.998	25.18	0.989	0.78	0.992
FVL-10	0.175	0.995	27.42	0.998	0.88	0.987
FVL-11	0.158	0.990	24.44	0.998	0.81	0.988



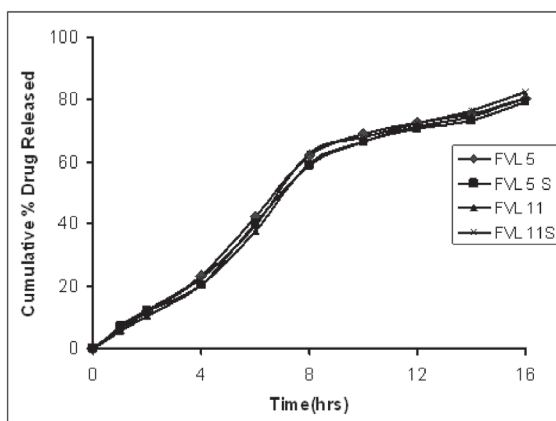
Graph 1. Drug release profiles for controlled release verapamil hydrochloride pellets



Graph 2. Drug release profiles for controlled release verapamil hydrochloride pellets

formulations and were shown in the graph 1 and 2. Formulations FVL1 to FVL 4 extended the drug release up to 14hrs. Formulations FVL 5 to FVL 11 extended the drug release up to 18hrs. The drug release rate decreased as the concentration of ethyl cellulose polymer increased. Among the

formulations prepared formulations FVL 6to FVL 11 showed the drug release up to 80 % at the end of 16hrs. It was observed that increase in the concentration of polymers ethyl cellulose resulted in extending the drug release over a prolonged period of time. The sub coating on



Graph 3. Drug release profiles verapamil hydrochloride pellets before and after stability

pellets with HPMCP at varied concentrations influenced on initial drug release. This was due to swelling of the polymer upon prolonged exposure to dissolution fluids (8). The increase in the HPMCP polymeric concentration in formulations showed initial delay in drug release i.e. up to 4hrs and further the rate of release was increased. All the pellet formulations were found to be linear with first order release rate with R^2 values in the range of 0.985 to 0.999, thus the rate of drug release from all the pellet formulations were concentration dependent and were linear with first order release rate constant (K_1). The Higuchi's plots for all the pellet formulations were found to be linear with R^2 values in the range of 0.969 to 0.998 and the drug release from the matrix tablet formulations was found to be by diffusion process. The release exponent (n values) for all the pellet formulations were in the range of 0.62 to 0.89, indicated that the drug release was by non-Fickian diffusion. Thus the drug release from the pellet formulations was by diffusion of the drug from the polymeric matrix followed by erosion of the polymer. Thus mechanism of drug release from all the pellet formulations was by both polymer erosion and diffusion of the drug from the matrix systems. The HPMCP sub coating upon continuous exposure to dissolution fluids lead to swelling which in turn responsible of erosion of pores or channels in

the EC coating layer thus leading to diffusion of drug from the coated layers. The dissolution profiles of verapamil hydrochloride pellet formulations were compared with marketed controlled release formulation of verapamil hydrochloride extended release pellets. The similarity factors were calculated for these pellet formulations. The similarity factor f_2 values were in the range of 28 – 89. The formulations FVL4 and FVL 5 showed the similarity factor values above 50 indicated that the release profiles for these formulations were similar to that of marketed formulation.

SEM analysis was performed on the selected pellet formulations prepared by pan coating. The pellets prepared by PC were having smooth surface with minimal pores indicated the uniform coating of the pellets. The SEM images of the pellets were shown in the fig.4 and 5. The spectra of Verapamil hydrochloride exhibited principle peaks at wave numbers of 2961 cm^{-1} (C-H Stretching), 2236 cm^{-1} (Ca=N Stretching), 1593 cm^{-1} (Ca=N Stretching), 1518 cm^{-1} (C=C Aromatic Stretching) and 1260 cm^{-1} (C-O Stretching). The spectra of pellet formulations FVL5 & FVL 11 (Fig. 2 and 3) exhibited all the principle peaks present in the verapamil hydrochloride pure drug. The results revealed that there were no major interaction between the drug and the polymers during coating process. The stability studies indicated that there was no visible and physical changes observed in the pellet formulations after storage. It was also observed that there was no significant change in drug release from the pellets. The slow and controlled drug release characteristics of the pellets remained unaltered. The comparative dissolution profiles of verapamil hydrochloride pellets before and after stability were shown in the graph 3. Thus the drug release characteristics of controlled release pellets designed were found to be quite stable.

Conclusion

The multi unit dosage form, pellets that were formulated by pan coating showed

optimized controlled release of the drug verapamil hydrochloride for extending the drug release for a prolonged period of time. Sugar sphere cores were coated with the hydrophobic ethyl cellulose and hydrophilic HPMCP. These pellets gave a more controlled fashion of drug release than sustained matrix formulations.

References

1. Palsson B.O, Wheatley T.A. and Dressman J.B. (1990). Mechanism of release from pellets coated with an ethylcellulose based film. *Journal of Controlled Release*. 14: 203-213.
2. Wu, X.Y., Eshun, G and Zhou, Y. (1998). Effect of interparticulate interaction on release kinetics of microsphere ensembles, *Journal of Pharmaceutical Sciences*. 87: 586-593.
3. Z Hon, Y and Wu, X.Y. (2003). Modeling and analysis of dispersed drug release into a finite medium from sphere ensembles with a boundary layer. *Journal of Controlled Release*. 90: 23-36.
4. Iyer, R.M., Augsburger, L.L., Parikh and D.M. (1993). Evaluation of drug layering and coating: Effect of process mode and binder level, *Drug Development and Industrial Pharmacy*. 19: 981-998.
5. Mustafa S.K, Suheyla K and Levent O. (2007). Formulation of Controlled Release Glipizide Pellets Using Pan Coating Method. *Hacettepe University Journal of the Faculty of Pharmacy*. 27: 93-106.
6. Bodea, A. and Leucuta, S.E. (1998) Optimization of propranolol hydrochloride sustained-release pellets using box-behnken design and desirability function. *Drug Development and Industrial Pharmacy*. 24: 145-155.
7. Follath.F, Ha.H.R and Schutz.E. (1986). Pharmacokinetics of conventional and slow release verapamil. *British Journal of Clinical Pharmacology*. 21: 149- 153.
8. Raymond C.R. (2009) *Handbook of Pharmaceutical Excipients*. 6th Edition.
9. Botzolakis J.E and Augsburger L.L.(1988). Disintegrating agents in hard gelatin capsules. Part I: mechanism of action. *Drug Development and Industrial Pharmacy*. 14: 29–41.
10. The United States Pharmacopeia (2004), USP 27, Webcom Limited: Toronto, 2003.
11. Santos H and Veiga F. (2002) Physical properties of chitosan pellets produced by extrusion-spheronization: influence of formulation variables. *International Journal of Pharmaceutics*. 246: 153-169.
12. United States Pharmacopoeia.(2004) *Verapamil Hydrochloride Extended-Release Capsules monograph*. 27th Edition.
13. Quality control. (2004) *Pharmaceutical statistics: Practical and clinical applications*. In: 4th ed. Bolton S, Bon C, editors. New York: Marcel Dekker. 408-411.
14. Moore.J.W. and Flanner.H.H. (1996). Mathematical comparison of dissolution profiles. *Pharmaceutical Technology*. 20: 64–74.

Identification and Validation of an Allele Specific Marker Associated with Pungency in *Capsicum* spp.

T. Chakradhar¹, B. Pradeep Reddy¹, N.Srinivas¹ and P.Chandra Obul Reddy²

¹ Centromere Biosolutions, Agri Incubation Park, International Crop Research Institute for Semi Arid Tropics (ICRISAT), Patancheru-502328, Hyderabad, India

²Department of Botany, Y.V. University, Kadapa-516003, Andhra Pradesh, India

*For Correspondence - coreddy@yogivemanauniversity.ac.in

Abstract

Pungency or heat in *Capsicum* spp. is due to the accumulation of unique secondary compounds known as capsaicinoids in their placental tissues. Detecting presence or absence of pungency at the nursery stage is a challenging task in CMS based hybrid pepper breeding programs. In this study a DNA sequence possibly related to pungency trait with high similarity to *Pun1* or *At3* gene was investigated. Nucleotide alignment of the obtained sequences and corresponding fragment from the data base has revealed a 16bp deletion in *C.annuum* 'Maor'. A multiplex agarose based co-dominant marker was designed to detect the identified polymorphism and named it as *Cen1*. This *Cen1* marker is validated in a panel of 27 pepper genotypes belonging to *C.annuum*, *C.chinensis*, *C.frutescens* and *C.baccatum* for its wide utility. All these *Capsicum* accessions were correctly discriminated with phenotype. In addition, the ability of *Cen1* marker to discriminate homozygous and heterozygous plants was demonstrated in F_1 hybrids crossed from a non pungent 'Maor' and a pungent 'Habanero'. The *Cen1* marker was also associated with phenotypic character in the tested genotypes. Moreover the linkage association of *Cen1* with *At3* or *Pun1* gene has also been discussed. Therefore the developed functional marker in this study will be highly useful in marker assisted selection (MAS) programmes, germplasm characterization and seed purity testing of chilli.

Key words: *Capsicum* spp. Marker assisted selection, *Pun1*, Capsaicinoids, Pungency, Allele.

Introduction

Pungency or heat is unique trait of *Capsicum* genus and is thought evolved to deter mammalian herbivores there by promoting seed dispersal by birds (1). Pungency in peppers is due to the production of group of alkaloids called 'capsaicinoids' in placental tissues of developing fruits approximately twenty days post anthesis. After biosynthesis they are secreted towards the outer epidermal cells and finally accumulated in structures called 'blisters' located on the placental surface (2, 3). Capsaicinoids are synthesized by condensation of branched chain fatty acids and vanillylamine, derived from phenylalanine, (4). Although more than ten different capsaicinoids structures exist (5), 'capsaicin' is responsible for sensation of pungency, accounting for almost 90% of all capsaicinoids (6, 7). In non-pungent pepper fruits vanillyl alcohol will be formed instead of vanillylamine which upon condensing branched chain fatty acid moiety, forms 'capsinoids' the non pungent alkaloids facilitating their application in human medicine as pain relievers (8, 9, 10).

It has been known for almost a century ago that mutations at single genetic locus, *Pun1* (formerly known as *C*) is responsible for loss of pungency in sweet peppers (11, 12). Several studies with different *Capsicum* population could map *Pun1* locus to pepper chromosome 2.

Recent studies by candidate gene approach concluded that *Pun1* encodes for a 'putative acyltransferase AT3' that has a qualitative role in determining pungency (13). Later studies have identified another allelic series *Pun2* in wild pepper *C. chacoense* and a quantitative role was attributed to it (14). Capsaicin biosynthesis is variable by environmental stress, fruit position and also by the height of the area (15, 16).

Phenotyping of pungency trait is an important task and can be a bottleneck in some pepper breeding programs. To facilitate this process, several methods have been developed from organoleptic tests well known as Scoville Test (17) to analytical methods based on separation techniques as gas chromatography (GC) and high performance liquid chromatography (HPLC) coupled to detection techniques as ultraviolet (UV) or mass spectrometry (MS) (18). These methods have some advantages and/or disadvantages, and they share great requirements of time and labor.

Biased selection pressure for sweet pepper to be used as vegetable during domestication has resulted in large deletions of *At3* or *Pun1* gene. So far three different allelic mutations were observed in *At3* or *Pun1* gene (19). Among them most prominent and widely exploited one is *pun1*¹ which involves a 2.5 kb deletion spanning the putative promoter region extending through 5'UTR and first exon of coding region (20). The *pun1*¹ allele is specific to *C. annuum* derived cultivars and several markers were identified that co-segregated with this allele (21-24). Another recessive allele of *Pun1* is *pun1*² identified in *C. chinensis* with 4bp deletion in the first exon of *At3* gene associated phenotypically with absence of blisters in placental epidermal cells (3). A tightly linked marker for *pun1*² using fluorescent primer was developed by Wyatt et al., (19). The third allele *pun1*³ was reported from *C. frutescens* with 210bp deletion including the stop codon (14).

In this paper, we report a new genetic source of allele that controls pungency. We

designed a novel co-dominant functional marker for the identified null allele and attempted to associate with phenotype in *Capsicum* spp. The versatility of developed marker was demonstrated among the panel of pepper genotypes and also in F₁ hybrids.

Material and Methods

For sequencing analysis of candidate gene *At3* four different pepper accessions were selected based on the differential banding pattern observed in one of the selected plants while genotyping pungency trait using ARMS-PCR marker (25). The samples include the non-pungent *C. annuum* 'Maor', *C. frutescens* 'Grif' and pungent *C. annuum* 'SCM-334', *C. chinensis* 'Orange Habanero'. The developed marker was tested in a wide range (twenty seven) of pungent and non pungent pepper genotypes belonging to various species of *Capsicum*. The details of species and cultivar of each genotype is given in Table-1. The *capsicum* accessions studied were obtained from Vibha seeds Ltd, India and the seeds were selfed in the green house conditions between 20-25°C at Yogi Vemana University, Kadapa, A.P, India, using standard horticultural practices. The co-dominant nature of the marker was demonstrated on F₁ hybrids obtained by a cross between *C. annuum* 'Maor' X *C. chinensis* 'Orange Habanero'

Organoleptic test was performed to score the pungency of genotypes under study. At least two persons tasted the matured fruits randomly from three plants per accession. A sample was declared non pungent when all samples tasted were non-pungent. If at least one among the tasted fruit is happened to be pungent then that accession was considered as pungent. However capsaicinoid content was also quantified using ELISA (enzyme linked immunosorbent assay) kit from Beacon Analytical (Portland, ME, USA) according to manufacturer's protocol taking five mature dried fruits from three replicates per accession.

Genomic DNA from young leaf tissue was extracted as per the modified protocol of Doyle

and Doyle (1990) with minor changes (26). The obtained PCR products were gel purified using QIAquick Gel Extraction Kit (Qiagen, USA) and cloned into pJET1.2 vector according to manufacturer's protocol (Thermo scientific, USA). Sequencing of cloned fragments was done with MWG (Eurofins Genomic India Pvt Ltd). A contig was created with the overlapping PCR clones using Geneious v5.3 software (27). Primers used in this study were designed using fast PCR (<http://fastpcr.software.informer.com/>).

To amplify the *At3* gene, sequence information already submitted to gene bank was used to design gene specific primers (F.P 5'-CCATGGATTGTTGCTCGGGCCTCC-3' and R.P 5'-CCGTACCGCCCCATTGCGATTCC-3'). Using these primers *At3* or *Pun1* gene amplified from selected pepper accessions and sequenced in both direction using the same primers. A co-dominant marker designed specific to the newly identified genetic locus consists of three primers Cen1F.P (5'-CCATTAGTCGT TCATTTTTG TTTG-3'), Cen1 R.P_1(5'-TCTGCCCTTGTT GGATTTTA-3') and Cen1R.P_2 (3'-GCATG TGGTATCATGCATG-5'). The PCR analysis was carried out in 20 μ l reaction system consisting of 50-100ng of template DNA, 0.5 μ l of 20 μ M each primer, 1 μ l of 20mM dNTPs, 2 μ l of 10X PCR buffer and 1U of taq polymerase (NEB, USA). A 20mM TMAC (Tetramethyl ammonium chloride) was used for reaction used with *Cen1* marker. PCR was performed in Bio-rad thermal cycler system1000 (Bio-rad, USA) for 35 cycles and conditions for *At3* gene amplification include an initial denaturation of 4 min at 94°C, followed by 35 cycles of 94°C/1min, 58°C/1min, 72°C/2min with final extension of 5 min.

PCR cycles for *Cen1* marker includes 94°C for 5 min, with 35 cycles of 94°C/1 min, 60°C / 1.30 min, 72 °C/2min min and a final extension of 8 min at 72 °C. The amplified products were resolved on 1.5% agarose gel (Lonza,USA) with added ethidium bromide (50ng/ul) in electrophoresis system (Hoefer, Inc. USA) at 80volts containing 1X TAE buffer. The gels were

visualized under UV light with an image analysis system GelDoc XR⁺ (Bio rad, USA).

Results and Discussion

We hypothesized that there would be a new source of allele that could be the source of genetic basis for loss of pungency in *Capsicum* spp. other than reported ones (19). To execute this, *Pun1* or *At3* was amplified from three *C.annuum* genotypes and one *C.chinensis* using gene specific primers and analysed their sequences. *Pun1* or *At3* which encodes for acyltransferase-3 is the only locus that has qualitative role on pungency in domesticated peppers (28). By sequence analysis it come to know that we could amplify another gene '*catf-2*' which has high homology (87%) with *At3* or *Pun1* gene (29). It was known from literature that *catf-2* also belongs to acyltransferase proteins and co-expressed in placental tissue of capsicum along with other gene involved in capsaicinoids biosynthesis (13). Hence we further analysed the obtained sequences by multiple alignment using clustalW program (Fig. 2) and a comparative study with other deposited pepper accessions of *catf2* and *At3* from GeneBank (# AB206920, # AY819027.1, # AY819031.1, # AY819030.1 and # EF104910.1) was also done. Alignment of the consensus sequences of different genotypes revealed several SNPs and indels. A 16bp deletion was found in *C.annuum* 'Maor' a non-pungent type between 2,644bp-2,659bp (Fig. 2). Multiple alignment of deduced amino acid sequence of the obtained sequence with other acyltransferases showed highly conserved motif (LVSYYPYAG), characteristic of genes belonging to BAHD super family of acyltrasferases (data not shown) (30). A three primer PCR marker was developed based on identified polymorphism and named it as *Cen1*. While designing the primers a second reverse primer was designed to complement the deleted region so that a 166bp & 494bp bands were observed only in pungent types and 478bp was observed in non pungent types (Fig. 1a & b). The *Cen1* marker was validated in accessions used for sequencing and also tested on panel of 27 genotypes of pepper

belonging to *annum-chinensis-frutesense* complex of *Capsicum* to reliably differentiate pungent and non pungent types (Table1). During phenotyping by taste, 9 among 16 *C.annuum*, 4 in *C.chinensis*, 3 of 4 in *C.frutescens*, 2 in *C.baccatum* and the single

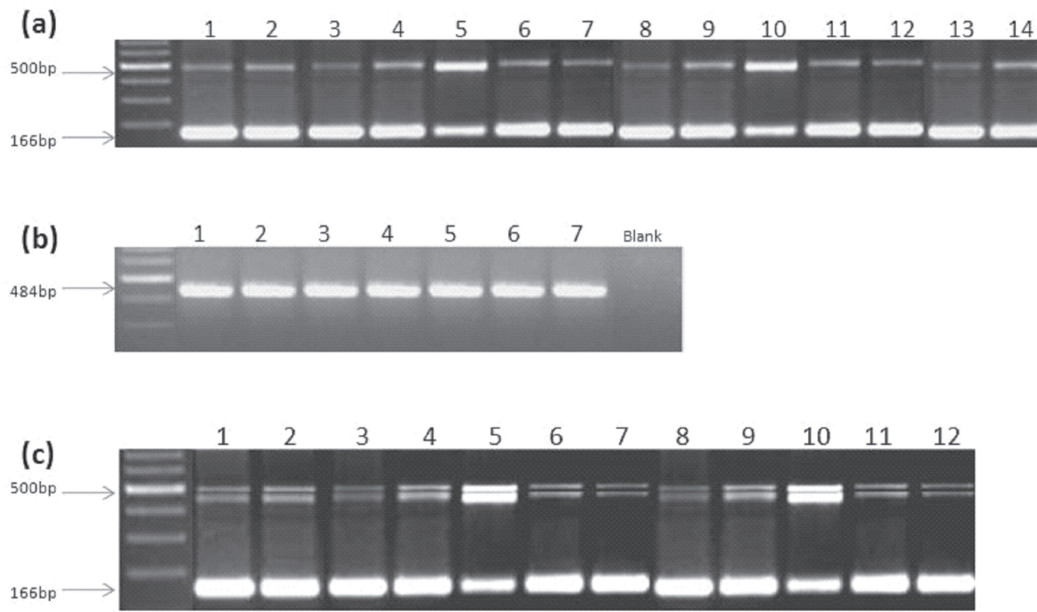


Fig. 1. a) Agarose gel showing genotypic data with *Cen1* marker .1: 'Jalapeno'2: 'Asain'3: 'CH-19'4: 'SCM334' 5: 'Bukesh' 6: 'BG 2816' 7: 'Habanero' 8: 'NMCA30036' 9: 'Bhut Jolokia' 10: 'C-238' 11: 'Aji' 12: 'Manzano' 13: 'PI 355819' 14: 'Red Savina' b) Genotyping data with non pungent accessions 1: 'Maor' 2: 'Bell' 3: 'Paprika' 4: Aleppo' 5: 'Yolo Wondor' 6: 'New Mexico' 7: 'Grif 9182'. c) co-dominant genotyping of F1 hybrids developed from a non pungent 'Maor'x 'Habanero'.

```

Maor      AAATGAGATGATCATATACT-----CCACATGCAGCAGGCAGAGGTCCT
Grif9185 AAATGAGATGATCATATACTTCCAACATGCATGATACCACATGCAGCAGGCAGAGGTCCT
SCM334   AAATGAGATGATCATATACTTCCAACATGCATGATACCACATGCAGCAGGCAGAGGTCCT
Habanero AAATGAGATGATCATATACTTCCAACATGCATGATACCACATGCAGCAGGCAGAGGTCCT

Maor      CAATTCGACATGTTAACAAGCCTGGGCTATTAGTCTATTTGTAGAGACTACTCTTAAACG
Grif9185 CAATTCGACATGTTAACAAGCCTGGGCTATTAGTCTATTTGTAGAGACTACTCTTAAACG
SCM334   CAATTCGACATGTTAACAAGCCTGGGCTATTAGTCTATTTGTAGAGACTACTCTTAAACG
Habanero CAATTCGACATGTTAACAAGCCTGGGCTATTAGTCTATTTGTAGAGACTACTCTTAAACG
    
```

Fig. 2. Multiple sequence alignment of four selected genotypes: *C. annum* "Maor", *C. annum* "SCM334", *C.chinensis* "Orange Hebenero" and *C.frutescens* "Grif9185". The part dotted denote the deletion portion.

genotype of *C. pubescens* turned out to be pungent both in organoleptic as well ELISA based tests. During organoleptic test heat sensation was observed in pungent accessions 10 days after pollination (DAP) and found decreased gradually 20 days after DAP, indicating strict developmental regulation of genes involved in capsaicinoid biosynthesis. A further study is required to identify the gene that play qualitative role in pungency. *Pun1* ARMS-PCR marker identified previously by Garcer-Claver was used to screen the same genotypes to know the

accuracy of the markers in predicting the phenotype (25). Few of the accessions which assessed as pungent by both organoleptic and HPLC were genotyped as non pungent with ARMS-PCR marker (data not shown) where as the *Cen1* marker developed in this study revealed perfect association with the phenotype with two exceptions, one in *C. frutescens* and another in *C. baccatum* 'C-238'. The result implies that the deletion may be unique to *C. annuum* spp occurred as result of duplication in a recent evolutionary event. Domestication of *Capsicum*

Table 1. Capsicum spp. Genotypes and their respective phenotyping for pungency obtained with *Cen1* marker

S.No	Samples of germplasm and F1 hybrids of <i>C. annuum</i> 'Maor' X <i>C. chinensis</i> 'Habanero'	Phenotype	Genotype
1	<i>C. annuum</i> var. <i>annuum</i> cv. 'Aleppo'	Non pungent	B
2	<i>C. annuum</i> var. <i>annuum</i> cv. 'New Mexico'	Non pungent	B
3	<i>C. annuum</i> var. <i>annuum</i> cv. 'Jalapeno'	Pungent	A
4	<i>C. annuum</i> var. <i>annuum</i> cv. 'Bell'	Non pungent	B
5	<i>Capsicum annuum</i> var. <i>glabriusculum</i>	Pungent	A
6	<i>C. annuum</i> cv. 'Asain'	Pungent	A
7	<i>C. annuum</i> cv. 'Paprika'	Non pungent	B
8	<i>C. annuum</i> cv. 'CH-19'	Pungent	A
9	<i>C. annuum</i> cv. 'Maor'	Non pungent	B
10	<i>C. annuum</i> cv. 'SCM334'	Pungent	A
11	<i>C. annuum</i> cv. 'Yolo Wonder'	Non pungent	B
12	<i>C. annuum</i> cv. 'Cal wonder orange'	Non pungent	B
13	<i>C. annuum</i> cv. 'Bukesh'	Pungent	A
14	<i>C. annuum</i> cv. 'Agridulce'	Pungent	A
15	<i>C. annuum</i> cv. 'Aviculare'	Pungent	A
16	<i>C. annuum</i> cv. 'czech Black'	Pungent	A
17	<i>C. pubescens</i> cv. 'Manzano'	Pungent	A
18	<i>C. frutescens</i> cv. 'Wild'	Pungent	A
19	<i>C. frutescens</i> cv. 'BG 2816'	Pungent	A
20	<i>C. frutescens</i> cv. 'Grif 9182'	Non pungent	B
21	<i>C. frutescens</i> cv. 'PI 355819'	Pungent	A
22	<i>C. chinense</i> cv. 'Orange Habanero'	Pungent	A
23	<i>C. chinense</i> cv. 'Red Savina'	Pungent	A
24	<i>C. chinense</i> cv. 'NMCA30036'	Pungent	A
25	<i>C. chinense</i> cv. 'Bhut Jolokia'	Pungent	A
26	<i>C. baccatum</i> var. <i>pendulum</i> cv. 'C-238'	Pungent	A
27	<i>C. baccatum</i> cv. 'Aji'	Pungent	A

species happened independently early during evolution and hence each taxa appear to carry different mutations for non-pungency (16, 31). The reason for not detecting the trait in *C.frutescens* and in *C.baccatum* could be because of existence of different source of alleles that could be responsible for loss of pungency (14). The *Cen1* marker developed in this study was also used to demonstrate zygosity status of the allele i.e. to distinguish between homozygous and heterozygous plants. The results using the parental lines, 'Moar and 'Habanero' and their corresponding pungent F₁ hybrids revealed the presence of three fragments in F₁ heterozygous plants with amplicons of pungent allele specific 500 & 166 bp and non-pungent allele specific 484bp. (Fig.1 c). All F₁ hybrids exhibited a pungent phenotype indicating the dominant nature of the allele.

Conclusions

Identification of pungent and non pungent genotypes at the seedling stage much earlier than fruit setting is a challenge in pepper breeding programs. This study provides a new allele specific versatile marker (*Cen1*) for the identification of the pungent trait in capsicum. The results, after assessing a large number of capsicum genotypes, have clearly demonstrated the feasibility of this allele specific deletion based co-dominant marker in breeding applications like germplasm screening, genetic purity test and marker assisted back crossing.

References

1. Tewksbury, J. and Nabhan, G.P. (2001). Directed deterrence by capsaicin in chillies. *Nature*, 412: 403–404.
2. Suzuki, T., Fujiwake, H. and Iwai, K. (1980). Intracellular localization of capsaicin and its analogues, capsaicinoid, in *Capsicum* fruit: Microscopic investigation of the structure of the placenta of *Capsicum annum* var. *annum* cv. Karayatsubusa. *Plant Cell Physiol*, 21: 839–853.
3. Stewart, C., Mazourek, M., Stellari, G.M., O'Connell, M. and Jahn, M. (2007). Genetic control of pungency in *C.chinensis* via the *Pun1* locus. *Journal of Experimental Botany*, 58: 979–991.
4. Curry, J., Aluru, M., Mendoza, M., Nevarez, J., Melendrez, M. and O'Connell, M.A. (1999). Transcripts for possible capsaicinoids biosynthetic genes are differentially accumulated in pungent and non pungent *Capsicum* spp. *Plant Sci*, 148: 47-57.
5. Mazourek, M., Pujar, A., Borovsky, Y., Paran, I., Mueller, L. and Jahn, M.M. (2009). A dynamic interface for capsaicinoid systems biology. *Plant Physiol*, 150: 1806–182.
6. Kozukue, N., Han, J.S., Kozukue, E., Lee, S.J., Kim, J.A., Lee, K.R., Levin, C.E. and Friedman, M. (2005). Analysis of eight capsaicinoids in peppers and pepper-containing foods by high-performance liquid chromatography and liquid chromatography-mass spectrometry. *J Agric Food Chem*, 53: 9172–9181.
7. Choi, S.H., Suh, B.S., Kozukue, E., Kozukue, N., Levin, C.E. and Friedman, M. (2006). Analysis of the contents of pungent compounds in fresh Korean red peppers and in pepper-containing foods. *J Agric Food Chem*, 54: 9024–9031.
8. Kobata, K., Kawaguchi, M. and Watanabe, T. (2002) Enzymatic synthesis of a capsinoid by the acylation of vanillyl alcohol with fatty acid derivatives catalyzed by lipases. *Biosci Biotechnol Biochem*, 66:319–327.
9. Luo, X.J., Peng, J. and Li, Y.J. (2011) Recent advances in the study of capsaicinoids and capsinoids. *Eur J Pharmacol*, 650: 1-7.
10. Sasahara, I., Furuhashi, Y., Iwasaki, Y., Inoue, N., Sato, H., Watanabe, T. and Takahashi, M. (2010). Assessment of the biological similarity of three capsaicin

- analogs (capsinoids) found in non-pungent chili pepper (CH-19 Sweet) fruits. *Biosci Biotechnol Biochem*, 74:274–278.
11. Webber, H. (1911). Preliminary notes on pepper hybrids. *Am Breeders Assoc Annu Report*, 7:188–199.
 12. Deshpande, R.B. (1935). Studies in Indian chillies: Inheritance of pungency in *Capsicum annuum* L. *Indian J Agric Sci*, 5:513–516.
 13. Lang, Y., Yanagava, Y., Sasakuma, T. (2006). A gene encoding a putative Acyltransferase involved in pungency of *Capsicum*. *Breeding Science*, 56: 55-62.
 14. Stellari, G.M., Mazourek, M. and Jahn, M.M. (2010). Contrasting modes for loss of pungency between cultivated and wild species of *Capsicum*. *Heredity*, 104:460-471.
 15. Zewdie, Y. and Bosland, P.W. (2000). Evaluation of genotype, environment, and genotype-by-environment interaction for capsaicinoids in *Capsicum annuum* L. *Euphytica*, 111:185–190.
 16. Tewksbury, J.J., Reagan, K.M., Machnicki, N.J., Carlo, T.A., Haak, D.C., Penaloza, A.L.C. and Levey, D.J. (2008). Evolutionary ecology of pungency in wild chillies. *Proc Natl Acad Sci*, 105: 11808–1181.
 17. Scoville, W. L. (1912). Note *Capsicum*. *J. Am. Pharm. Assoc*, 1: 453.
 18. Wall, M.M. and Bosland, P.W. (1998). Analytical methods for color and pungency of chiles (*Capsicum*). In: Wetzels D, Charalambous G (eds) *Instrumental methods in food and beverage analysis*. Elsevier, Amsterdam, pp 347–373.
 19. Wyatt, L.E., Eannetta, N.T., Stellari, G.M. and Mazourek, M. (2012). Development and application of a suite of non-pungency markers for the *Pun1* gene in pepper (*Capsicum* spp.). *Mol Breeding*, 30: 1525-1529.
 20. Stewart, C., Kang, B.C., Liu, K., Mazourek, M., Moore, S.L., Yoo, E.Y., Kim, B.D. and Paran, I. (2005). The *Pun1* gene for pungency in pepper encodes a putative acyltransferase. *The Plant Journal*, 42: 675–688.
 21. Blum, E., Liu, K., Mazourek, M., Yoo, E.Y., Jahn, M. and Paran, I. (2002). Molecular mapping of the *C* locus for presence of pungency in *Capsicum*. *Genome*, 45: 702–705.
 22. Minamiyama, Y., Kinoshita, S., Inaba, K. and Inoue, M. (2005). Development of a cleaved amplified polymorphic sequence (CAPS) marker linked to pungency in pepper. *Plant Breeding*, 124: 288–291.
 23. Lee, C.J., Yoo, E.Y., Shin, J.H., Lee, J., Hwang, H.S. and Kim, B.D. (2005). Non pungent capsicum contains a deletion in the capsaicinoid synthase gene which allows early detection of pungency with SCAR marker. *Mol. Cells*, 19: 262-267.
 24. Truong, H.T.H., Kim, K.T., Kim, S., Kim, H.R., Cho, M-C. and Woo, J-G. (2009). Development of gene-based markers for the *Pun1* pungency gene in pepper (*Capsicum* spp.) for marker assisted selection. *Hortic Environ Biotechnol*, 50: 358–365.
 25. Garces-Claver, A., Fellman, S.M., Gil-Ortega, R., Jahn, M. and Andres, A.M.S. (2007). Identification, validation and survey of a single nucleotide polymorphism (SNP) associated with pungency in *Capsicum* spp. *Theor Appl Genet*, 115: 907–916.
 26. Doyle, J.J. and Doyle, J.L. (1990). Isolation of plant DNA from fresh tissue. *Focus*, 12: 13–15.
 27. Drummond, A.J., Ashton, B., Buxton, S., Cheung, M., Cooper, A., Duran, C., Field,

- M., Heled, J., Kearse, M., Markowitz, S., Moir, R., Stones-Havas, S., Sturrock, S., Thierer, T. and Wilson, A. (2010). Geneious v5.3. Available at <http://www.geneious.com>.
28. Aza-Gonzalez, C., Nunez-Paleniuss, G.H. and Ochoa-Alejo, N. (2011). Molecular biology of capsaicinoid biosynthesis in chili pepper (*Capsicum* spp.) *Plant Cell Rep*, 30: 695–706.
29. Kim, M., Kim, S., Kim, S. and Kim, B.D. (2001). Isolation of cDNA clones differentially accumulated in the placenta of pungent pepper by suppression subtractive hybridization. *Mol. Cell*, 11: 213–219.
30. Pierre, St, B. and De Luca, V. (2000). Evolution of acyltransferase genes: origin and diversification of the BAHD superfamily of acyltransferases involved in secondary metabolism. *Recent Adv. Phytochem.* 34, 285–315.
31. Pickersgill, B. (2007). Domestication of plants in the Americas: insights from Mendelian and molecular genetics. *Ann Bot*, 100: 925–940.

Selection of Foot and Mouth Disease Virus Candidate Vaccine Strain for Serotype O

S. Yuvaraj, M. Madhanmohan, Ralla Kumar, Kankipati Manikumar, Jangam Anil Kumar, V. A. Srinivasan and Ramesh Matur*

Foot and Mouth Disease Virus Laboratory, Research and Development Centre, Indian Immunologicals Limited, Gachibowli, Hyderabad 500032, Andhra Pradesh, India

*For Correspondence – maturr@indimmune.com

Abstract

India is endemic for foot and mouth disease with the prevalence of O, A and Asia 1 serotypes. Serotype O accounts for nearly 80 % of the FMD outbreaks which were grouped as Middle East-South Asia (ME-SA) topotype by phylogenetic analysis. Serotype O outbreaks are dominated by Ind 2001 lineage. Among these Ind 2001 lineage field isolates five candidate strains were selected and used for raising rabbit convalescent sera (RCS). These RCS samples were used for antigen matching studies with 21 field isolates containing 11 Ind 2001 isolates and few representative isolates from other lineages like PanAsia, PanAsia-2 and minor group by the two-dimensional microneutralization test (2D-MNT). The serological spectrum of the selected five Ind 2001 isolates was compared with the field isolates by calculation of the relative homology value (r) from the serum neutralization antibody titers. Among the five vaccine candidates, O/KEPt/07/2010 showed broad serological spectrum followed by O/PUJ/01/2012 and O/UPMe/10/2009.

Key words: Serotype O, Ind 2001 lineage, Rabbit convalescent serum and Antigenic relationship (r 'value)

Introduction

Foot and mouth disease (FMD) is a disease of cloven hoofed animals causing vesicular eruptions of the tongue and foot epithelium and

has very high morbidity but a low mortality. The disease is prevalent in most of the developing countries of Asia, South America and Africa (1). FMD is considered as an important criterion for the trade of animal and animal by-products in the lucrative European and American markets (2). The countries which achieved complete FMD free status was mainly through a regular vaccination programme combined with strict bio security regulations. The causative agent for FMD is foot and mouth disease virus (FMDV) belonging to the family *Picornaviridae* and genus *Aphthovirus*.

Globally seven serotypes of foot and mouth disease virus are reported viz., O, A, C, Asia 1, Southern African Territory 1 (SAT1), SAT2 and SAT3. Among these, serotype O is reported in most of the FMD prevalent countries. Serotype O isolates exists as 11 distinct topotypes which are further divided into different lineages within each topotypes. FMDV serotypes O, A and Asia 1 are prevalent in the Indian subcontinent among which serotype O accounts for more than 80 % of the outbreaks (3, 4, 5). All the Indian serotype O isolates fall under a single topotype Middle East – South Asia (ME-SA) which is also most commonly reported in many of the Asian countries. In India, ME – SA topotype exists as three distinct lineages viz., PanAsia, PanAsia-2 and Ind 2001 along with a minor group.

Quasi species property of FMDV causes a continuous change in the viral antigenic epitopes

to escape the host immune mechanisms (6). In order to maintain a vaccine with broader serological spectrum for the newly evolving field strains of FMDV, a continuous matching of field isolates with the commonly used vaccine strains becomes necessary (7). Use of serologically appropriate strains for vaccination will help in the control of disease outbreaks.

Recent outbreaks are predominated by Ind 2001 lineage isolate reported throughout the country (4). Since 2003, O/IND/R2/75 vaccine strain is used in commercial trivalent vaccines in India. Vaccine matching studies of Ind 2001 field isolates with bovine vaccinate serum from O/IND/R2/75 showed that all the isolates are homologous to the current vaccine strain showing a higher relative homology value (r' value >0.30) (8). However, increased number of outbreaks due to this Ind 2001 lineage isolates necessitates selection of a new vaccine candidate panel among this lineage. This would be helpful for the adoption in vaccination programme within a short period of time, if any further antigenic variants arise in the field. Thus, the current study was planned to select a panel of candidate strains among the widely distributed and highly prevalent Ind 2001 lineage group.

Materials and methods

Cells and viruses: A baby hamster kidney (BHK-21) cell was obtained from the tissue culture laboratory of R&D centre, Indian Immunologicals Limited (IIL), Hyderabad. Five strains from Ind 2001 lineage namely O/UPMe/10/2009, O/KAM/04/2010, O/KEPt/07/2010, O/TNNa/12/2011 and O/PUJ/01/2012 were selected for the antigen matching studies with the field isolates. Twenty one serotype O isolates isolated from 12 different states or union territories of India from 2001 to 2012 outbreaks were included in the study (Table 1). The field isolates for vaccine matching study were included from all of the prevalent serotype O lineages in India. All these isolates are maintained in the virus repository of FMDV laboratory, IIL, Hyderabad.

Preparation of rabbit convalescent serum (RCS): The viral master bank cultures stored in the virus repository were revived by passaging once or twice in the baby hamster kidney cell line-21 (BHK-21) monolayer flasks to produce a complete cytopathic effect (CPE). The cultures showing complete CPE within 24 hrs were used for the preparation of rabbit convalescent serum (RCS). The RCS was raised in New Zealand White rabbits by inoculating 1 ml of BHK-21 monolayer adapted viral suspension cultures through intravenous route. The rabbits were given booster dose on 21 days post inoculation (dpi) and bled on 35 dpi (9).

Microneutralization test: RCS samples of the five Ind 2001 candidate vaccine panel isolates namely O/UPMe/10/2009, O/KAM/04/2010, O/KEPt/07/2010, O/TNNa/12/2011 and O/PUJ/01/2012 were used for vaccine matching studies by using two-dimensional microneutralization test (2D-MNT) with BHK-21 cells (10). Briefly, in a 96 well cell culture plate (Nuncclon™ Denmark) the serum samples was two fold diluted and added with different log dilutions of the virus suspension samples with appropriate controls. The BHK-21 monolayer cells were added to all wells and the plates were sealed and incubated for 48 hrs at 37°C. After 48 hrs the plates were stained with 0.4 % naphthalene black stain containing formaldehyde. The serum neutralizing end point titer was calculated as reciprocal of the last dilution that neutralizes 100TCID₅₀ virus particles in 50% of the wells. The MNT was repeated three times and the mean antibody titers were statistically analyzed and average value was taken for calculation of r' value (9, 11).

Determination of r' value: The serum neutralization antibody titer of the RCS against 100 TCID₅₀ (tissue culture infecting dose) of the homologous candidate strain and the same dose of a field isolate are compared to determine the antigenic relationship of the field virus to the candidate vaccine strain as follows.

If the antigenic relationship between the isolates was more than 0.3 the isolates were

considered homologous and known to be protective against this field isolate. Conversely if less than 0.30 the isolates were said to be heterologous and to be different from the vaccine strain.

Results

With the phylogenetic analysis of Ind 2001 lineage field isolates, five strains from different branches of Ind 2001 group were selected as vaccine candidate strains. The serum

neutralization antibody titer was estimated by MNT and used for calculation of the 'r' value. Antigenic relationship between five of the selected candidate Ind 2001 strains and the twenty one selected field isolates was expressed as relative homology 'r' value and are as shown in Table 2.

Of the 21 type O field isolates used for antigen matching 17 of them showed an 'r' value of >0.3 with O/KEPt/07/2010 RCS. RCS samples from O/PUJ/01/2012 and O/UPMe/10/2009

Table 1. List of serotype O foot and mouth disease viruses used in this study.

S. No	Virus	Source			
		Village	District	State	Tissue
1	O/MER/57/2001	Eleven Miles	Rihboi	Meghalaya	TE
2	O/MAA/28/2002	Hungaewadi	Ahmednagar	Maharashtra	TE
3	O/KETr/119/2002	Mannuthy	Thrissur	Kerala	TE
4	O/POP/144/2002	Thevankudy	Karikal	Pondicherry	TE
5	O/ORC/20/2003	NA	Cuttack	Orissa	TE
6	O/RAJ/47/2003	Bassi	Jaipur	Rajasthan	TE
7	O/APR/01/2005	Kokapet	Ranga Reddy	Andhra Pradesh	TE
8	O/PUL/88/2005	Ludhiana	Ludhiana	Punjab	TE
9	O/APR/20/2006	NA	Rangareddy	Andhra Pradesh	TE
10	O/KEI/18/2008	Manakkad	Idukki	Kerala	TE
11	O/CHRn/05/2009	Godmara	Rajnandgaon	Chattisgarh	TE
12	O/UPMe/10/2009	Meerut	Meerut	Uttar Pradesh	TE
13	O/APR/19/2009	Kokapet	Ranga Reddy	Andhra Pradesh	TE
14	O/APR/23/2009	NA	Ranga Reddy	Andhra Pradesh	TE
15	O/KEKm/27/2009	Veechoor	Kottayam	Kerala	TE
16	O/KAM/04/2010	Hd Kote	Mysore	Karnataka	TE
17	O/KEKm/06/2010	Kurichy	Kottayam	Kerala	TE
18	O/KEPt/07/2010	Peringara	Patahnamthitta	Kerala	TE
19	O/MAP/07/2011	Baramati	Pune	Maharashtra	TE
20	O/TNNa/12/2011	Jedarpalayam	Nammakkal	Tamil Nadu	TE
21	O/PUJ/01/2012	Jalandhar	Jalandhar	Punjab	TE

TE- Tongue epithelium; NA – Not available

showed an 'r' value of >0.30 with 15 and 16 of the 21 field strains used in this study respectively. But only 8 isolates out of twenty one field isolates showed an 'r' value > 0.30 with both O/KAM/04/2010 and O/TNNA/12/2011 RCS samples (Table 2).

Ind 2001 lineage and minor group isolates:
 Among the selected five strains for antigenic characterization, O/KEPt/07/2010 RCS was

homologous to all Ind 2001 isolates used in the study with an 'r' value >0.35. And O/PUJ/01/2012 RCS showed an 'r' value of >0.35 with Ind 2001 isolates except for O/APR/23/2009 (0.18). O/UPMe/10/2009 showed an 'r' value >0.3 with all Ind 2001 isolates except for O/CHRn/05/2009 (0.05) and O/APR/23/2009 (0.05). Seven (63.6%) of the 11 Ind 2001 lineage isolates showed an 'r' value <0.3 with both O/KAM/04/2010 and O/TNNA/12/2011 strains RCS.

Table 2. Relative homology ('r' value) of field isolates with the selected Ind 2001 candidate strains. The antigenic relationship ('r' value) between the field isolates and the selected candidate Ind 2001 strains (O/UPMe/10/2009, O/KAM/04/2010, O/KEPt/07/2010, O/TNNA/12/2011 and O/PUJ/01/2012) was derived from log SN₅₀ titer values calculated by MNT with the rabbit convalescent sera samples (RCS).

S. No	Virus	Group	Ind 2001 strains 'r' value				
			O/UPMe/10/2009	O/KAM/04/2010	O/KEPt/07/2010	O/TNNA/12/2011	O/PUJ/01/2012
1	O/MAA/28/2002	PanAsia	0.87	0.11	>1.00	0.33	0.64
2	O/POP/144/2002	PanAsia	0.34	0.11	0.28	0.05	0.29
3	O/APR/20/2006	PanAsia	>1.00	>1.00	>1.00	>1.00	>1.00
4	O/MAP/07/2011	PanAsia	0.44	0.07	0.71	0.06	0.35
5	O/KETr/119/2002	PanAsia-2	0.28	0.76	0.23	0.15	0.13
6	O/RAJ/47/2003	PanAsia-2	0.75	>1.00	0.71	0.09	0.89
7	O/KEI/18/2008	Ind 2001	>1.00	0.07	>1.00	0.93	0.65
8	O/CHRn/05/2009	Ind 2001	0.05	0.03	0.67	0.04	0.41
9	O/UPMe/10/2009	Ind 2001	1.00	>1.00	>1.00	0.90	>1.00
10	O/APR/19/2009	Ind 2001	>1.00	0.25	>1.00	0.07	>1.00
11	O/APR/23/2009	Ind 2001	0.05	0.14	0.38	0.05	0.18
12	O/KEKm/27/2009	Ind 2001	>1.00	0.36	>1.00	0.26	>1.00
13	O/KAM/04/2010	Ind 2001	0.31	1.00	0.70	0.01	0.34
14	O/KEKm/06/2010	Ind 2001	>1.00	0.07	>1.00	>1.00	0.81
15	O/KEPt/07/2010	Ind 2001	0.88	0.21	1.00	0.11	0.34
16	O/TNNA/12/2011	Ind 2001	0.88	0.24	>1.00	1.00	0.33
17	O/PUJ/01/2012	Ind 2001	0.59	0.64	>1.00	0.02	1.00
18	O/MER/57/2001	Minor	>1.00	0.21	>1.00	>1.00	0.08
19	O/ORC/20/2003	Minor	0.26	0.03	0.20	0.11	0.11
20	O/APR/01/2005	Minor	0.18	0.69	0.15	0.01	0.06
21	O/PUL/88/2005	Minor	>1.00	0.15	0.91	>1.00	>1.00

All the five selected candidate strain RCS showed an 'r' value of <0.3 with at least one or more of the 4 minor group isolates. One field isolate from the minor group, O/ORC/20/2003 showed an 'r' value of <0.3 with all five RCS samples used in the analysis.

PanAsia and PanAsia-2 lineage isolates : All four PanAsia field strains used in the study showed an 'r' value of >0.3 with O/UPMe/10/2009 RCS sample. O/KEPt/07/2010 and O/PUJ/01/2012 RCS samples were homologous to all the PanAsia isolates tested except O/POP/144/2002. O/KAM/04/2010 and O/TNNA/12/2011 RCS samples showed a relatively lesser 'r' value (<0.30) with all PanAsia field isolates used in the study. An isolate of the PanAsia group, O/APR/20/2006 was homologous to all the RCS samples tested.

Both the PanAsia-2 lineage field isolates used in this study were homologous to O/KAM/04/2010 RCS tested. The PanAsia-2 lineage isolate O/RAJ/47/2003 was homologous to O/UPMe/10/2009, O/KEPt/07/2010 and O/PUJ/01/2012 RCS samples. However, another PanAsia-2 isolate O/KETr/119/2002 was heterologous to these three candidate strains. Neither of the two PanAsia-2 isolates showed an 'r' value of >0.3 with RCS of O/TNNA/12/2011.

Discussion

In India, Ind 2001 lineage isolates started showing its distribution throughout the country since 2009 (3, 4). Currently used type O vaccine strain, O/IND/R2/1975 was reported to neutralize all Ind 2001 lineage isolates (PD-FMD, 2011).

The use for RCS for the vaccine matching studies had been reported to produce the results comparable to that of BVS (9, 12). Among the 21 isolates used in the study, 11 of them were from Ind 2001 with 4 and 2 from PanAsia and PanAsia-2 respectively and as much as four isolates were from minor groups. The selected candidate Ind 2001 strains showed a complete cytopathic effect (CPE) in BHK-21 monolayer cells within 18 to 24 hrs with high titers. When these strains were used for immunizing

rabbits, all the animals showed high neutralizing ($\log SN_{50} > 2.0$ in MNT) homologous antibody titers.

Based on the analysis of 'r' value between the field isolates and five selected candidate strain RCS samples the antigenic diversity was calculated. Among the five selected strains, only O/KEPt/07/2010 was homologous to all Ind 2001 isolates (100 %) and showed an 'r' value of >0.70 with all PanAsia isolates. RCS from O/KEPt/07/2010 showed an antigenic coverage of at least 80.9 % of the total 21 field isolates tested. RCS from O/PUJ/01/2012 and O/UPMe/10/2009 were able to antigenically cover 90.9 % and 81.8 % of Ind 2001 isolates used in this study and neutralized 71.4 % and 76.1 % of the 21 field isolates respectively with an 'r' value >0.30. Other two strains O/KAM/04/2010 and O/TNNA/12/2011 RCS showed a reduced antigenic reactivity even within the Ind 2001 isolates neutralizing only <50 % Ind 2001 isolates. More than 50 % of total 21 isolates used in this study were divergent from O/KAM/04/2010 and O/TNNA/12/2011 strains.

Although all the selected candidate strains showed good immunogenicity, O/KEPt/07/2010 showed a broad serological spectrum among the five with the field strains tested. The antigenic analysis of isolates in this study provided a panel of suitable vaccine candidate strains for further vaccine matching studies to select an alternate strain in case of an emergency.

Conclusion

The antigen matching studies with newly evolved strains under the field conditions is necessary for the development of an effective vaccine strain in case of emergency in short time. In this study, antigenic comparison of the 21 field isolates was carried out with the RCS samples raised against five Ind 2001 lineage isolates (commonly reported lineage post 2009) by MNT. Among the five sera tested, O/KEPt/07/2010 RCS showed a broad serological spectrum with isolates from different lineages followed by O/PUJ/01/2012 and O/UPMe/10/2009.

References

1. Rweyemamu, M., Roeder, P., Mackay, D., Sumption, K., Brownlie, J., Leforban, Y., Valarcher, J.F., Knowles, N.J. and Saraiva, V. (2008). Epidemiological patterns of foot-and-mouth disease worldwide. *Transbound Emerg Dis.*, 55: 57–72.
2. Forman, S., Le Gall, F., Belton, D., Evans, B., François, J.L., Murray, G., Sheesley, D., Vandersmissen, A. and Yoshimura, S. (2009). Moving towards the global control of foot and mouth disease: an opportunity for donors. *Rev sci tech Off int Epiz.*, 28: 883-896.
3. PD-FMD Annual Report, 2010-11. (2011). Project Directorate on Foot and mouth disease, Mukteswar.
4. Subramaniam, S., Pattnaik, B., Sanyal, A., Mohapatra, J.K., Pawar, S.S., Sharma, G.K., Das, B. and Dash, B.B. (2012). Status of Foot-and-mouth Disease in India. *Transbound Emerg Dis.*, DOI: 10.1111/j.1865-1682.2012.01332.x
5. Pattnaik, B., Subramaniam, S., Sanyal, A., Mohapatra, J.K., Dash, B.B., Ranjan, R. and Rout, M. (2012). Foot-and-mouth Disease: Global Status and Future Road Map for Control and Prevention in India. *Agric Res.*, 1: 132–147.
6. Holland, J.J., de la Torre, J.C. and Steinhauer, D.A. (1992). RNA virus populations as quasispecies. *Current Topics in Microbiol Immunol.*, 176: 1-20.
7. Paton, D.J., Valarcher, J.F., Bergmann, I., Matlho, O.G., Zakharov, V.M., Palma, E.L. and Thomson, G.R. (2005). Selection of foot-and-mouth disease vaccine strains-a review. *Rev sci tech Off int Epiz.*, 24: 981–993.
8. PD-FMD Annual Report, 2009-10. (2010). Project Directorate on Foot and mouth disease, Mukteswar.
9. Srinivasan, V.A., Ouldrige, E.J., Head, M. and Rweyemamu, M.M. (1983). A serological study of Indian type O foot and mouth disease virus isolates. *Rev sci tech Off int Epiz.*, 2: 145-151.
10. Rweyemamu, M.M., Booth, J.C., Head, M. and Pay, T.W.F. (1978). Microneutralization tests for serological typing and subtyping of foot-and-mouth disease virus strains. *J Hyg.*, 81: 107–123.
11. Rweyemamu, M.M. (1984). Antigenic variation in foot and mouth disease; studies based on the virus neutralization reaction. *J Biol Stand.*, 12: 323-337.
12. Rudreshappa, A.G., Sanyal, A., Mohapatra, J.K., Subramaniam, S., Das, A.B., Singanallur, N.B., Jangam, A., Muthukrishnan, M., Villuppanoor, S.A. and Pattnaik, B. (2012). Emergence of antigenic variants with in serotype A foot and mouth disease virus in India and evaluation of a new vaccine candidate panel. *Vet Microbiol.*, 158: 405-409.

***In Silico* Design of Inhibitors for β -Secretase: Implications for Alzheimer's Disease**

S. Sai Madhukar¹, Anand Solomon², Viswanath Das³, K. Anil Kumar⁴ and S. Krupanidhi⁶*

¹Department of Health Informatics, Karolinska Institute of Medical Sciences, Stockholm, Sweden

² Sankar Foundation Research Institute, Vishakapatnam 530047, India

³ School of Biological Sciences and Centre for Biodiscovery, Victoria University of Wellington, Wellington, New Zealand

⁴ Tata Chemicals Ltd, Innovation Center, Pune 412108, India, ⁶ Department of Biotechnology, Vignan University, Vadlamudi 522213. India.

*For Correspondence - krupanidhi.srirama@gmail.com

Abstract

β -secretase is regarded as one of the best characterized targets for Alzheimer's disease therapy. β -secretase 1 protease plays an important role in cleaving amyloid precursor protein and further the formation of pathogenic β -amyloid plaques in the brain, thereby causing Alzheimer's disease. The present work reports the docking studies of a series of analogues based derivatives of phenyl-piperazine, cyclic urea, N-phenyl-1-arylamide and N-phenylbenzenesulfonamide. The structure of β -secretase 1 complexed with a ligand, 2-amino-6-propylpyrimidin-4(3H)-one was retrieved from Protein Data Bank and used in the present study. All the derivatives and clinically used drugs for Alzheimer's disease, such as, tacrine, razadyne, exelon and aricept were energy minimized and docked with the receptor. The docked positions of all derivatives were compared with tacrine as the standard drug. Four of the derivatives showed better docking score and identical hydrogen bonds with that of tacrine.

Key words: β -secretase, amyloid precursor protein, β -amyloid plaques, phenyl-piperazine, cyclic urea, N-phenyl-1-arylamide, N-phenylbenzenesulfonamide.

Introduction

Zilka and Novak (1) portrayed that Alois Alzheimer in the year 1907 was the first person

to describe symptoms and pathology of progressive and lethal neurodegenerative disorder called Alzheimer's disease (AD). It is an irreversible disorder and slowly destroys the memory and thinking skills (2-4). It has been the biggest unmet medical need in neurology, though, once considered the same as a rare disorder. AD is treated as a major public health problem seriously affecting millions of older people and their families. Further, Ferreira *et al*, (5) elucidated that AD is a metabolic syndrome for the reason that there is a decline in the glucose oxidation due to neuronal mitochondrial dysfunction.

Amyloid precursor protein (APP) is a ubiquitous membrane protein with four domains. Of which, three are extended outside the cell membrane and a small domain across the cell membrane (6). The small domain functions as an anchor for APP. Its role both in receptor function and neuronal growth is well authenticated (7). APP is cleaved into several functional fragments by a set of proteases, namely secretases. A large portion of cleaved APP is released outside the cell and helps in regulation of nerve growth. The small domain, a 39-42 amino acid peptide, however, becomes a free peptide, changing its form from helix to β -sheet and stacks into long tangled fibrils called as beta amyloid ($A\beta$) plaques (8,9). Further, its abundance in the synapse of neurons as a

consequence of unmanaged proteolysis became the primary cause for the ailment in AD patients.

β -secretase (BACE 1) is aspartic protease that is generally involved in the maturation of cytosolic proteins. This enzyme is normally translocated in the endoplasmic reticulum and the Golgi, where new proteins are processed. Both β -secretase and γ -secretase cleave the membrane APP close to c-terminus one after the other and the resultant small peptide stacks at synaptic junctions as A β plaques and thus impairs the neuronal propagation (9). Therefore, intracellular transport of β -secretase into the endoplasmic reticulum and the Golgi needs to be understood along with its possible inhibitors as a prelude to the pathogenesis of AD. Invariably the inhibition of both the enzymes viz., β -secretase and γ -secretase possibly helps in averting Alzheimer's by eliminating the formation of A β peptides. The major drawback of inhibiting γ -secretase is that it affects the Wnt/notch signal pathway which is related to the growth of the somatic cells (10-12). Thus, inhibiting β -secretase would prove to be a more suitable option for the A β mediated AD therapy.

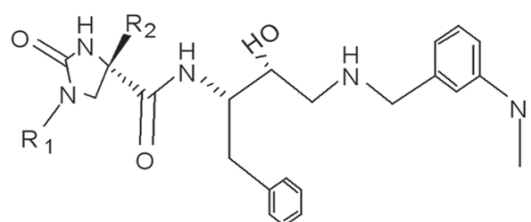
In general, the drug targets for novel human drugs focus on the latest developments in the fields of medicinal chemistry, transmembrane receptor biology and enzymes. Neuronal metabolic dysfunctions have been suggested as the primary cause for the neurodegenerative illness⁵. Vassar (3,10) reviewed the initial characterization of BACE-1 and BACE-2 along with their post-translational modifications and based on the available literature on BACE-1, he deduced that BACE is the prime therapeutic target for AD. It is also shown that casein kinase 1 (CK1) represents yet another therapeutic target for prevention of A β formation in AD that prompted a deep concern because of the fact that CK1 couples with Wnt mediated signal pathways (11). Hence, the docking studies have been performed to design suitable lead-molecules (drugs) for the target enzyme (BACE 1) to prevent the formation of physiological culprit viz., A β peptides.

Methodology

Generation of the three dimensional structure of molecules: The cyclic urea derivatives (13) viz., N-phenyl-1-arylamide (Table-1A, 1B), phenyl-piperazine derivatives (9) (Table-2) and N-phenylbenzenesulfonamide derivatives (15) (Table-3) were minimized using 100 cycles of steepest decent and 1000 cycles of conjugate gradient algorithms with OPLS_2005 force field. The structures of the derivatives used in this study are given in table 1A, 1B, 2, and 3. The same method of minimization was adopted for the structures of existing drugs in the market viz., tacrine, razadyne, excelon and aricept (Table 4).

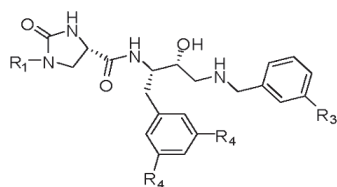
Protein preparation: The structure of BACE-1 complexed with a ligand viz., EVO (2-amino-6-

Table 1A. Cyclic urea derivatives



Compound	R ₁	R ₂
3	Benzyl	H
4	H	H
5	n-Butyl	H
6	Phenethyl	H
7	Phenoxy-ethyl	H
8	Benzyl	Methyl
9	Benzyl	Benzyl
10	3,5-Dibromophenyl	H
11	Phenyl	H

Table 1B. Cyclic Urea derivatives



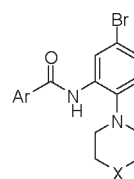
Compound	R ₁	R ₃	R ₄
12	(3-Methoxy)benzyl	-N(CH ₃) ₂	H
13	(3,5-Dimethoxy)benzyl	-N(CH ₃) ₂	H
14	(4-F)Benzyl	-N(CH ₃) ₂	H
15	(3,4-diF)Benzyl	-N(CH ₃) ₂	H
16	(2,4-diF)Benzyl	-N(CH ₃) ₂	H
17	(3,5-diF)Benzyl	-N(CH ₃) ₂	H
18	(2,4,5-triF)Benzyl	-N(CH ₃) ₂	H
19	(2-CF ₃)Benzyl	-N(CH ₃) ₂	H
20	(4-CF ₃)Benzyl	-N(CH ₃) ₂	H
21	Benzyl	-CF ₃	H
22	Benzyl	-OCF ₃	H
23	(3,5-diF)Benzyl	i-Propyl	H
24	(3,5-diF)Benzyl	t-Butyl	H
25	Benzyl	-N(CH ₃) ₂	F
26	(3,5-diF)Benzyl	t-Butyl	F

propylpyrimidin-4(3H)-one) was retrieved from PDB database (3HVG). The structure of the protein was minimized after taking into consideration the inaccuracies in the protein structure, such as missing hydrogen bonds, incorrect bond order assignments, charge states, the orientation of various groups, etc.

Receptor grid generation: The receptor grid generation searches for favourable interactions between the ligand molecules and target protein. By using the options in each tab of the receptor grid generation panel, the receptor structure was defined and the co-crystallized ligand was

excluded. The position and size of the active sites represented by the receptor grids and glide constraints were determined by using BACE-1 as the receptor (Fig.1-4).

Table 2. Phenyl-piperazine derivatives



Compound	Ar	X
3a		N-Boc
3b		N-Benzyl
6a		N-Boc
6b		N-Benzyl
7a		N-Boc
7b		N-Benzyl
8a		N-Boc
8d		
9a		N-Boc
9d		
10a		N-Boc

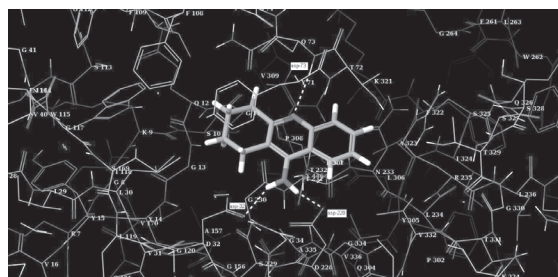


Fig. 1. Tacrine bound to BACE-1 at Asp-73, Asp-32 and Asp-228.

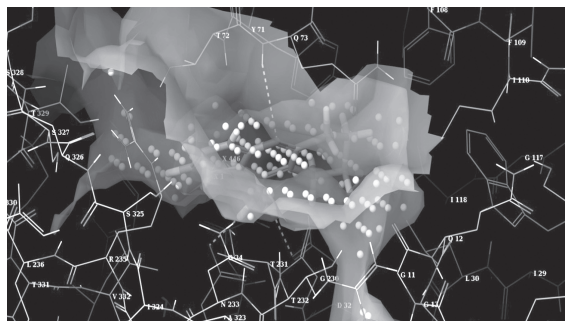


Fig. 2. The site map of tacrine bound to BACE-1.

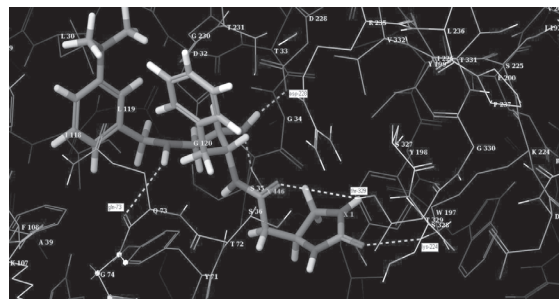
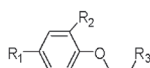


Fig. 3. Derivative 4 bound to BACE-1 at Asp-228, Gln-73, Thr-329 and Lys-224.

Table 3. N-phenyl-1-arylamide and N-phenylbenzenesulfonamide derivatives.



Compound	R ₁	R ₂	R ₃
26	Br	1-Naphthalenylacetamide	
27	Br	Phenylpropanamide	
28a	Br	4-Bromobenzenesulfonamide	
28b	Br	Benzenesulfonamide	
33a	Br	1-Naphthalenylacetamide	
33b	Br	1-Naphthalenylacetamide	
33c	Br	1-Naphthalenylacetamide	
33d	Br	1-Naphthalenylacetamide	
33e	Br	1-Naphthalenylacetamide	
33f	Br	1-Naphthalenylacetamide	
33g	H	1-Naphthalenylacetamide	

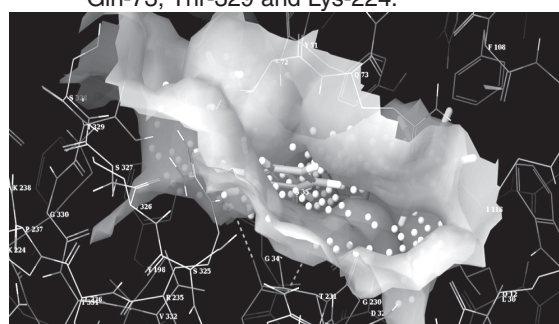
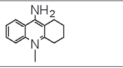
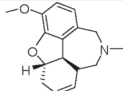
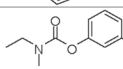
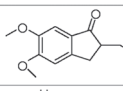
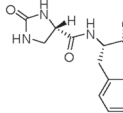
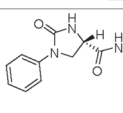
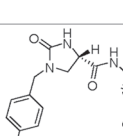


Fig. 4. The site map of derivative 4 bound to BACE-1.

Table 4. Existing drugs for Alzheimer's disease

Name	Structure
Tacrine	
Razadyne	
Exelon	
Aricept	

Table 5. The docking scores of the four drugs and derivatives

Name	Structure	Docking score
Tacrine		-5.38
Razadyne		-4.63
Exelon		-3.92
Aricept		-5.26
Compound 4		-5.85
Compound 11		-5.42
Compound 14		-5.50

Docking studies: Using GLIDE docking in Schrödinger, docking of the mentioned derivatives with BACE-1 receptor was performed (Table-5). A maximum of 10 docked poses were generated for each of the derivatives.

Calculation of ADMET properties: Using QikProp software in Schrödinger Suite, the properties and descriptors of the derivatives and also of the existing drugs were calculated (Table-6).

Results and Discussion

Docking results of the known drugs: All the four existing drugs for AD (Table-4) are acetylcholinesterase inhibitors (16). They are presently approved by the US Food and Drug Administration to treat patients with cognitive deficits seen in AD; however, these inhibitors have limited effectiveness in delaying progression

of AD (17).

In the present study, the focus is on BACE-1 since its involvement in signal transduction is least. The drugs shown in Table-4 were docked with BACE-1 and tacrine was used as the reference drug because it showed the maximum docking score (Table 5).

Docking results of all compounds: The rest of the derivatives were also docked with BACE-1; the docking scores of derivatives were compared with that of tacrine along with hydrogen bonding interactions. It is inferred from fig. 3 and 4 that derivative compound 4 showed a similar hydrogen bonding as that of tacrine with a higher docking score (Table 5) and the site map of compound 4 bound to four amino acid residues of BACE-1 .

In addition to BACE-1, the CK1 family of serine–threonine protein kinases, found in all eukaryotic organisms, is considered as the target to avert AD and its isoforms have been reported to play a role in phosphorylation of ‘Disheveled’ in the Wnt signaling pathway (11). The reason behind must have been that the inhibitor of CK1 (IC261) was also reported to inhibit γ -secretase (18). As the participation of γ -secretase is known in notch signal pathway (12), which is related to the growth of the somatic cells, CK1 inhibitors might not have been the correct choice.

Epidemiologic evidence also revealed that non-steroidal anti-inflammatory drugs (NSAIDs) delay the onset of dementia seen in AD. Further, it is suggested upon revisiting the original Alzheimer’s Disease Anti-inflammatory Prevention Trial hypothesis that NSAIDs reduce AD risk, wherein asymptomatic individuals treated with conventional NSAIDs such as naproxen experienced reduced AD incidence, with sufficiently a long delay ranging between 2 to 3 years (19).

It is observed that derivative compounds viz., 4, 11, 14, and 24 showed identical hydrogen bonding with the protein receptor as that of tacrine (Table 5 and 6). It is also noticed that the

Table 6. ADMET properties of tacrine and the four derivatives

Principal Descriptors		Tacrine	Compound 4	Compound 11	Compound 14	Compound 24
Solute	Molecular Weight	198.267	439.556	501.63	533.64	564.674
Solute	Dipole Moment (D)	4.645	6.653	7.398	9.552	9.251
Solute	Total SASA	428.308	794.461	847.06	878.55	920.461
Solute	Hydrophobic SASA	184.95	340.323	302.4	326.81	361.544
Solute	Hydrophilic SASA	54.839	162.518	131.31	120.28	119.224
Solute	Carbon Pi SASA	188.52	291.62	413.36	384.49	357.799
Solute	Weakly Polar SASA	0	0	0	46.968	81.894
Solute	Molecular Volume (A ³)	706.265	1450.57	1587.2	1652.1	1749.67
Solute	vdW PSA	33.824	123.247	106.42	105.95	103.206
Solute	No. of Rotatable Bonds	1	12	11	13	13
Solute as Donor	Hydrogen Bonds	1.5	4	3.25	3.25	3.25
Solute as Acceptor	Hydrogen Bonds	2	7.7	7.95	7.95	6.95
Solute Globularity	Sphere = 1	0.895	0.78	0.777	0.769	0.763
Solute Ionization						
Potential (eV)		8.076	7.989	8.036	8.045	9.226
Solute Electron						
Affinity (eV)		0.548	“0.276	“0.036	0.012	0.229
Predictions for Properties						
QP Polarizability	Angstroms ³	23.269M	46.977M	54.251M	55.287M	58.937M
QP log P	For hexadecane/gas	6.901	15.939M	17.679M	17.741M	18.255M
QP log P	For octanol/gas	10.756	25.890M	27.645M	28.341M	29.120M
QP log P	For water/gas	6.352	17.171M	16.935M	16.318M	15.217M
QP log P	For octanol/water	2.574	2.733	3.977	4.595	5.708
QP log S	For aqueous solubility	“3.093	“3.658	“4.897	“5.311	“6.529
QP log S	Conformation independent	“2.93	“4.072	“5.63	“6.268	“7.276
QP log K	HSA Protein Binding	0.062	0.04	0.444	0.521	0.954
QP log BB	For brain/blood	0.047	“1.542	“1.151	“1.061	“0.986
No. of Primary Metabolites		3	8	7	8	7
Predicted CNS Activity (“ “ to ++)		+	“ “	“ “	“ “	“
HERG K ⁺ Channel Blockade: log IC ₅₀		“4.122	“5.834	“6.466	“6.451	“6.427
Apparent Caco-2 Permeability (nm/sec)		2991	47	101	129	133
Apparent MDCK Permeability (nm/sec)		1616	31M	65M	153M	245M
QP log K _p for skin permeability		“1.77	“4.398	“3.49	“3.196	“3.271
Jm, max transdermal transport rate		2.718	0.004	0.002	0.002	0
Lipinski Rule of 5 Violations		0	0	1	1	2
Jorgensen Rule of 3 Violations		0	1	1	1	2
% Human Oral Absorption in GI (±20%)		100	73	73	79	72
Qual. Model for Human Oral Absorption		High	Medium	Medium	Medium	Low

A * indicates a violation of the 95% range.
 # stars = 1 An M indicates MW is outside training range.
 QP Breakdown (< for descriptor over training max)

<i>log Po/w</i>					
H-bond Donor	"0.45	"1.2	"0.975	"0.975	"0.975
H-bond Acceptor	"0.974	"3.75	"3.872	"3.872	"3.385
Volume	4.608	9.463	10.355	10.778	11.415
Ac x Dn [^] .5/SASA	0.254	0.86	0.751	0.724	0.604
FISA	"0.38	"1.125	"0.909	"0.832	"0.825
Non-con Amines	0	"0.527	"0.527	"0.527	"0.527
Non-con Amides	0	"0.626	"0.626	"0.626	"0.626
WPSA & PISA	0.221	0.341	0.484	0.629	0.731
Constant	"0.705	"0.705	"0.705	"0.705	"0.705
Total	2.574	2.733	3.977	4.595	5.708
<i>-log S</i>					
H-bond Donor	"0.602	"1.606	"1.305	"1.305	"1.305
H-bond Acceptor	"1.047	"4.032	"4.163	"4.163	"3.639
SASA	8.116	15.055	16.052	16.648	17.443
Ac x Dn [^] .5/SASA	0.572	1.938	1.691	1.631	1.361
Rotor Bonds	"0.163	"1.954	"1.791	"2.116	"2.116
N Protonation	0	"1.22	"1.22	"1.22	"1.22
Non-con Amides	0	"0.74	"0.585	"0.587	"0.568
WPSA	0	0	0	0.205	0.357
Constant	"3.783	"3.783	"3.783	"3.783	"3.783
Total	3.093	3.658	4.897	5.311	6.529
<i>log BB</i>					
Hydrophilic SASA	"0.456	"1.781	"1.451	"1.355	"1.366
WPSA	0	0	0	0.115	0.201
Rotor Bonds	"0.06	"0.723	"0.663	"0.783	"0.783
N Protonation	0	0.399	0.399	0.399	0.399
FOSA	0	0	0	0	0
Constant	0.564	0.564	0.564	0.564	0.564
Total	0.047	"1.542	"1.151	"1.061	"0.986
<i>log PMDCK</i>					
Hydrophilic SASA	"0.562	"1.666	"1.346	"1.233	"1.222
WPSA	0	0	0	0.257	0.449
	0	0	0	0	0
Non-con Amines	0	"0.608	"0.608	"0.608	"0.608
COOH/SO ₃ H Acids	0	0	0	0	0
Constant	3.771	3.771	3.771	3.771	3.771
Total	3.209	1.497	1.817	2.187	2.389

ADMET properties of these four derivatives showed much similarity with tacrine (Table-6). Therefore, based on these results it can be concluded that these four derivative compounds viz., 4, 11, 14 and 24 (Table-5) illustrate promises as potential lead-drugs for the treatment of AD and further studies using *in vitro* and *in vivo* models would generate substantial information for understanding the working mechanism of these drugs.

Conclusions

Through the docking analysis and calculated ADMET properties it can be inferred that, four of the derivatives showed similar ADMET properties with that of tacrine. Furthermore, these four derivatives exhibited a similar hydrogen bonding as that of tacrine with the receptor BACE-1. Since the docking scores of these four derivatives have been better than that of tacrine with the receptor BACE-1, it can be concluded that these four derivatives have a good potential for screening as drugs for AD; however, further *in vitro* and *in vivo* studies need to be planned for confirmation.

Abbreviations

AD, Alzheimer's disease; APP, amyloid precursor protein; A β , amyloid beta; β -secretase 1, BACE-1; CK1, casein kinase 1; NSAID, non-steroidal anti-inflammatory drugs; PDB, Protein Data Bank.

References

1. Zilka, N. and Novak, M. (2006) The tangled story of Alois Alzheimer, Bratisl. Lek. Listy, 107, 343-45.
2. Rego, A.C. (2010) Central and peripheral metabolic changes in neurodegenerative diseases. Curr. Drug Targets, 11, 1192.
3. Vassar, R. (2001) The beta-secretase, BACE: a prime drug target for Alzheimer's disease. J. Mol. Neurosci., 17, 157-70.
4. Iserloh, U., Pan, J., Stamford, A.W., Kennedy, M.E., Zhang, Q., Zhang, L., Parker, E.M., McHugh, N.A., Favreau, L., Strickland, C. and Voigt, J. (2008) Discovery of an orally efficacious 4-phenoxy-pyrrolidine-based BACE-1 inhibitor. Bioorg. Med. Chem. Lett., 18, 418-22.
5. Ferreira, I.L., Resende, R., Ferreira, E., Rego, A.C. and Pereira, C.F. (2010) Multiple defects in energy metabolism in Alzheimer's disease. Curr. Drug Targets, 11, 1193-206.
6. Reinhard, C., Hebert, S.S. and De Strooper, B. (2005) The amyloid-beta precursor protein: integrating structure with biological function. EMBO J., 24, 3996-4006.
7. Turner, P.R., O'Connor, K., Tate, W.P. and Abraham, W.C. (2003) Roles of amyloid precursor protein and its fragments in regulating neural activity, plasticity and memory. Prog. Neurobiol., 70, 1-32.
8. Morgan, C., Colombres, M., Nunez, M.T. and Inestrosa, N.C. (2004) Structure and function of amyloid in Alzheimer's disease. Prog. Neurobiol., 74, 323-49.
9. Cole, S.L. and Vassar, R. (2008) BACE1, structure and function in health and Alzheimer's disease. Curr. Alzheimer Res., 5, 100-20.
10. Cole, S.L. and Vassar, R. (2007) The Basic Biology of BACE1: A Key Therapeutic Target for Alzheimer's Disease. Curr. Genomics. 8, 509-30.
11. Davidson, G., Wu, W., Shen, J., Bilic, J., Fenger, U., Stanek, P., Glinka, A. and Niehrs, C. (2005) Casein kinase 1 gamma couples Wnt receptor activation to cytoplasmic signal transduction. Nature, 438, 867-72.
12. Takada, R., Hijikata, H., Kondoh, H. and Takada, S. (2005) Analysis of combinatorial effects of Wnts and Frizzleds on beta-catenin/armadillo stabilization and Dishevelled phosphorylation. Genes Cells, 10, 919-28.

13. Park, H., Min, K., Kwak, H.S., Koo, K.D., Lim, D., Seo, S.W., Choi, J.U., Platt, B. and Choi, D.Y. (2008) Synthesis, SAR and X-ray structure of human BACE-1 inhibitors with cyclic urea derivatives. *Bioorg. Med. Chem. Lett.*, 18, 2900-4.
14. Garino, C., Pietrancosta, N., Laras, Y., Moret, V., Rolland, A., Quelever, G. and Kraus, J.L. (2006) BACE-1 inhibitory activities of new substituted phenyl-piperazine coupled to various heterocycles: chromene, coumarin and quinoline. *Bioorg. Med. Chem. Lett.*, 16, 1995-9.
15. Huang, W., Yu, H., Sheng, R. and Li J., Hu, Y. (2008) Identification of pharmacophore model, synthesis and biological evaluation of N-phenyl-1-arylamide and N-phenylbenzenesulfonamide derivatives as BACE 1 inhibitors. *Bioorganic & Medicinal Chemistry Letters*, 16, 10190-7.
16. Bolognesi, M.L., Simoni, E., Rosini, M., Minarini, A., Tumiatti, V. and Melchiorre, C. (2011) Multitarget-directed ligands: innovative chemical probes and therapeutic tools against Alzheimer's disease. *Curr. Top. Med. Chem.* 11, 2797-806.
17. Galluzzi, K.E., Appelt, D.M. and Brian, B.J. (2010) Modern care for patients with Alzheimer disease: rationale for early intervention. *J. Am. Osteopath Assoc.*, 110, S37-42.
18. Höttecke, N., Liebeck, M., Baumann, K., Schubeneil, R., Winkler, E., Steiner, H. and Schmidt, B. (2010) Inhibition of gamma-secretase by the CK1 inhibitor IC261 does not depend on CK1delta. *Bioorg. Med. Chem. Lett.*, 20, 2958-63.
19. Breitner, J.C., Baker, L.D., Montine, T.J., Meinert, C.L., Lyketsos, C.G., Ashe, K.H., Brandt, J., Craft, S., Evans, D.E., Green, R.C., Ismail, M.S., Martin, B.K., Mullan, M.J., Sabbagh, M. and Tariot, P.N. (2011) Extended results of the Alzheimer's disease anti-inflammatory prevention trial. *Alzheimers Dement.*, 7, 402-11.

Biosorption Performance of *Adenantha pavonina* Leaf Powder for the Removal of Lead using Central Composite Design

J. Srinivasa Rao^{1*}, C. Kesava Rao² and G. Prabhakar²

¹Department of Chemical Engineering, Bapatla Engineering College, Guntur, India

²Department of Chemical Engineering, S.V. University, Tirupathi, India

*For Correspondence - jsrbec@gmail.com

Abstract

Increase in population has led to the increase in demand for more products to cater the needs of humans and thus increasing the pollution levels. Heavy metal ground pollution is of major concern now a days as ground water is the basic need for mankind. The present investigation is removal of lead from aqueous solutions using a new biosorbent *Adenantha Pavonina* leaf powder. This investigation comprises of equilibrium studies on biosorption of lead and optimization using response surface methodology. The parameters influencing biosorption are agitation time, biosorbent size, pH of the aqueous solution, initial concentration of lead solution, dosage of biosorbent and temperature. The optimum pH for the removal of lead is found to be 5. The optimum biosorbent size for the present study is 63 μm . The Langmuir and Temkin isotherms fitted well with a correlation factor of 0.996, followed by Freundlich. The entire biosorption process followed pseudo second order kinetics. The optimized values obtained through central composite design and one factor at a time process is in good agreement.

Key words: Biosorption, *Adenantha pavonina* leaf powder, Central composite design, Isotherms, Kinetics.

Introduction

Water is no alien to all the living beings upon earth. It has no barrier or bars over

constituencies or continents, as it leaves only 1/4th of the land of whole ecosystem. It may cause anemia, headache, chills, diarrhea and reduction in hemoglobin formation (1). These contaminants are usually generated by different industrial as well as domestic processes and are hazardous to the environment, because they do not naturally degrade (2). Environmental engineers and scientists are faced with the challenging task to develop appropriate low cost technologies for effluent treatment (3). Beyond certain limits, heavy metals are toxic to living organisms and may cause serious hazard to public health (4). For the last decades, biosorption or sorption of contaminants by sorbents of natural origin has gained important credibility due to the good performance and low cost of these complexing materials (5–10). A multitude of biomass types comprising fungal biomass, bacterial biomass, algae, peat etc., have been studied for their biosorption of metals (11–14). Agricultural wastes such as tree bark, peanut skin, hull, tobacco, tomato root tissues and plants waste have been used to remove heavy metals from water (15–17). In view of the above, the authors tried to use a novel biosorbent *Adenantha pavonina* leaf powder to remove lead from aqueous solutions and report the application of Response Surface Methodology using Central Composite Design to develop a mathematical model and predict the response and check the adequacy of the model.

Experimental Procedure

Biosorbent: *Adenanthera Pavonina* leaves were obtained from Bapatla Engineering College surroundings, Guntur. The *Adenanthera Pavonina* leaves were washed thrice with tap water and once with distilled water in order to remove adhering mud, impurities etc. It was dried in sunlight for one week until all the moisture was evaporated. The crispy *Adenanthera Pavonina* leaves were then crushed and grinded to powder, separated using British Standard Sieves (BSS) and stored in dry vacuum packs to prevent moisture penetration and readily used as biosorbent.

Biosorption studies: Preliminary experiments were conducted in 250 ml Erlenmeyer flasks containing 50 ml of 20 mg/L metal solution using single step optimization procedure. The flasks were agitated on an orbital shaker at 180 rpm and samples were taken at predetermined time intervals (1, 3, 5, 10, 15, 20, 25, 30, 40, 50, 60, 90, 120, 150 & 180 min) & centrifuged at 14000 rpm and the supernatant liquid was analysed in Atomic Absorption Spectrophotometer (AAS) - Shimadzu make AA-6300 for final concentrations (18). Similarly the other variables were varied in a wide range: Biosorbent size (63, 75 and 105 μm), pH of the aqueous solution (2, 3, 4, 5, 6, 7 and 8), Initial concentration of lead solution (20, 50, 80, 120 and 150 mg/L), Biosorbent dosage (5, 10, 15, 20, 25, 30, 35, 40 and 50 g/L) and Temperature (283, 293, 303, 313 and 323 K).

Process optimization: Final experimental runs for optimization were obtained through Response Surface Methodology from Design of Experiments (DoE) using STATISTICA software. The extent of biosorption of lead calculated at the preliminary optimum conditions is verified with the final runs for the optimum conditions using Central Composite Design (CCD).

Results and Discussion

Effect of agitation time: Duration of equilibrium biosorption is defined as the time required for heavy metal concentration to reach a constant

value during biosorption. The equilibrium agitation time is determined by plotting the % biosorption of lead against agitation time as shown Fig.1 for the interaction time intervals between 1 to 180 min. For 63 μm size of 10 g/L biosorbent dosage mixed in 50 mL of aqueous solution ($C_0 = 20 \text{ mg/L}$), 55.66% of lead is biosorbed in the first 5 min. The % biosorption is increased briskly up to 60 min reaching 86.52%. Beyond 60 min, the % biosorption is constant indicating the attainment of equilibrium conditions. The maximum biosorption of 86.52% is attained for 60 min of agitation time. The rate of biosorption is fast in

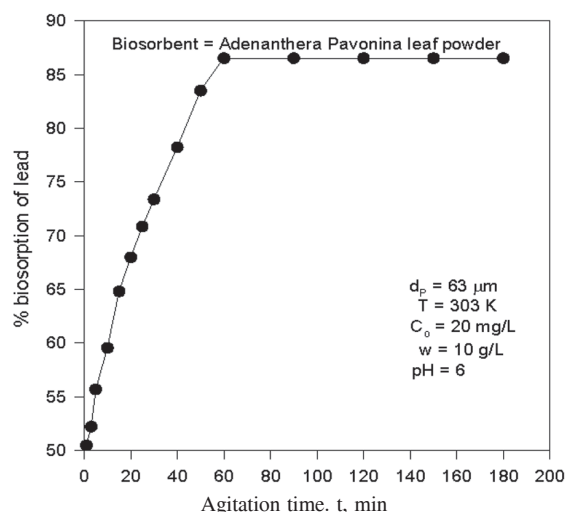


Fig. 1. Effect of agitation time on % biosorption of lead

the initial stages because adequate surface area of the biosorbent is available for the biosorption of lead. As time increases, more amount of lead gets biosorbed onto the surface of the biosorbent due to Vanderwaal's forces of attraction and resulted in decrease of available surface area. The biosorbate, normally, forms a thin one molecule thick layer over the surface. When this monomolecular layer covers the surface, the biosorbent capacity is exhausted. The maximum percentage of biosorption is attained at 60 minutes. The percentage biosorption of lead becomes constant after 60 min. Therefore, all other experiments are conducted at this agitation time.

Effect of biosorbent size: The variations in % biosorption of lead from the aqueous solution with biosorbent size are obtained. The results are drawn in Fig.2 with percentage biosorption of lead as a function of biosorbent size. The percentage biosorption is increased from 80.18% to 86.94% as the biosorbent size decreases from 105 to 63 μm . This phenomenon is expected, as the size of the particle decreases, surface area of the biosorbent increases; thereby the number of active sites on the biosorbent also increases.

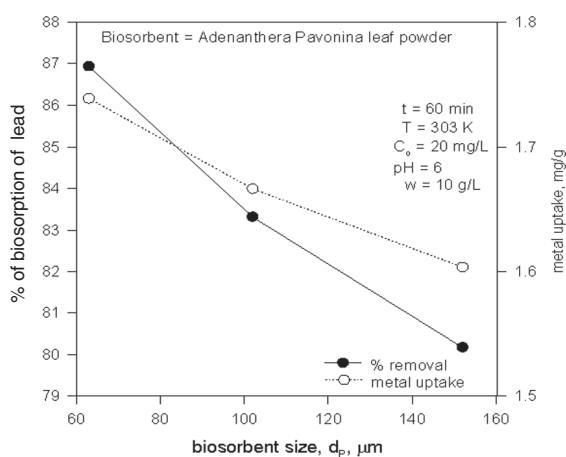


Fig. 2. % biosorption of lead as a function of biosorbent size

Effect of pH: pH controls biosorption by influencing the surface change of the biosorbent, the degree of ionization and the species of biosorbate. In the present investigation, lead biosorption data are obtained in the pH range of 2 to 8 of the aqueous solution ($C_0 = 20 \text{ mg/L}$) using 10 g/L of 63 μm size biosorbent. The effect of pH of aqueous solution on % biosorption of lead is shown in Fig.3. The % biosorption of lead is increased from 64.64% to 91.44% as pH is increased from 2 to 5 and decreased beyond the pH value of 6. % biosorption is decreased from pH 6 to 8 reaching 62.12% from 84.32%. Since the pH of aqueous solution influences the solution chemistry of the heavy metals, the binding of metal ions by surface functional groups is strongly pH dependent. The increase in % removal when

pH increases from 2 to 5 could be due to decrease in competition between hydrogen ions and metal species for appropriate sites on the biosorbent surface and also by the decrease in positive surface charge on the adsorbent. However, with increasing pH above 5 lead tends to hydrolyse and precipitate instead of adsorption and adsorbent was deteriorated with accumulation of metal ions, making the true adsorption studies unpredictable.

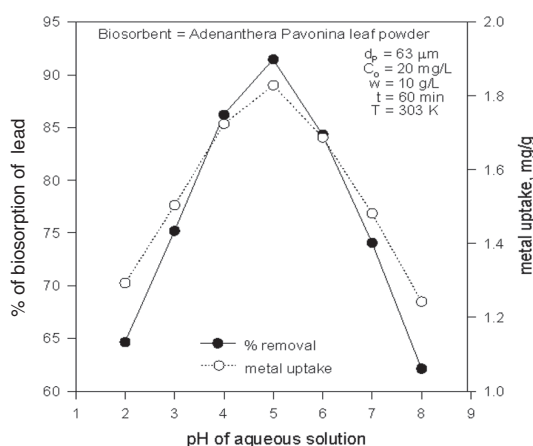


Fig. 3. Observation of pH along with % biosorption of lead

Effect of initial concentration of lead: The effect of initial concentration of lead in the aqueous solution on the percentage biosorption of lead is shown in Fig.4. The percentage biosorption of lead is decreased from 89.14% to 53.95% with an increase in C_0 from 20 mg/L to 150 mg/L. Such behavior can be attributed to the increase in the amount of biosorbate to the unchanging number of available active sites on the biosorbent.

Effect of biosorbent dosage: The percentage biosorption of lead is drawn against biosorbent dosage for 63 μm size biosorbent in Fig.5. The biosorption of lead increased from 79.54% to 89.98% with an increase in biosorbent dosage from 5 to 35 g/L. Such behavior is obvious because with an increase in biosorbent dosage,

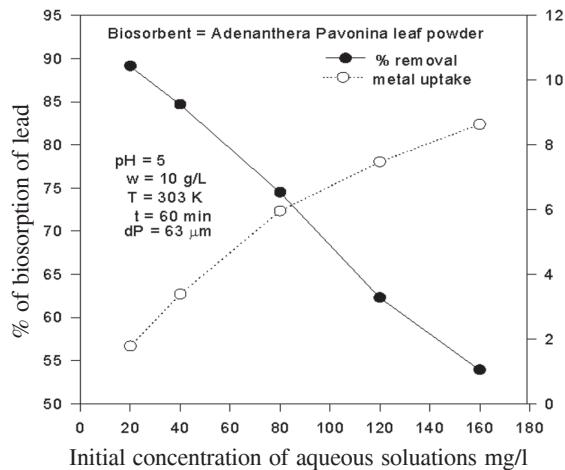


Fig. 4. Variation of initial concentration with % biosorption of lead

the number of active sites available for lead biosorption would be more. The change in percentage biosorption of lead is marginal from 89.98% to 90.29% when 'w' is increased from 35 to 50 g/L. Hence all other experiments are conducted at 35 g/L dosage.

Effect of temperature: The effect of temperature on the equilibrium metal uptake was significant. Adsorption processes are normally exothermic and as the temperature increases the % adsorption decreases in accordance with LeChatelier principle. The effect of changes in the temperature on the lead uptake is shown in Fig.6. Lead uptake marginally increased from 90.44 to 93.58% with increasing temperature from 283 K to 323 K indicating that the biosorption of lead on to *Adenantha Pavnina leaf powder* is endothermic process. The reverse phenomena could be activation of non living biomass under moderate temperatures and Increasing the temperature is known to increase the rate of diffusion of the adsorbate molecules across the external boundary layer and in the internal pores of the adsorbent particles, owing to decrease in the viscosity of the solution.

Isotherms

Langmuir isotherm: Irving Langmuir developed an isotherm named Langmuir isotherm (19).

The Langmuir relationship is hyperbolic and the final equation is: $(C_e/q_e) = 1/(bq_m) + C_e/q_m$

Further analysis of Langmuir equation is made on the basis of separation factor, (R_L) defined as $R_L = 1 / (1+bC_e)$

- $0 < R_L < 1$ indicates favorable adsorption
- $R_L > 1$ indicates unfavorable adsorption
- $R_L = 1$ indicates linear adsorption
- $R_L = 0$ indicates irrepressible adsorption

Langmuir isotherm is drawn for the present data and shown in Fig. 7. The equation obtained is $C_e/q_e = 0.1021C_e + 1.191$ with a good linearity (correlation coefficient, $R^2 \sim 0.996$) indicating strong binding of lead ions to the surface of *Adenantha Pavnina leaf powder*. The maximum metal uptake of (q_m) 9.7943 mg/g is observed and the separation factor obtained (R_L) is 0.843, indicating favorable biosorption.

Freundlich isotherm: Freundlich (20) presented an empirical biosorption isotherm equation and its final form is: $\ln q_e = \ln K_f + n \ln C_e$. From Fig. 8., the obtained Freundlich equation for the present data is $\ln q_e = 0.4439 \ln C_e + 0.3325$. The resulting equation has a correlation coefficient of 0.9778. The 'n' value (0.4439) in the above equations satisfies the condition of $0 < n < 1$ indicating favorable biosorption. The K_f obtained was 2.1503.

Temkin isotherm: Temkin and Pyzhev isotherm (21-22) equation in its final form is $q_e = (RT/b_T) \ln(A_T + (RT/b_T) \ln(C_e))$. From the linear plot Fig. 9., the equation obtained is: $q_e = 1.9571 \ln C_e - 0.0807$ with a correlation coefficient 0.9964. The best fit model is determined based on the linear regression correlation coefficient (R^2). From the Figs .7, 8 & 9, it is found that biosorption data are well represented by Temkin and Langmuir isotherm with higher correlation coefficient of 0.996 followed by and Freundlich isotherm with correlation coefficient of 0.9778. The isotherm constants are given in Table 1.

Kinetics : The kinetics in most cases follows the first order rate equation of Lagergren can be

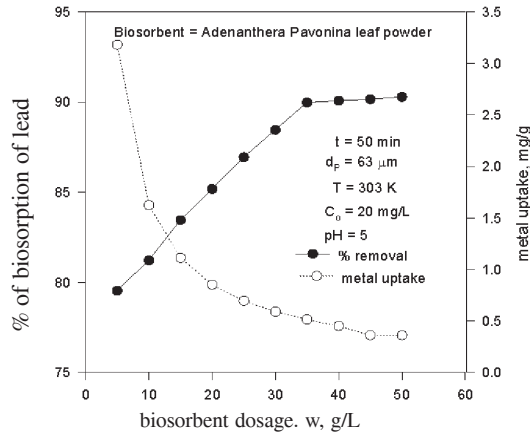


Fig. 5. Dependency of % biosorption of lead on biosorbent dosage

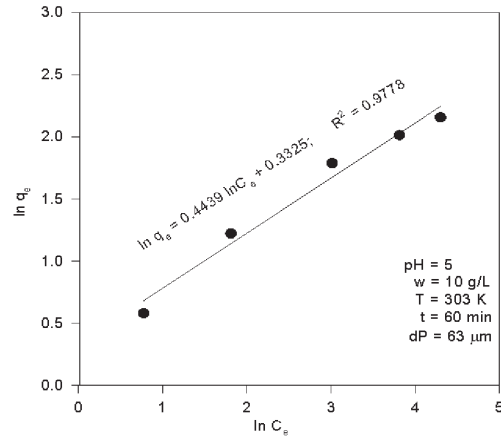


Fig. 8. Freundlich isotherm for biosorption lead

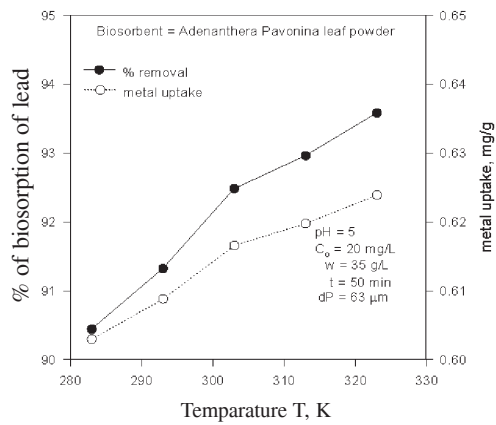


Fig.6. Effect of temperature on % biosorption of lead

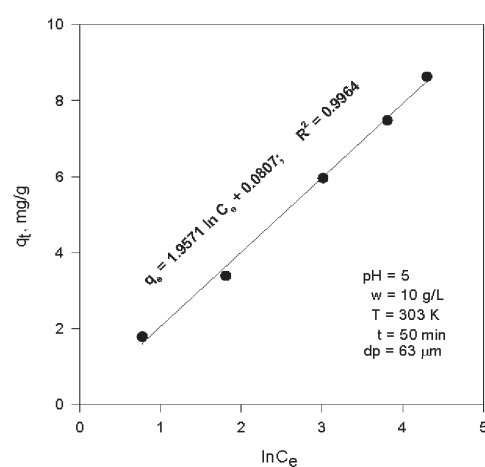


Fig. 9. Temkin isotherm for biosorption of lead

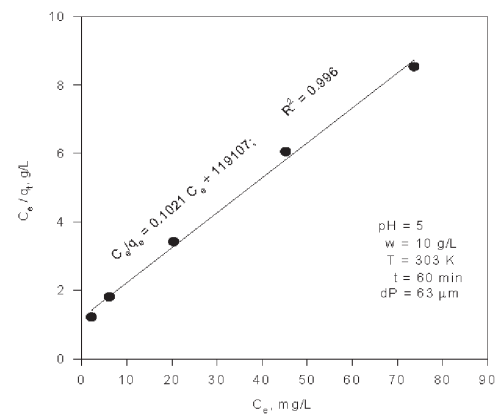


Fig. 7. Langmuir isotherm for biosorption of lead

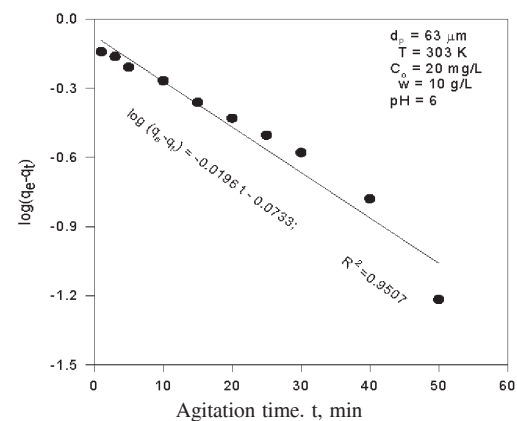


Fig. 10. First order kinetics for biosorption of lead

Biosorption Performance of *Adenanthera pavonina* leaf powder

presented as $\log (q_e - q_t) = \log q_e - (K_{ad} / 2.303) t$. Plot of $\log (q_e - q_t)$ versus 't' gives a straight line for first order kinetics, facilitating the computation of adsorption rate constant (K_{ad}).

The pseudo second order kinetic equation represented in linear form as: $(t/q_t) = (1/ K_{qe}^2) + (1/q_e) t$. The pseudo second order model considers the rate-limiting step as the formation of chemisorptive bond involving sharing or exchange of electrons between the biosorbate and biosorbent. The first order and the second order kinetics plots are given in Figs. 10 and 11 respectively. The correlation coefficients indicate that the system under consideration is more appropriately described by pseudo-second order model. The regression coefficient of 0.9897 shows that that the model can be applied for the entire adsorption process. The confirmation of pseudo second order kinetics indicates that in the adsorption process, concentrations of both adsorbent and adsorbate are involved in rate determining step. The rate equations obtained and comparative lead uptake capacities are given in Table 2 and Table 3 respectively. In the range of studied parameters, the metal uptake is very good for *Adenanthera Pavonina* leaf powder.

Thermodynamics of biosorption :

Biosorption is temperature dependant. In general, the temperature dependence is associated with three thermodynamic parameters namely change in enthalpy of biosorption (ΔH), change in entropy of biosorption (ΔS) and change in Gibbs free energy (ΔG). Enthalpy is the most commonly used thermodynamic function due to its practical significance. The negative value of ΔH will indicate the exothermic/endothemic nature of biosorption and the physical/chemical in nature of sorption. It can be easily

Table 1. Isotherms constants

Langmuir	Freundlich	Temkin
$q_m = 9.7943$ $b = 0.0857$ $R^2 = 0.996$	$k_f = 2.1503$ $n = 0.4439$ $R^2 = 0.9778$	$A_T = 1.042$ $b_T = 1287.181$ $R^2 = 0.9964$

Table 2. Rate Equations and coefficients for biosorption of lead on *Adenanthera pavonina* leaf powder

Order	Equation	K, min-1	R2
Lagergren first order	$\log (q_e - q_t) = -0.019698 t - 0.073348$	0.04513	0.9507
Pseudo second order	$t/q_t = 0.5935 t + 1.85514$	0.18987	0.9897

Table 3. Lead uptake capacities for different biosorbents

Authors	Biosorbent	qt, mg/g
S.A. Abo-El-Enein	rice husk ash	158
Erdal Kenduzler	Amberlyst 36	88
Vijayaraghavan	Sargassum	20.2
Fuat Guzel	black carrot	5.003
Mustafa Tuzen	<i>Pseudomonas aeruginosa</i> immobilized multiwalled carbon nanotubes	5.83
Present investigation	<i>Adenanthera pavonina</i> Leaf powder	9.7943

reversed by supplying the heat equal to calculated ΔH . The ΔH is related to ΔG and ΔS as

$$\Delta G = \Delta H - T \Delta S$$

$\Delta S < 1$ indicates that biosorption is impossible whereas $\Delta S > 1$ indicates that the biosorption is possible. $\Delta G < 1$ indicates the feasibility of sorption.

The Vant Hoff's equation is

$$\log (q_e / C_e) = \Delta H / (2.303 RT) + (\Delta S / 2.303 R)$$

$$\log (q_e / C_e) = - 0.43463 (1 / T) + 1.03393$$

where (q_e / C_e) is called the biosorption affinity.

The Vant Hoff's plot for the biosorption data obtained is shown in Fig. 12. The values are $\Delta G = -5989.933$, $\Delta H = 8.3156$ and $\Delta S = 19.7962$. ΔH is positive indicating that the biosorption is endothermic. The negative value of ΔG indicates the spontaneity of biosorption. As ΔS is

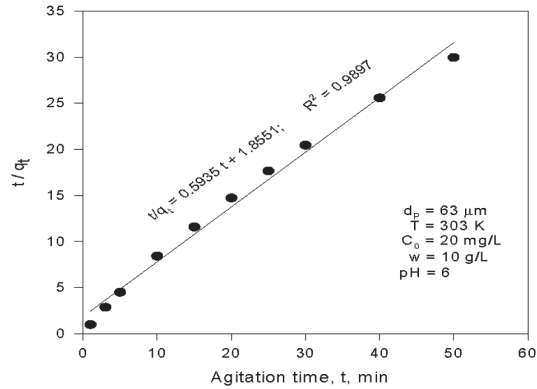


Fig. 11. Second order kinetics for biosorption of lead

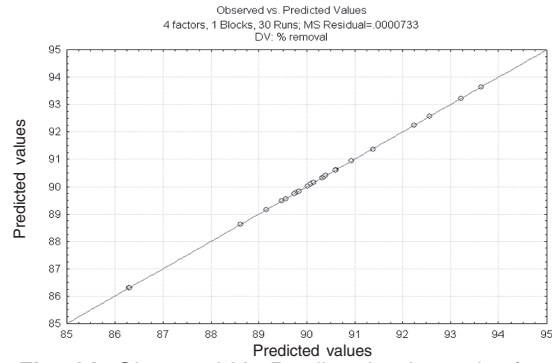


Fig. 14. Observed Vs Predicted values plot for % biosorption of lead

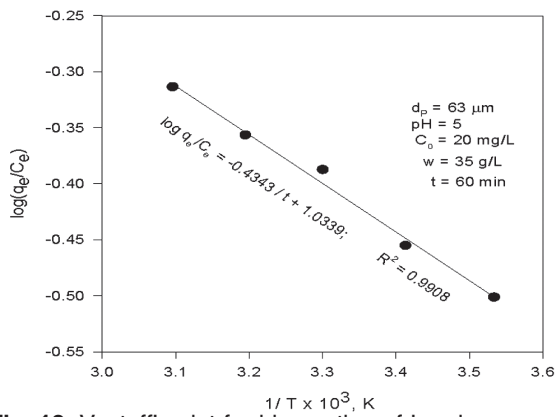


Fig. 12. Vantoff's plot for biosorption of Lead_d

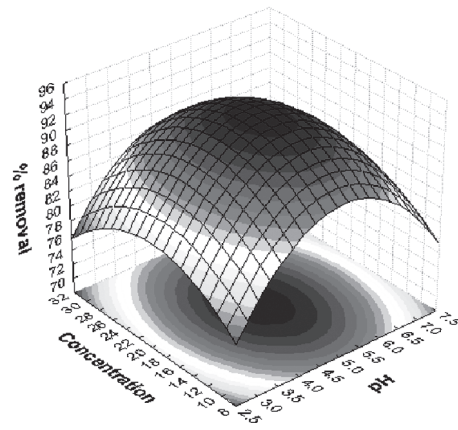


Fig. 15(a). Surface contour plot for the effects of pH and concentration of lead on biosorption

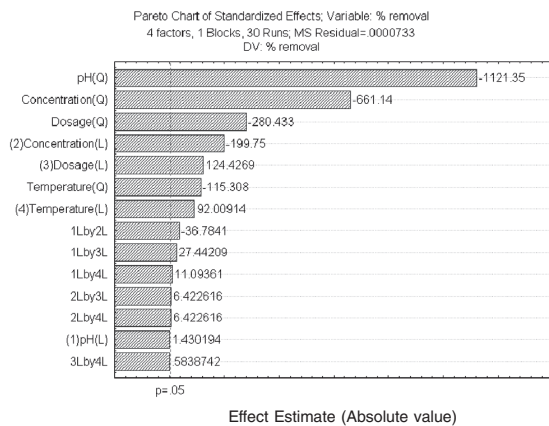


Fig. 13. Pareto Chart

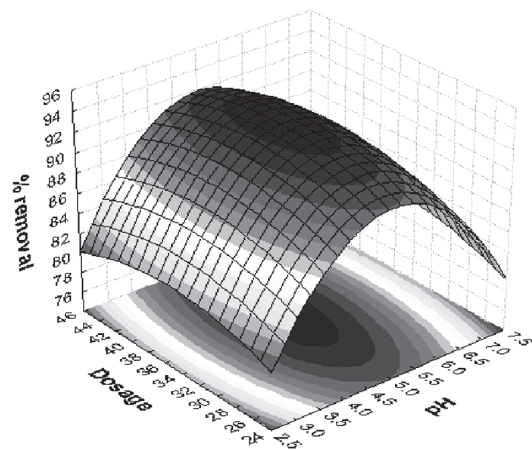


Fig. 15(b). Surface contour plot for the effects of pH and dosage on biosorption of lead

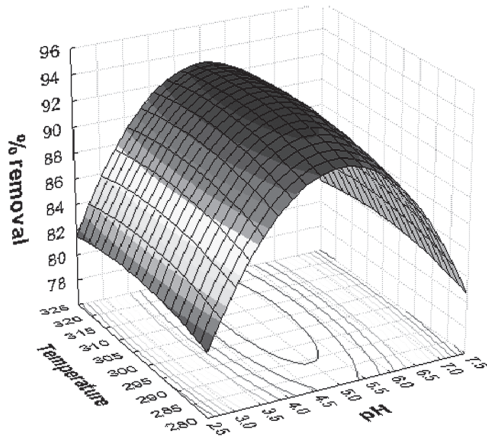


Fig. 15(c). Surface contour plot for the effects of pH and temperature on biosorption of lead

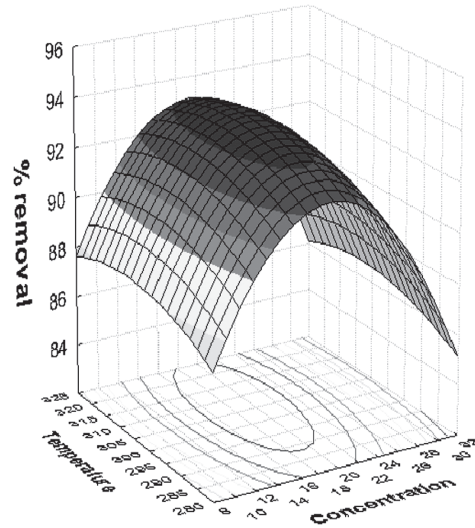


Fig. 15(e). Surface contour plot for the effects of concentration of lead and temperature on biosorption

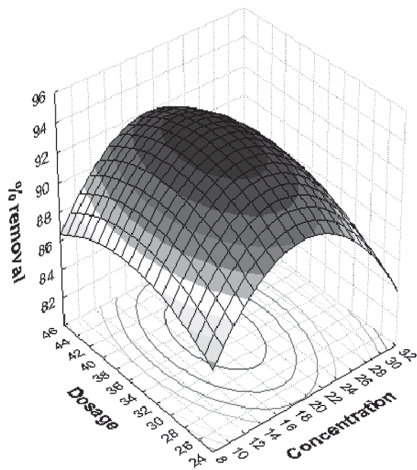


Fig. 15(d). Surface contour plot for the effects of concentration of lead and dosage on biosorption

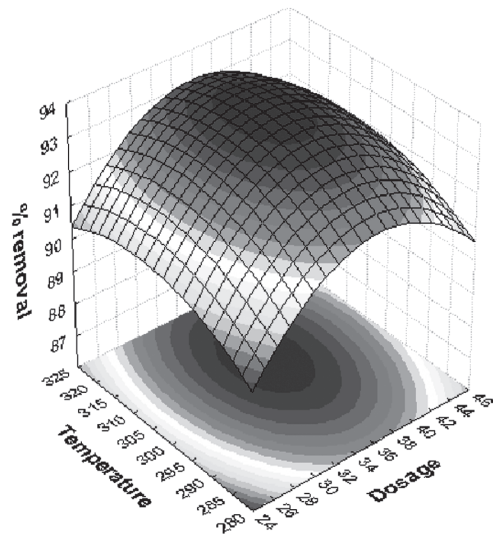


Fig. 15(f). Surface contour plot for the effects of dosage and temperature on biosorption of lead

more than zero, it indicates the irreversibility of biosorption.

Optimization using Response Surface Methodology (RSM):

In the present study, the relationship between four independent variables and percent of Pb ions biosorption fitted well with the quadratic model. Levels of different process variables in coded and un-coded form (Table 4), Results from CCD (Table 5), Analysis of variance (ANOVA) (Table 6), Estimated regression coefficients (Table 7) and Comparison of optimum values obtained from CCD and experimentation (Table 8) for biosorption of lead using *Adenantha pavonina* leaf powder are presented below. For the optimization of biosorption the regression equation: % biosorption of lead (Y) is function of the pH (X_1), Co (X_2), w (X_3), and T (X_4). Based on experimental runs and predicted values proposed by CCD design.

$$Y = -163.678 + 17.522X_1 + 1.636 X_2 + 1.25X_3 + 1.14X_4 - 1.834X_1^2 - 0.043X_2^2 - 0.018X_3^2 - 0.002 X_4^2 - 0.016 X_1X_2 + 0.012 X_1X_3 + 0.002 X_1X_4 + 0.001X_2X_3$$

Pareto Chart (Fig. 13), Observed Vs Predicted values plot (Fig. 14) and Surface contour plot (Fig. 15 a to f) for biosorption of lead on to *Adenantha Pavonina* leaf powder are presented below. The optimal set of conditions for maximum percentage biosorption of lead is pH = 5.0106 biosorption dosage (w) = 36.1803 g/L, initial lead concentration.(Co) = 19.2115 mg/L and temperature = 307.222 K and the % biosorption calculated at these values found to be 93.727 %.

Conclusion

The analysis of the experimental and theoretical data resulted that the equilibrium agitation time for lead biosorption is 60 minutes. The % removal of lead from an aqueous solution increases with a decrease in the particle size of the biosorbent

Table 4. Levels of different process variables in coded and un-coded form for biosorption of lead using *Adenantha pavonina* leaf powder

Variable	Name	Range and levels				
		-2	-1	0	1	2
X1	pH of aqueous solution	3	4	5	6	7
X2	Initial concentration, Co, mg/L	10	15	20	25	30
X3	Biosorbent dosage, w, g/L	25	30	35	40	45
X4	Temperature, T, K	283	293	303	313	323

and increases with increase in biosorbent dosage. With an increase in the initial concentration of lead in the aqueous solution, the percentage removal of lead from the aqueous solution is decreased. Percentage removal of lead from the aqueous solution increases significantly with increase in pH from 2 to 5, thereafter percentage removal decreases for further increase in pH. In the range of variables studied, percentage removal is increased from 50.44% to 93.9%. The maximum uptake capacity of 9.7943 mg/g is obtained at temperature 303 K. The present study involves the use of statistical experimental design to optimize process conditions for maximal biosorption of lead from aqueous solution using CCD involving RSM. The maximum biosorption of lead (93.727%) onto *Adenantha Pavonina* leaf powder is observed when the processing parameters are set as follows: pH = 5.0106, w = 36.1803 g/L, Co = 19.2115 mg/L and T = 307.222 K. The kinetic studies show that the biosorption of lead is better described by pseudo second order kinetics. It is also found that data are well represented by Temkin isotherm with higher correlation coefficient of 0.9964, followed by Langmuir and Freundlich isotherms. The biosorption of lead on to *Adenantha Pavonina* leaf powder is irreversible, spontaneous and endothermic in nature. Therefore the above said *Adenantha Pavonina* leaf powder is effective and efficient biosorbent and is capable of removing lead.

Acknowledgements

The author's whole heartedly thanks the Bapatla Engineering College and TEQIP-World Bank for supporting the authors and sparing the equipment for Research Purpose.

Table 5. Results from CCD for lead biosorption by *Adenanthera pavonina* leaf powder

Run no.	$X_1(w)$	$X_2(C_o)$	$X_3(pH)$	$X_4(T)$	% biosorption of lead	
					Experimental	Predicted
1	-1.0000	-1.0000	-1.0000	-1.0000	90.08	93.53571
2	-1.0000	-1.0000	-1.0000	1.0000	90.32	93.02117
3	-1.0000	-1.0000	1.0000	-1.0000	90.36	91.35117
4	-1.0000	-1.0000	1.0000	1.0000	90.62	91.55438
5	-1.0000	1.0000	-1.0000	-1.0000	89.48	92.16800
6	-1.0000	1.0000	-1.0000	1.0000	89.78	92.37071
7	-1.0000	1.0000	1.0000	-1.0000	89.84	90.74071
8	-1.0000	1.0000	1.0000	1.0000	90.12	91.66117
9	1.0000	-1.0000	-1.0000	-1.0000	90.08	92.98650
10	1.0000	-1.0000	-1.0000	1.0000	90.40	93.20421
11	1.0000	-1.0000	1.0000	-1.0000	90.60	91.88421
12	1.0000	-1.0000	1.0000	1.0000	90.94	92.81967
13	1.0000	1.0000	-1.0000	-1.0000	89.16	92.36154
14	1.0000	1.0000	-1.0000	1.0000	89.56	93.29650
15	1.0000	1.0000	1.0000	-1.0000	89.74	92.01650
16	1.0000	1.0000	1.0000	1.0000	90.14	93.66921
17	-2.0000	0.0000	0.0000	0.0000	86.30	91.71979
18	2.0000	0.0000	0.0000	0.0000	86.32	93.17862
19	0.0000	-2.0000	0.0000	0.0000	90.02	93.15779
20	0.0000	2.0000	0.0000	0.0000	88.62	92.63962
21	0.0000	0.0000	-2.0000	0.0000	91.38	91.40462
22	0.0000	0.0000	2.0000	0.0000	92.24	89.59279
23	0.0000	0.0000	0.0000	-2.0000	92.56	93.24463
24	0.0000	0.0000	0.0000	2.0000	93.22	94.38279
25	0.0000	0.0000	0.0000	0.0000	93.64	96.48333
26	0.0000	0.0000	0.0000	0.0000	93.64	96.48333
27	0.0000	0.0000	0.0000	0.0000	93.64	96.48333
28	0.00000	0.0000	0.0000	0.0000	93.64	96.48333
29	0.00000	0.0000	0.0000	0.0000	93.64	96.48333
30	0.00000	0.0000	0.0000	0.0000	93.64	96.48333

Experimental conditions [Coded Values] and observed response values of central composite design with 24 factorial runs, 6- central points and 8- axial points.
 Agitation time fixed at 60 min and biosorbent size at 63 μm

Table 6. Analysis of variance (ANOVA) of lead biosorption for entire quadratic model

Source of variation	SS	dfS	Mean square(MS)	F-value	P> F
Model	117.1011	14	8.36436	114059	0.00000
Error	0.0011	15	0.000073		
Total	117.1022				

df, degree of freedom; SS, sum of squares; F, factor F; P, probability. R²=0.98424; R² (adj): 0.96952

Table 7. Estimated regression coefficients for the lead biosorption onto *Adenantha pavonina* leaf powder

Terms	Regression	Standard error coefficient	t-value of the coefficient	P-value
constant	-163.678	1.647415	-99.35	0.000000
X ₁	17.522	0.069110	253.54	0.000000
X ₂	-1.834	0.001635	-1121.35	0.000000
X ₃	1.636	0.013742	119.05	0.000000
X ₄	-0.043	0.000065	-661.14	0.000000
X ₁ *X ₁	1.250	0.014033	89.08	0.000000
X ₂ *X ₂	-0.018	0.000065	-280.43	0.000000
X ₃ *X ₃	1.140	0.010116	112.73	0.000000
X ₄ *X ₄	-0.002	0.000016	-115.31	0.000000
X ₁ *X ₂	-0.016	0.000428	-36.78	0.000000
X ₁ *X ₃	0.012	0.000428	27.44	0.000000
X ₁ *X ₄	0.002	0.000214	11.09	0.000000
X ₂ *X ₃	0.001	0.000086	6.42	0.000011
X ₂ *X ₄	0.000	0.000043	6.42	0.000011
X ₃ *X ₄	0.000	0.000043	0.58	0.567982 ^a

^ainsignificant ($P \geq 0.05$)

Table 8. Comparison of optimum values obtained from CCD and experimentation

Variable	CCD	Experimental value
pH of aqueous solution	5.0106	5.0
Biosorption dosage, w, g/L	36.1803	35
Initial lead concentration, mg/L	19.2115	20
Temperature, K	307.222	303
% biosorption	93.727	92.48

References

1. Changzhou, Yan., Guoxin, Li., Peiying, Xue., Qunshan, Wei. and Qingzhao, Li. (2010). Competitive effect of Cu(II) and Zn(II) on the biosorption of lead(II) by *Myriophyllum spicatum*. *Journal of Hazardous Materials*, 179: 721-728.
2. El-Naas, M.H., Abu Al-Rub, F., Ashour, I. and Al Marzouqi, M. (2007). Effect of competitive interference on the biosorption of lead(II) by *Chlorella vulgaris*. *Chemical Engineering and Processing*, 46: 1391-1399.
3. Sarabjeet Singh, A. and Dinesh, G. (2007). Microbial and plant derived biomass for re-

- removal of heavy metals from wastewater. *Bioresource Technology*, 98: 2243-2257.
4. Arzu, Y. and Dursun, A. (2006). Comparative study on determination of the equilibrium, kinetic and thermodynamic parameters of biosorption of copper(II) and lead(II) ions onto pretreated *Aspergillus niger*. *Biochemical Engineering Journal*, 28: 187–195.
 5. Bailey, S.E., Olin, T.J., Bricka, R.M. and Adrian, D.D. (1999). A review of potentially low-cost sorbents for heavy metals. *Water Res.*, 33 (11): 2469–2479.
 6. Roberts, E.J. and Rowland, S.P. (1973). Removal of mercury from aqueous solutions by nitrogen-containing chemically modified cotton. *Environ. Sci. Technol.*, 7 (6): 552–555.
 7. Roy, D., Greenlaw, P.N. and Shane, B.S. (1993). Adsorption of heavy metals by green algae and ground rice hulls. *J. Environ. Sci. Health.*, A 28 (1): 37.
 8. Srivastava, S.K., Singh, A.K. and Sharma, A. (1994). Studies on the uptake of lead and zinc by lignin obtained from black liquor – a paper industry waste material. *Environ. Technol.*, 15: 353–361.
 9. Ozer, A., Tumen, F. and Bildik, M. (1997). Cr(III) Removal from Aqueous Solutions by Depectinated Sugar Beet Pulp. *Environmental Technology*, 18(9): 893-901.
 10. Niu, H., Xu, X.S. and Wang, J.H. (1993). Removal of lead from aqueous solutions by *Penicillium* Biomass, *Biotechnol. Bioeng.*, 49: 785-787.
 11. Kuyucak, N. and Volesky, B. (1990). Biosorption by algal biomass, *Biosorption of heavy metals* B. Volesky, (CRC Press, Boca Raton, FL), 173-198.
 12. Ferguson, J. and Bubela, B. (1974). The concentration of Cu (II), Pb (II), and Zn (II) from aqueous solutions by particulate algae matter, *Chem. Geol.*, 13: 163-186.
 13. Ho, Y.S., Wase, D.A.J. and Forster, C.F. (1995). Batch nickel removal from aqueous solution by sphagnum moss peat, *Water Research*, 29(5): 1327-1332.
 14. Chen, X.H., Gosset, T. and Thevenot, D.R. (1990). Batch copper ion binding and exchange properties of peat. *Water Res.*, 24: 1463–1471.
 15. Randall, J. M. and Hantala, E. (1975). Removing heavy metal ions from water. U.S. Patent 3925192.
 16. Scott, C. D. (1992). Removal of dissolved metals by plant tissue, *Biotechnology and Bioengineering* 39: 1064-1068.
 17. Lujan, J. R., Darnal, D. W., Stark, P. C., Rayson, G. D. and Gardea Torresdey, L.G. (1994). Metal ion binding by algae and higher plant tissues. *Solvent Extr. Ion Exch.*, 12(4): 803-816.
 18. Awwad, A. M. and Salem, N. M. (2012). Biosorption of copper(II) and lead(II) ions from aqueous solutions by modified loquat (*Eriobotrya japonica*) leaves (MLL). *J. Chem. Eng. Mater. Sci.*, 3(1): 7-17
 19. Langmuir, I. (1916). The constitution and fundamental properties of solids and liquids. *Journal of American Chemical Society.*, 38: 2221–2295.
 20. Freundlich, H. (1939). Adsorption in solution. *J. Amer. Chem. Soc.*, 61: 2-28.
 21. Aharoni, A. and Ungarish, M. (1977). Kinetics of activated chemisorption-part-2. Theoretical models. *J Chem Soc Faraday Trans*, 73: 456-464.
 22. Boparai, HK., Joseph, M. and O'Carroll, DM. (2011). Kinetics and thermodynamics of Cadmium ion removal by adsorption onto nano zerovalent iron particles. *J. Hazard. Mater*, 186: 458-465.

Age Dependent Lead Induced Perturbations in Serum Markers; Protective Effect of Nutrient Metal Mixture

V. Kavitha^a, K. Praveen Kumar^b and G. Rajarami Reddy^{a,*}

^aDepartment of Zoology, S.V University, Tirupati, A. P, India.

^bDepartment of Biotechnology, S.V University, Tirupati, A. P, India.

*For correspondence – gottipolu2002@yahoo.com

Abstract

Lead (Pb) is a widespread toxic metal found in the environment. Lead affects multiple organs in the body and results in alteration of various serum parameters. The present study was designed to examine the effect of lead on serum markers and further examine the protective effect of nutrient metal mixture of calcium, iron and zinc. Pups of wistar rats were lactationally exposed to 0.2% lead acetate through drinking water of mother from postnatal day (PND) 1 to PND 21. Another group of pups received 0.2% Pb-acetate together with a mixture of calcium, iron and zinc (0.02%) whereas control animals received only deionized water without Pb. Various serum markers like glucose, urea, creatinine, bilirubin, total cholesterol, alkaline phosphatase (ALP), serum glutamic pyruvate transaminase (SGPT) and serum glutamic oxaloacetic transaminase (SGOT) levels were estimated in control and experimental rats of PND 28, PND 45, 4 months and 12 months aged rats. These serum markers were significantly altered in Pb - exposed rats in all age groups when compared to control rats. The nutrient metal mixture of calcium, iron and zinc significantly reversed the Pb induced changes in serum markers indicating protection against Pb - induced toxicity.

Keywords: Lead, Nutrient metal mixture, Serum markers.

Introduction

Human exposure to heavy metal lead (Pb) is a global health problem because of its wide

spread use in industrial and commercial products. Pb is one of the oldest known and most widely studied occupational and environmental toxins (1, 2), usually found in Pb acid batteries, pipes, paints, gasoline additives, ceramic glazers, glass and crystals, cosmetics etc.

Unlike most chemicals for which health impacts of low level doses are still uncertain, exposure to Pb, even at very low levels (10 µg/dl), is highly toxic (3). Pb has a more severe effect on the cardiovascular and haematological systems especially in Fe deficient people. Because the combination of Fe deficiency and Pb exposure cause more severe effects on the blood forming system, women and children tend to show more severe effects (4). Lead impairs the synthesis of a substance called "heme" which is extremely important to human life because it carries oxygen to tissues of the body. In chronic exposure, Pb induces anemia by both interfering with heme biosynthesis and by diminishing red blood cell survival. Pb inhibits the body's ability to make hemoglobin by interfering with several enzymatic steps in the heme pathway. Specifically, Pb decreases heme biosynthesis by inhibiting δ-aminolevulinic acid dehydratase (ALAD) and ferrochelatase activity (5, 6). Blood parameters are probably the more rapid and detectable variations under stress and are useful in assessing the health conditions. Besides blood indices, serum parameters are also broadly affected by Pb exposure. Pb alters the serum urea and creatinine levels (7, 8) indicating renal

failure. Pb induces hypercholesterolemia and alters the liver marker enzymes such as ALT, AST and ALP (9-11).

Nutrient metals like calcium, iron and zinc play an important role in reducing Pb toxicity. Dietary Ca deficiency increases the absorption of Pb by the gastrointestinal tract and increases Pb concentrations in critical organs of the body (12, 13). Nutritional Fe deficiency also enhances Pb absorption and promotes Pb toxicity more prominently in young children and women (14). A negative relationship between dietary Fe intake and blood Pb levels was also found in a study of preschool children (15). Studies show that as dietary Zn increases, Pb absorption and its subsequent toxicity decrease, indicating that Zn exerts its effect on Pb in the gastrointestinal tract (16, 17). Interactions between Zn and Pb are possible beyond the level of the gastrointestinal tract, as Zn involves the inhibition of heme synthesis by Pb (14, 18). Since the nutrient metals play an important role in the treatment of Pb poisoning, the present study was therefore aimed at investigating the potential of Ca, Fe and Zn nutrient metal mixture in countering age dependent Pb induced toxicity in the haematological system of rats.

Material and Methods

Maintenance of experimental animals: Adult albino rats (Wistar) were obtained from Sri Venkateswara Traders, Bangalore, and from these animals a colony of rats were developed and maintained in rat cages under normal laboratory conditions (at constant temperature $28 \pm 2^\circ\text{C}$ and relative humidity $60 \pm 10\%$ with a 12 hour light/dark cycle) throughout the course of the present study. The animals were fed on rat feed supplied by Sri Venkateswara Traders, Bangalore and water was provided ad libitum.

Chemical exposure: Young rats from PND1 were lactationally exposed to 0.2% Pb by adding Pb-acetate to deionized drinking water of the mother. Pb-exposure dose was obtained from published work (19). All pups, twenty four hours after birth

(PND1) were pooled and new litters consisting of eight males were randomly selected and placed with each dam. Pb-exposure was continued up to PND21 and stopped at weaning. Calcium (Ca^{2+}), Zinc (Zn^{2+}) and Iron (Fe^{2+}) in a mixture was supplemented as 0.02% in 0.2% Pb-water given to another group of pups through mother's milk up to PND 21 and stopped at weaning. Control animals received only deionized water without Pb.

Collection of blood and serum and estimation of biochemical parameters:

The control and experimental animals at the end of PND 28, PND 45, 4 months and 12 months after the treatment were sacrificed by cervical decapitation and the blood samples were collected. Blood was allowed to stand for 30 min at room temperature and then centrifuged using refrigerated centrifuge to separate the serum. Serum was stored at -40°C , and used for the analysis of various parameters like glucose, urea, bilirubin, creatinine, total cholesterol, serum Alkaline Phosphatase (ALP), serum glutamate oxaloacetate transaminase (SGOT) and serum glutamate pyruvate transaminase (SGPT). Serum parameters were estimated by using the kits purchased from Biosystems, A15 hematology Analyzer (20). Results were expressed as mg/dl for serum glucose, urea, creatinine, bilirubin, cholesterol and as IU/L for serum ALP, SGOT, SGPT.

Statistical analysis: The data obtained from six separate samples were expressed as mean \pm SD. Data was analyzed by two-way Analysis of Variance (ANOVA) following Standard Statistical Software Package to compare the effects among various groups. The 0.05 level of probability was used as the criterion for significance.

Results

Serum glucose levels of rats of different age groups were shown in figure 1. From the results obtained in our studies, it is clear that Pb-exposure showed a significant decrease in the glucose levels of PND 28, PND 45, 4 months and 12 months aged rats (Fig 1). The decrease in glucose content of Pb exposed rats was 13.63% in 28

days rats, 9.34% in 45 days rats, 24.36% in 4 months rats and 11.2% in 12 months rats. Maximum decrease (24.36%) was observed at 4 months of postnatal development. The decrease in glucose content was most significant at 4 months age and not significant in remaining age groups of rats ($P < 0.05$). $Ca^{2+} + Fe^{2+} + Zn^{2+}$ supplementation reversed the effects of Pb on glucose levels of experimental animals at different time periods (Fig. 1). Maximum effect of nutrients was observed at 4 months PND (Fig. 1).

The serum urea levels of control, Pb exposed and nutrient supplemented rats were shown in figure 2. Serum urea levels increased progressively from PND 28 days to 12 months old rats (Fig. 2). The Pb-exposure showed a significant increase in the urea level of rat's different age groups. The increase in urea levels of Pb exposed rats decreased progressively from PND 28 days to 12 months aged rats. The increase in urea of Pb exposed rats was 45.7% in 28 days rats, 43.24% in 45 days rats, 17.9% in 4 months rats and 12.8% in 12 months aged rats. Maximum increase in urea levels was observed in 28 days young rats (45.7%) than other age groups (Fig. 2). The increase in serum urea content was significant at all the age points of rats except in 12 months age rats. The administration of $Ca^{2+} + Fe^{2+} + Zn^{2+}$ nutrients reversed the Pb induced increase in urea levels.

Creatinine levels were estimated in serum of control, Pb exposed and $Ca^{2+} + Fe^{2+} + Zn^{2+}$ nutrient supplemented rats of PND 28, 45, 4 months and 12 months age and presented in fig 3. The creatinine levels in control rats decreased from PND 28 to 45 and increased from 45 days to 12 months aged rats (Fig 3). The Pb-exposure showed a significant increase in the creatinine levels of different age groups of rats. The increase in creatinine levels of Pb exposed rats from control was 60% in PND 28 days, 31.25% in PND 45 days, 26.98% in 4 months and 20% in 12 months age. Maximum increase in creatinine levels was observed in 28 days young rats (60%) than other age groups (Fig. 3). The increase in creatinine

levels was significant in 28 days and 4 months age rats. Administration of mixture of $Ca^{2+} + Fe^{2+} + Zn^{2+}$ produced recovery from Pb induced increase in creatinine levels. The maximum reversal effect was observed in PND 28 rats than other age groups (Fig. 3).

Serum bilirubin levels of control, Pb exposed and nutrient supplemented rats of different age groups were shown in figure 4. Serum bilirubin levels of control rats were increased from 28 to 45 days and decreased in 4 months and 12 months aged animals (Fig. 4). The Pb-exposure showed a significant increase in the bilirubin levels of rats of different age groups. The increase in bilirubin level was 91.6%, 55.5%, 132.3% and 25% respectively in PND 28, 45, 4 months and 12 months age. The increase was greater in 4 months aged rats (132.3%) than other age groups of rats. The increase in bilirubin levels was significant in all age groups except in 12 months age rats. Administration of nutrient mixture ($Ca^{2+} + Fe^{2+} + Zn^{2+}$) produced reversal effect on Pb induced increase in bilirubin levels which was maximum at 4 months rats than other age groups (Fig. 4).

The cholesterol level was estimated in serum of control, Pb exposed and $Ca^{2+} + Fe^{2+} + Zn^{2+}$ supplemented rats of PND 28, 45, 4 months and 12 months aged rats (Fig. 5). The cholesterol level gradually decreased in the serum of control rats from 28 days to 4 months age and again increased in 12 months aged rats (Fig. 5). The cholesterol levels were significantly altered in Pb-exposed developing, young, adult and aged rats. The increase in serum total cholesterol in Pb exposed rats was 38.29%, 105%, 44.11% and 28.8% respectively in PND 28, 45, 4 months and 12 months aged rats. Maximum increase was observed at PND 45 days young rats. The increase in cholesterol levels was significant in all age groups except in 12 months age rats (Fig. 5). The administration of $Ca^{2+} + Fe^{2+} + Zn^{2+}$ supplements produced recovery from the Pb induced increase in cholesterol levels (Fig 5).

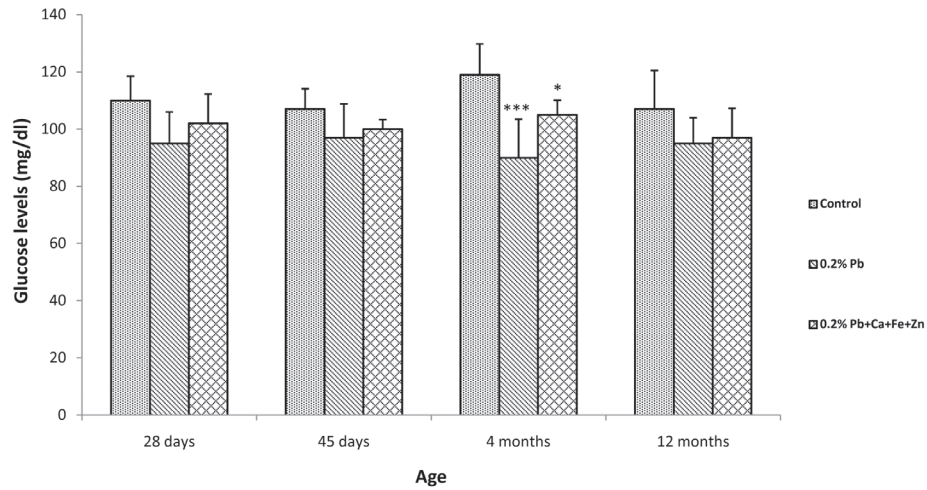


Fig. 1. Effects of Pb exposure and nutrient metals supplement to Pb on serum glucose levels. Pups were exposed to deionized water (control), or Pb acetate (0.2 %), calcium, zinc and iron combination together with Pb (0.02 % in 0.2 % Pb water) from PND 1 to PND 21. Serum glucose levels were estimated in control, Pb exposed and supplemented rats of different age groups (PND 28, 45, 4 and 12 months). All the values are mean \pm SD of six individual observations. The 0.05 level of probability was used as the criterion for significance. * $p < 0.05$, ** $p < 0.01$, *** $p < 0.001$.

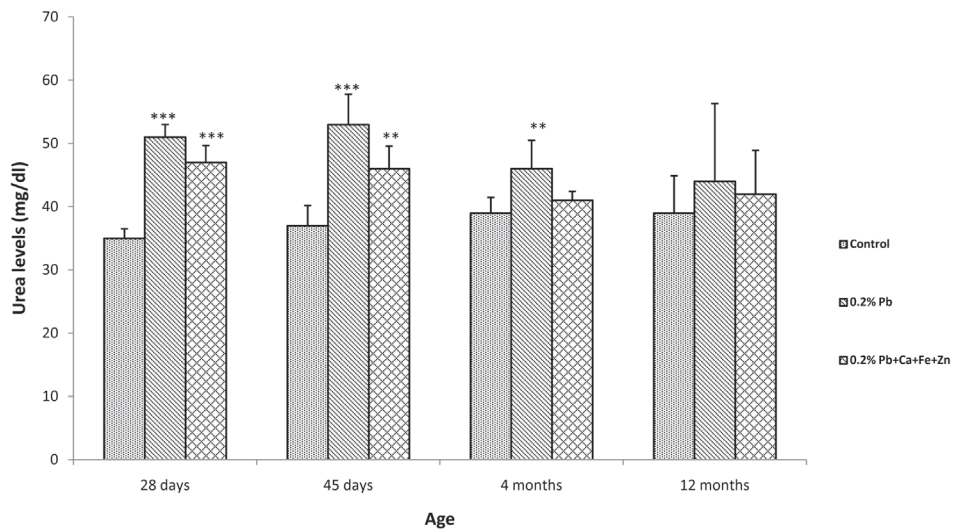


Fig. 2. Effects of Pb exposure and nutrient metals supplement to Pb on serum urea levels. Pups were exposed to deionized water (control), or Pb acetate (0.2 %), calcium, zinc and iron combination together with Pb (0.02 % in 0.2 % Pb water) from PND 1 to PND 21. Serum urea levels were estimated in control, Pb exposed, supplemented rats of different age groups (PND 28, 45, 4 and 12 months). All the values are mean \pm SD of six individual observations. The 0.05 level of probability was used as the criterion for significance. * $p < 0.05$, ** $p < 0.01$, *** $p < 0.001$.

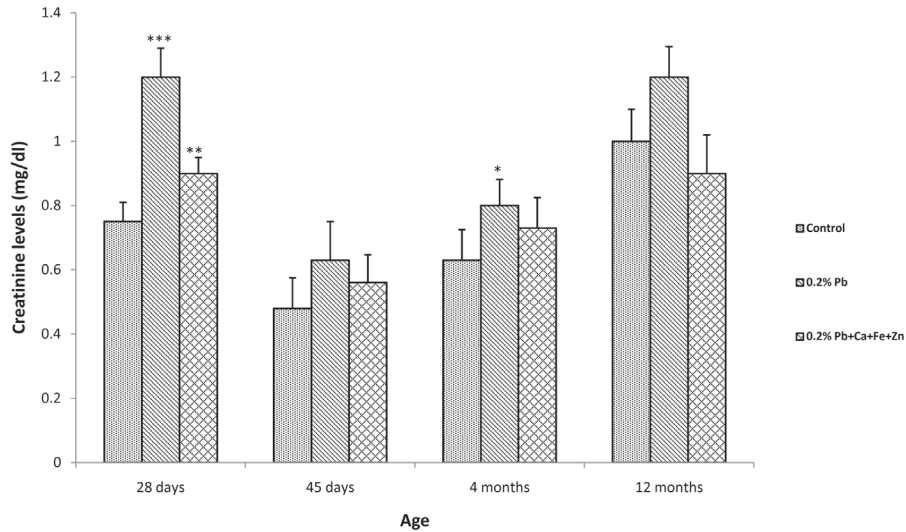


Fig. 3. Effects of Pb exposure and nutrient metals supplement to Pb on serum creatinine levels. Pups were exposed to deionized water (control), or Pb acetate (0.2 %), calcium, zinc and iron combination together with Pb (0.02 % in 0.2 % Pb water) from PND 1 to PND 21. Serum creatinine levels were estimated in control, Pb exposed, supplemented rats of different age groups (PND 28, 45, 4 and 12 months). All the values are mean \pm SD of six individual observations. The 0.05 level of probability was used as the criterion for significance. * $p < 0.05$, ** $p < 0.01$, *** $p < 0.001$.

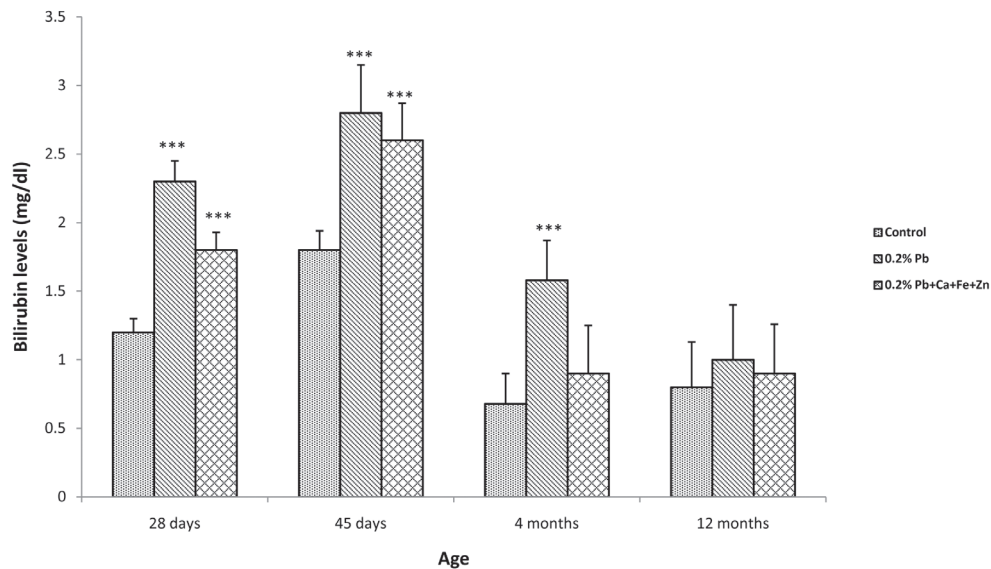


Fig. 4. Effects of Pb exposure and nutrient metals supplement to Pb on serum bilirubin levels. Pups were exposed to deionized water (control), or Pb acetate (0.2 %), calcium, zinc and iron combination together with Pb (0.02 % in 0.2 % Pb water) from PND 1 to PND 21. Serum bilirubin levels were estimated in control, Pb exposed, supplemented rats of different age groups (PND 28, 45, 4 and 12 months). Values are mean \pm SD of six separate experiments. The 0.05 level of probability was used as the criterion for significance. * $p < 0.05$, ** $p < 0.01$, *** $p < 0.001$.

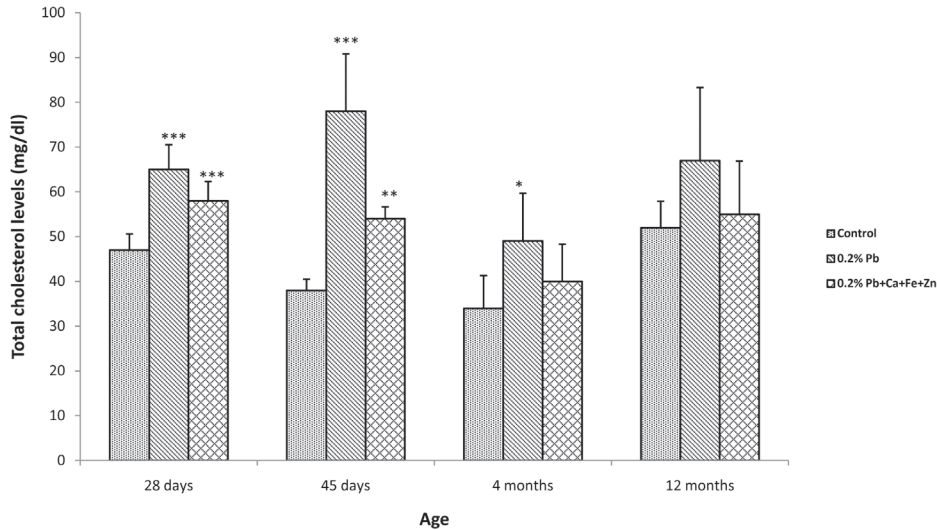


Fig. 5. Effects of Pb exposure and nutrient metals supplement to Pb on serum total cholesterol levels. Pups were exposed to deionized water (control), or Pbacetate (0.2 %), calcium, zinc and iron combination together with Pb (0.02 % in 0.2 % Pb water) from PND 1 to PND 21. Serum total cholesterol levels were estimated in control, Pb exposed, supplemented rats of different age groups (PND 28, 45, 4 and 12 months). Values are mean \pm SD of six separate experiments. The 0.05 level of probability was used as the criterion for significance. * $p < 0.05$, ** $p < 0.01$, *** $p < 0.001$.

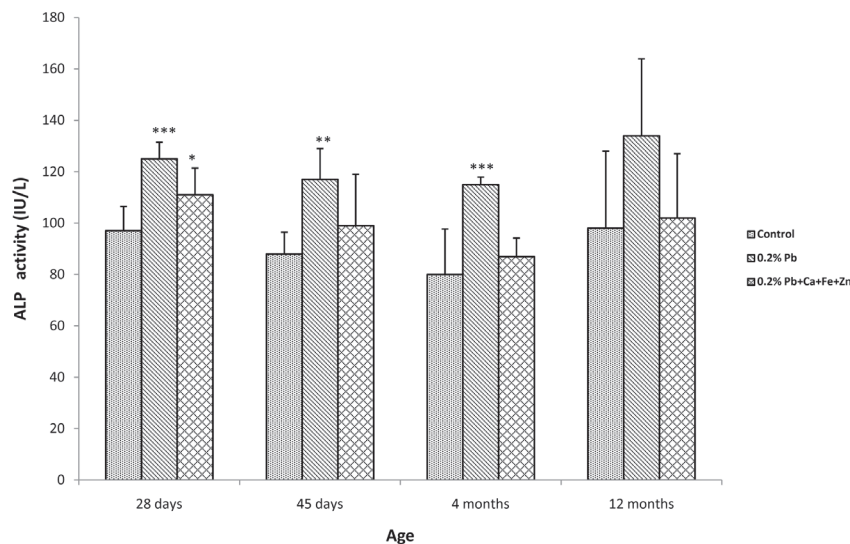


Fig. 6. Effects of Pb exposure and nutrient metals supplement to Pb on serum ALP activities. Pups were exposed to deionized water (control), or Pbacetate (0.2 %), calcium, zinc and iron combination together with Pb (0.02 % in 0.2 % Pb water) from PND 1 to PND 21. Serum ALP activities were estimated in control, Pb exposed, supplemented rats of different age groups (PND 28, 45, 4 and 12 months). Values are mean \pm SD of six separate experiments. The 0.05 level of probability was used as the criterion for significance. * $p < 0.05$, ** $p < 0.01$, *** $p < 0.001$.

Activity of the serum alkaline phosphatase was estimated in the serum of control, Pb exposed and $\text{Ca}^{2+} + \text{Fe}^{2+} + \text{Zn}^{2+}$ supplemented rats at different time periods such as PND 28, PND 45, 4 months and 12 months are presented in Fig 6. The activity of ALP of control rats was decreased from 28 days to 4 months and increased in 12 months aged control rats (Fig 6). Pb exposure however significantly increased the activity of ALP in all age groups of rats. The increase in ALP activity was 28.86%, 32.95%, 43.75% and 36.73% respectively in PND 28, 45, 4 months and 12 months aged rats. The increase in ALP activity due to Pb exposure was greater in 4 months rats than other age groups (Fig 6) and significant in all the age groups except in 12 months rats. The administration of $\text{Ca}^{2+} + \text{Fe}^{2+} + \text{Zn}^{2+}$ supplement however, produced significant reversal from the Pb induced increase in ALP activity (Fig 6).

Activities of serum glutamic pyruvic transaminase (SGPT) and serum glutamic oxaloacetic transaminase (SGOT) were estimated in serum of control, Pb exposed and $\text{Ca}^{2+} + \text{Fe}^{2+} + \text{Zn}^{2+}$ supplemented rats at different time periods (PND 28, 45, 4 months and 12 months) (Fig 7 & 8). Exposure to Pb resulted in an increase in both the SGPT and SGOT activities in different age groups of rats. Pb exposure resulted in an increase of 68.42% in PND 28, 75% in PND 45, 69% in 4 months, 38.63% in 12 months aged animals and an increase of 81% in PND 28, 102.9% in PND 45, 66.6% in 4 months, 42.1% in 12 months aged animals for SGPT and SGOT activities respectively (Fig 7 & 8). Increases in the activities of SGPT and SGOT were significant in all age groups. The supplementation of $\text{Ca}^{2+} + \text{Fe}^{2+} + \text{Zn}^{2+}$ reversed the effect caused by Pb exposure in SGPT and SGOT activities (Fig 7 & 8).

Discussion

In the present study, age related changes in haematological parameters were observed following exposure of rats to Pb. The haematological system is one of the important

target systems in Pb induced toxicity. Pb interferes with heme synthetic pathway at various steps and cause haematological disturbances. Besides haematological parameters like blood cell count, Hb content various serum parameters were also affected due to lead exposure. In the present study, serum glucose level was decreased following Pb exposure in all age groups of rats. The reduction in serum glucose concentration following the administration of Pb observed in the present study may be due to inhibition of the uptake and transport of glucose by Pb (21). Pb appears to exert a direct or indirect effect on serum glucose of experimental rats and results in abnormal glucose metabolism. Many environmental and occupational agents including Pb have been shown to cause detrimental effects on endocrine function related to glucose metabolism (22). The observed decrease of glucose concentration in serum of treated rats may also be due to altered endocrine function and stimulating the the glycogenesis and ultimately leading to decrease of glucose level in the serum.

In the present study, serum urea levels increased in Pb exposed animals when compared to the control animals of different age groups. Urea serves an important role in the metabolism of nitrogen-containing compounds by animals and is the main nitrogen-containing substance in the urine of mammals. Serum urea has been reported to increase in acute and chronic Pb exposure (7, 23-25). Urea is the principal end product of protein catabolism. Enhanced protein catabolism together with accelerated amino acid deamination for gluconeogenesis is probably a contributing factor for the elevated levels of urea. On the other hand, the elevated serum urea levels may also be due to the destruction of RBC's.

The result of the present study also showed significant increase in serum creatinine levels in Pb exposed rats indicating renal deficiency. Creatinine is formed in muscle and is chiefly filtered out of the blood by the kidneys. Increased serum creatinine levels following Pb exposure was also reported earlier (7, 26) which supports

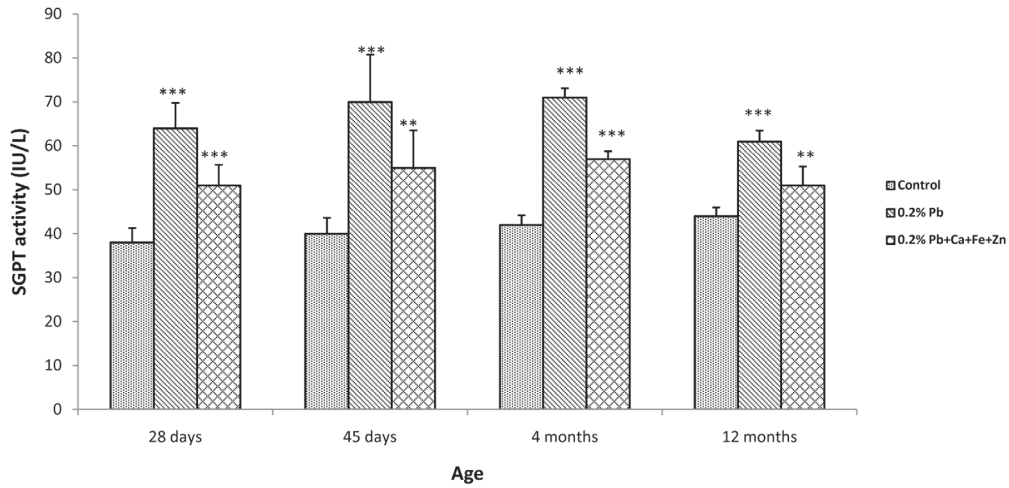


Fig. 7. Effects of Pb exposure and nutrient metals supplement to Pb on SGPT activity. Pups were exposed to deionized water (control), or Pb acetate (0.2 %), calcium, zinc and iron combination together with Pb (0.02 % in 0.2 % Pb water) from PND 1 to PND 21. SGPT activities were estimated in control, Pb exposed, supplemented rats of different age groups (PND 28, 45, 4 and 12 months). Values are mean \pm SD of six separate experiments. The 0.05 level of probability was used as the criterion for significance. * $p < 0.05$, ** $p < 0.01$, *** $p < 0.001$.

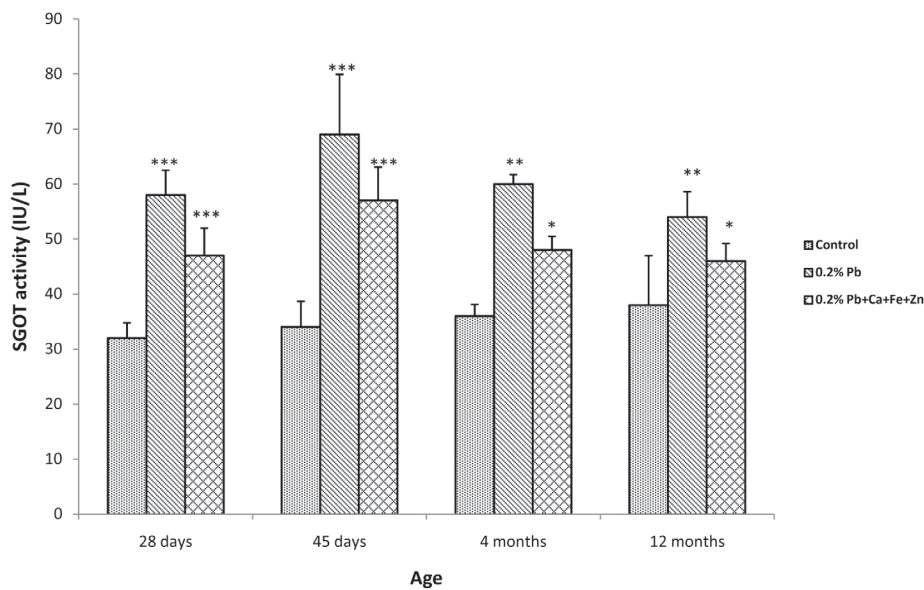


Fig. 8. Effects of Pb exposure and nutrient metals supplement to Pb on SGOT activity. Pups were exposed to deionized water (control), or Pb acetate (0.2 %), calcium, zinc and iron combination together with Pb (0.02 % in 0.2 % Pb water) from PND 1 to PND 21. SGOT activities were estimated in control, Pb exposed, supplemented rats of different age groups (PND 28, 45, 4 and 12 months). Values are mean \pm SD of six separate experiments. The 0.05 level of probability was used as the criterion for significance. * $p < 0.05$, ** $p < 0.01$, *** $p < 0.001$.

the findings of our present study. The observed elevation in the serum creatinine levels in Pb exposed rats suggests renal function impairment which might result from intrinsic renal lesions, decreased perfusion of the kidney obstruction of lower urinary tract or due to deranged metabolic process caused by this metal. In the present study, serum bilirubin levels increased in Pb exposed animals when compared to the control animals of different age groups. Increased bilirubin level was also observed in automobile workers (27) and Pb exposed rats (28) supporting the findings of our study. Bilirubin is the yellow breakdown product of normal heme catabolism. Increase in serum total bilirubin level in the Pb exposed rats may be due to greater haemolysis of red blood cells.

Although cholesterol is important and necessary for mammals, high levels of cholesterol in the blood can damage arteries and are potentially linked to diseases such as those associated with the cardiovascular system. Pb induced hypercholesterolemia, observed in this study could be due to increased hepatic cholesterogenesis accompanied with a decrease in triglyceride and phospholipid contents in the liver and consequently causing an increase in the blood (29). This relationship between Pb exposure and plasma cholesterol suggests an altered lipid metabolism. Increase in serum cholesterol levels was also reported earlier in Pb exposed rats (30-33). The increase in the total cholesterol of Pb exposed rats indicate that the rats were under stress and that cholesterol may be utilized for the repair of the damaged cell membrane due to the toxic impact.

In the present study, administering Pb acetate to rats resulted in a significant increase of blood alkaline phosphatase in different age groups. Alkaline phosphatase is responsible for removing phosphate groups from many types of molecules, including nucleotides, proteins, and alkaloids. Liver enzyme ALP is a marker enzyme for liver function and integrity (34, 11). Serum ALP level usually increase in acute hepatotoxicity or mild hepatocellular injury (34, 35). In this study,

administration of Pb showed significant increase in plasma ALP activity. Similar increase in serum ALP activity was also observed earlier in Pb exposed rats (28, 31, 32, 36-39) Increase in the level of serum ALP due to Pb exposure may be due to the loss of this enzyme and diffusion through cell membrane. The present data suggest that Pb exerts possible hepatotoxic effect as the increase in ALP is indicative of liver damage.

Measuring the concentrations of transaminases in the blood is important in the diagnosing and tracking many diseases. An increased serum marker (SGPT and SGOT) following Pb exposure to rats was observed previously (28, 31, 36, 38) supporting the present findings of our study. Pb may accumulate in liver and exert its toxic effect via pro oxidative damage to hepatic cell membranes causing transaminases to liberate into the serum. The increases in activities of SGOT and SGPT observed in Pb exposed rats might be due to increased cell membrane permeability or cell membrane damage of hepatocytes caused by Pb acetate. The elevation of serum SGOT and SGPT may be also due to the possible release of these enzymes from the cytoplasm, into the blood circulation rapidly after rupture of the plasma membrane and cellular damage.

Supplementation of rats with nutrient metals calcium, iron and zinc reversed the effect of Pb on serum parameters. Ca is one of the most important elements in the diet because it is a structural component of bones, teeth, and soft tissues and is essential in many of the body's metabolic processes. Fe is one of the important nutrients as it is necessary for oxygen transport in the blood and is important for the normal functioning of all the cells in the body. Zn is a biological trace element and component of many enzymes and in many cells and is bound to a storage protein, metallothionein. Supplementation with calcium, iron and zinc decreases Pb gastrointestinal absorption and decreases tissue accumulation (40). Our earlier studies indicated reversal of the Pb induced neurochemical alterations with calcium or zinc supplements (17).

Extensive clinical and experimental evidence supports the significance of Pb-Ca²⁺ interactions (41). Ca²⁺ is a divalent cation just like Pb. The same transport mechanism is operative for absorption of Pb and Ca²⁺ from the gastrointestinal tract resulting competitive interaction between Pb and Ca²⁺ (42). Absorption of Pb by gastrointestinal tract is inversely related to the amount of Ca²⁺ present (43, 44). Ca²⁺ and Pb compete for similar binding sites on intestinal mucosal proteins, which are important in the absorptive process (45). The supplemented Ca, Fe and Zn may compete for similar binding sites as that of Pb on gastrointestinal tract. These nutrient metals offered protection against the alterations caused by Pb in the different age groups of rats. Increased Fe intake has also been suggested as one part of a multi-tiered approach to lessening Pb- toxicity (46). The mechanism by which Fe deficiency potentiates Pb toxicity is not clear, but there are several metabolic pathways in which Fe/Pb interaction is occur. The effects of Pb and Fe on the heme biosynthetic pathways have been extensively investigated and characterized. Pb inhibits two major enzymes of the heme biosynthetic pathway: δ -aminolevulinic acid dehydratase (ALAD) and ferrochelatase. It has also been suggested that these two metals might compete directly for specific erythrocyte binding sites (47). Interactions between Zn²⁺ and Pb have been investigated at absorptive and enzymatic sites (48). Zn²⁺ and Pb compete for similar binding sites on the metallothionein like transport protein in the gastrointestinal tract (49). In addition to forming strong bonds with SH and other groups like OH, NH₂ and Cl in amino acids which interfere with basic enzymatic processes, toxic metals exert part of their effects by replacing essential metals such as Zn²⁺ at their sites in enzymes (50). Potential mechanisms of interaction between Pb and Zn²⁺ include an inhibition of Pb gastrointestinal absorption by Zn²⁺, which has been demonstrated in rats (51). Thus supplementation with Ca²⁺+Fe²⁺+Zn²⁺ reduced the inhibitory effect of Pb on the activity of blood parameters and reversed the enzyme activity nearer to control level.

The effect of Pb in haematological system is influenced directly by the dose, duration of Pb exposure and by age. The results of the present study showed that the exposure of Pb in early life can continue to influence the serum parameters even in later life suggesting the storage of Pb in critical organs of the body like bones for a long time and released oftenly into the blood stream. The supplementation of nutrient metal mixture offered protection against the Pb induced alterations in serum parameters by reducing the absorption of Pb and by interacting with Pb at various sites of the body. Thus the present data suggest that the early life exposure to Pb can continue to affect the serum markers and nutrient metal supplements provide protection against Pb induced toxicity.

Acknowledgements

This study was supported by council of scientific and industrial research (CSIR), grant no. 37(1349)/08/EMR-II.

References

1. Reddy, G.R., Devi, B.C. and Chetty, C.S. (2007). Developmental lead neurotoxicity: Alterations in brain cholinergic system. *Neurotoxicology*, 28: 402–407.
2. Gidlow, D.A. (2004). Lead toxicity. *Occup Med (Lond)*; 54:76-81.
3. Silbergeld, E. and Kevin Tonat. (1994) Investing in Prevention: Opportunities to Prevent Disease and Reduce Health Care Costs By Identifying Environmental and Occupational Causes of Noncancer Disease, *Toxicology and Industrial Health*, 10(6): 677
4. Gulson, B.L. (1995). Tooth analyses of sources and intensity of lead exposure in children. *Environ Health Perspect* 104:306-312.
5. Ahamed, M. and Siddiqui, M.K.J., (2007). Low level lead exposure and oxidative stress: current opinions. *Clin. Chim. Acta* 383, 57–64.

6. Oskarsson, A. and Fowler, B.A. (1985). Effects of lead on the heme biosynthetic pathway in rat kidney. *Exp. Mol. Pathol.* 43, 409–417.
7. Ghorbe, F., Boujelbene, M., Makni-Ayadi, F., Guermazi, F., Kammoun, A., Murat, J., Croute, F., Soleilhavoup, J.P. and Feki, A.E. (2001). Effect of Chronic Lead Exposure on Kidney Function in Male and Female Rats: Determination of a Lead Exposure Biomarker ; *Physiology and Biochem.* 5(109): 457-463, 467.
8. Ashour, A. (2002). Can garlic lobes, olive oil or black seed oil offer protection for some serum biochemical constituents against lead toxicity in rabbits? *Al-Aqsa Univ J* 6: 74-95.
9. Shalan, M.G., Mostafa, M.S., Hasouna, M.M., Nabi, S.E. and Refaie, A. (2005). Amelioration of lead toxicity on rat liver with vitamin C and silymarin supplements. *Toxicology.* 206:1-15.
10. Patil, A.J., Bhagwat, V.R., Patil, J.A., Dongre, N.N., Ambekar, J.G. and Das, K.K. (2007). Occupational lead exposure in battery manufacturing workers, silver jewelry workers, and spray painters in Western Maharashtra (India): effect on liver and kidney function. *J. Basic Clin. Physiol. Pharmacol.* 18(2): 87-100.
11. Adaramoye, O.A., Osaimoje, D.O., Akinsanya, M.A., Nneji, C.M., Fafunso, M.A. and Ademowo, O.G. (2008). Changes in antioxidant status and biochemical indices after acute administration of artemether, artemether-lumefantrine and halofantrine in rats. *Basic Clin. Pharmacol. Toxicol.*, 102: 412-418.
12. Six, K. M. and Goyer, R. A. (1970) Experimental enhancement of lead toxicity by low dietary calcium. *J. Lab. Clin. Med.* 76: 933-942.
13. Farias, P., Borja-Aburto, V.H., Rios, C., Hertz-Picciotto, I., Rojas- Lopez, M. and Chavez-Ayala, R. (1996). Blood lead levels in pregnant women of high and low socioeconomic status in Mexico City. *Environ Health Perspect* 104:1070-1074.
14. Mahaffey, K.R. (1995). Nutrition and lead: strategies for public health. *Environ Health Perspect* 103(6):191-196.
15. Hammad, T.A., Sexton, M. and Langerberg, P. (1996). Relationship between blood and lead and dietary iron intake in preschool children. A cross-sectional study. *Ann. Epidemiol.* 6: 30-33.
16. Prasanthi, R.P.J., Reddy, G.H., Devi, C.B. and Reddy, G.R. (2005). Zinc and calcium reduce lead induced perturbations in the aminergic system of developing rat brain. *Biometals* 18:615–626
17. Prasanthi, R.P.J., Devi, C.B., Basha, D.C., Reddy, N.S. and Reddy, G.R. (2010). Calcium and zinc supplementation protects lead (Pb)-induced perturbations in antioxidant enzymes and lipid peroxidation in developing mouse brain. *Int J Devl Neurosci* 28:161–167
18. Lauwerys, R., Roels, H., Buchet, J.P., Bernard, A.A., Verhaeven, L. and Konings, J. (1983). The influence of orally-administered vitamin C or zinc on the absorption of and the biological response to lead. *J Occup Health* 25:668-678.
19. Reddy, G.R. and Zawia, N.H. (2000). Lead exposure alters Egr-1 DNA binding in the neonatal rat brain. *Int. J. Dev. Neurosci.* 18: 791-795.
20. Biosystem, S.A. Costa Brava 30. Barcelona (Spain).
21. Fowler, B.A., Kimmel, C.A. and Woods, J.S. (1980). Chronic low-level lead toxicity in the rat: III. An integrated assessment of long-term toxicity with special reference to the kidney. *Toxicol. Appl. Pharmacol.* 56: 59-77.

22. Baccarelli, A. (1999). Occupational agents and endocrine function: an update of the experimental and human evidence. *Med Lav.* 90: 650-670.
23. Ashour, A., Yassin, M., Nahed, M., Abu Aasi, M. and Ali, M. (2007) Blood, Serum Glucose and Renal Parameters in Lead-Loaded Albino Rats and Treatment with Some Chelating Agents and Natural Oils *Turk J Biol* 31 25-34.
24. Missoun, F., Slimani, M. and Aoues, A. (2010). Toxic effect of lead on kidney function in rat Wistar *African Journal of Biochemistry Research* 4(2), 21-27.
25. Moneim, A.E., Dkhil, M.A. and Quraishy, S.A. (2011). The potential role of flaxseed oil on lead acetate induced kidney injury in adult male albino rats. *African Journal of Biotechnology.* 10(8), 1436-1451.
26. Kim, Y., Yoo, C.I. and Lee, C.R. (2002). Evaluation of activity of erythrocyte 5-nucleotidase (P5N) in lead exposure workers, with focus on the effect on hemoglobin. *Ind Health* 40: 23-27.
27. Khan, A.A., Safeena Inam., Muhammad Idrees., Azra Dad., Khitab Gul. and Haji Akbar. (2010). Effect of automobile workshop on the health status of automechanics in N. W. F. P., Pakistan *African Journal of Environmental Science and Technology* 4(4), 192-200.
28. Koreim, K. M. M. (2009). Lead toxicity and the protective role of *Cupressus sempervirens* seeds growing in Egypt. *Rev. Latinoamer. Quím.* 37/3: 230-242.
29. Formica, J.V. and Regelson, W. (1995). Review of the biology of quercetin and related bioflavonoids. *Federal Chemical Toxicology* 33: 1061-1080.
30. Upasani, C.D. and Balaraman, R. (2001). Effect of vitamin E, vitamin C and Spirullina on the levels of membrane bound enzymes and lipids in some organs of rats exposed to lead. *Indian Journal of Pharmacology* 33:185-191.
31. Moussa, S.A. and Bashandy, S.A. (2008). Biophysical and biochemical changes in the blood of rats exposed to lead toxicity. *Romanian J Biophys.* 18 (2): 123-133.
32. Hamadouche, N.A., Slimani, M., Merad-Boudia, B. and Zaoui, C. (2009). Reproductive toxicity of lead acetate in adult male rats. *Am. J. Sci. Res.*, 3: 38-50.
33. Ismail, I.A.A., Agha, S.Z.A. and Ossama Ahmed Shehwan, O.A. (2006). Hematological and Biochemical Studies for Gasoline Toxicity Among Gasoline Workers In Gaza Strip. *J Al-Aqsa Univ*, 10.
34. Jens, J.J. and Hanne, H. (2002). A Review on Liver Function Test. The Danish Hepatitis C. Retrieved from: http://home3.inet.tele.dk/omni/hemochromatosis_iron.htm.
35. Cornelius, C.E. (1979). Biochemical evaluation of hepatic function in dogs. *J. Am. Anim. Hosp. Assoc.*, 15: 25-29.
36. Flora, S., Pande, M., Kannan G.M. and Mehta, A. (2004). Lead induced oxidative stress and its recovery following co-administration of melatonin or n-acetylcysteine during chelation with succimer in male rats. *Cell Mol Biol* ; 50:543-551.
37. Odunola, O.A., Kazeem, A., Akinwumi; Babatunde Ogunbiyi and Oladimeji Tugbobo. (2007). Interaction and Enhancement of the Toxic Effects of Sodium Arsenite and Lead Acetate in Wistar Rats. *African Journal of Biomedical Research*, Vol. 10; 59 – 65.
38. Suradkhar, S.G., Ghodasara, D.J., Priti Vihol, Jatin Patel., Vikas Jaiswal and Prajapati, K.S. (2009). Haemato-Biochemical Alterations induced by lead acetate toxicity in Wistar Rats. *Veterinary World*, 2(11):429-431

39. Krishna, H. and Ramachandran, A.V. (2009). Biochemical alterations induced by the acute exposure to combination of chlorpyrifos and lead in Wistar rats. *Biology and Medicine*, 1 (2): 1-6.
40. Peraza, M.A., Fierro, F., Barber, D.S., Casarez, E. and Rael, L.T. (1998). Effects of micronutrients on metal toxicity. *Environ. Hlth. Perspect.* 106(1): 203-216.
41. Simons, T.J.B. (1993). Lead-calcium interactions in cellular lead toxicity. *Neurotoxicology* 14:77-86.
42. Mushak, P. (1991). Gastrointestinal absorption of lead in children and adults: Overview of biological and biophysicochemical aspects. *Chem. Speciat. Bioavaiaabl.* 3: 87-104.
43. Mahaffey, K. (1985). Factors modifying susceptibility to lead toxicity. In: Ed. Mahaffey, K., *Dietary and Environmental Lead: Human Health Effects*. Elsevier Science Publishers, Amsterdam. 373-419.
44. Goyer, R.A. (1995). Nutrition and metal toxicity. *Am. J. Clin. Nutr.* 61: 646S-650S.
45. Fullmer, C.S. (1992). Intestinal interactions of lead and calcium. *Neurotoxicology* 13:799-808.
46. CDC. (1997). Update: Blood lead levels. Centers for Disease Control and Prevention. *MMWR Morb Mortal Wkly Rep* 46(7):141-146.
47. Kaplan, M. L., Jones, A. G., Davis, M. A. and Kopito, L. (1975). Inhibitory effect of iron on the uptake of lead by erythrocytes. *Life Sci.* 16: 1545.
48. Flora, S.J.S., Jain, V.K., Behari, J.R. and Tandon, S.K. (1982). Protective role of trace metals in lead intoxication. *Toxicol. Lett.* 13: 52-56.
49. Kagi, J.H.R. and Vallee, B.L. (1961). Metallothionein, a cadmium and zinc containing protein from equine renal cortex. *J. Biol. Chem.* 236: 2435-2442.
50. Windham, B. (2004). Effects of toxic metals on learning ability and behavior. <http://www.home.earthlink.net/~berniew1/tmlbn.html>.
51. Cerklewski, F.L. and Forbes, R. M. (1976). Influence of dietary zinc on lead toxicity in the rat. *J. Nutr.* 106: 689-696.

**7th ANNUAL CONVENTION OF ASSOCIATION OF
BIOTECHNOLOGY AND PHARMACY &
INTERNATIONAL CONFERENCE ON PLANT BIOTECHNOLOGY,
MOLECULAR MEDICINE AND HUMAN HEALTH (ICPMH-2013)**

(October 18-20, 2013)

At

Department of Genetics

University of Delhi South campus, New Delhi – 110 021, India

Broad Areas of Focus

- Recent Advances in Plant Biotechnology
- Cellular, Tissue, and Metabolic Engineering
- Genomics, Proteomics and Bioinformatics
- Gene Expression, Regulation and Target Gene activation
- RNAi and Epigenetics in Plant and Human Health
- Plant and Animal based Vaccines and DNA Vaccines
- Molecular Medicine for Human Health
- Immunological responses and Inflammatory diseases
- Cellular inflammatory activation and Signalling pathways
- Novel Human Genes and Genetic Disorders
- Molecular Sensors and Markers
- Disease diagnosis and Molecular imaging
- Nanobiotechnology and Drug Development
- Medicinal Plants and Herbal Drugs
- Environment and Human health
- Other Related Areas

For further details contact

Dr. M. V. Rajam, FNASc, FNAAS, FABAP, FAPAS
Organizing Secretary, International Conference (ICPMH-2013)
Professor & Head, Department of Genetics
University of Delhi South Campus, New Delhi – 110 021
Email - rajam.mv@gmail.com
Tel: +91-11-24110866, TelFax - +91-11-24112437,
Mobile: 9818108515

NEWS ITEM

Science should bridge gap between haves and have-nots: PM Manmohan Singh



Prime Minister Manmohan Singh said at the inauguration of the centenary session of the Indian Science Congress in Kolkata that Science can help bridge the gap between haves and have-nots even as India seeks a sustained growth of national income. Singh called upon the scientific community to carve out a niche for India's leadership in some areas of science. He felt that it was time for research in public sector to be supplemented by private laboratories for faster growth. Unveiling the 'Science, Technology and Innovation Policy 2013', the PM pointed out that since 65% of India's population lives in rural areas, a 4% growth in agricultural productivity is imperative for food security. He said that we need breakthroughs in technology to tap more water and raise land productivity. He added that this transformation of agriculture must be the top priority of planning, science and technology policies. Referring to recent developments like genetically modified crops and nuclear energy, Singh said that these could not be addressed with fear as science must aim at an inclusive, modern

society and science scholarship must be informed of social realities. Singh emphasized that it is time for coordinated research between public and private laboratories to ensure faster growth.

President Pranab Mukherjee urges students to be more innovative

President of India, Pranab Mukherjee appealed the students to be more innovative and also asked educational institutes to promote new ideas and concepts to strengthen the education sector. Speaking at the inauguration of the D Y Patil Knowledge City, Mukherjee said that without innovation we become stagnant and development stopped. Therefore, we need to strive for innovation and bring new ideas in everyday life. Mukherjee said that Technology has become power and students should work on technological innovations to be successful and confident enough to claim that nobody can challenge their knowledge. Pointing out that the 12th Plan focused on providing quality education and further improving the health sector, the President said Quality education will provide more opportunities to students at international level. He also said that China and India were playing a major role in Asia and despite recession and sluggishness in the economy, the country had contributed substantially to the world output.

Govt. planning new authority to regulate higher education: Tharoor

The Minister for State for Human Resource Development, Dr. Shashi Tharoor admitting that there is a "clear gap in the overall regulation of higher education said that the government is planning to establish an over-arching authority to set and coordinate standards in higher education.

Delivering the keynote address at a seminar on “Higher Education: Affirmative Action and Skill Gaps”, the Minister said there is a need to establish a body with statutory authority to prescribe academic standards, norms of accreditation and mechanisms of financing and governance of institutions. He said that such a body will enhance the endeavour to promote credible standards of higher education and research in the country. He also emphasised on the need to turn the country’s huge demographic advantage into fruitful ways to take the country into the group of major developed economies.

Country’s education system burdened with demands of quantity, quality: Mukherjee

President Pranab Mukherjee said despite achievements, it is widely recognized that our country’s education system is burdened with demands of both quantity and quality. Speaking at the ninth convocation of Motilal Nehru National Institute of Technology (MNNIT), Mukherjee said that we need many more universities and technical institutions to be able to address the higher education needs of our increasing number of students. However, what we need most is to provide good quality education. He said that befitting our growing economic power status, we must raise the standards of our higher education to a level that we reach undisputedly among the top ten or at least top fifty in the world. In a globalised world, Indian institutions should aim not only at becoming top universities in India but also establish themselves as world class universities with international standards of research, teaching and learning. He said that progress of a country cannot be guaranteed unless all sections of society take part in nation building to their full potential. Mukherjee further said that the route to success may be a rocky

one, but the person who completes the route has actually finished a pilgrimage - his roots are firm, and his foundations are strong. Keep the flame of innovation alive; never be lulled into complacency and never be lured by short-cuts,” he added.

India needs new models of development: Sam Pitroda

National Innovation Council (NIC) chairman Sam Pitroda said that India needs to have new models of development, especially in the education sector. He commented that Today education is too exclusive and Western model of education is not workable in India as it is based on consumption. Pitroda said that we still use processes that were used 80 years ago as it is now obsolete and we find lots of resistance to change. Currently adviser to the Prime Minister of India, Manmohan Singh, on Public Information Infrastructure and Innovations, Pitroda said that innovation agenda for India is all about productivity, new wealth creations and opportunities. He added that the best way to kill innovation is to pack up various councils and committees with government officials.

SCIENTIFIC NEWS

Bacteria’s Self-Defense Mechanisms Revealed

Danish researchers have gleaned new insights into how bacteria control the amount of toxin in their cells. Many pathogenic bacteria are able to go into a dormant state by making persister cells that are not receptive to conventional antibiotics. This causes serious problems in the treatment of life-threatening disorders such as tuberculosis, where the presence of persister cells often leads to a resurgence of infection following medical treatment. At the molecular level, the

formation of persister cells is due to the presence of toxins that are produced by the bacteria themselves, and which enable them to enter the dormant state. During this hibernation period, the bacteria constantly regulate the amount of toxin at exactly the same level and thus maintain the dormant state. By isolating and crystallizing the toxin molecules and their molecular companions—the antitoxins—and by subsequently exposing the crystals to strong X-rays, the scientists gained unique insight into how bacteria control the amount of toxin in the cell. The new findings can eventually lead to the development of completely new forms of treatment of bacterial infections that work at first by blocking toxin function and production, and consequently by using conventional antibiotics to fight the pathogenic bacteria.

B. Jhansi Rani

Treating Obesity-Related Diseases with Parasitic Worms

New research has revealed that many parasitic worms, once inside a host, secrete a sugar-based anti-inflammatory molecule that might help treat metabolic disorders linked with obesity. Although the latest pharmaceutical agents have made parasitic worm infection less of a threat in some areas, these organisms are still a major cause of disease and infirmity throughout much of the developing world. However, parasites are not all bad, according to new research by a team of scientists at the University of Georgia (UGA; Atlanta, GA, USA), the Harvard School of Public Health (Boston, MA, USA), the Université François Rabelais (Tours, France), and the Central South University, Changsha (Hunan, China). The sugar molecule (glycan) is released by parasites to help them evade the body's immune system. By lessening inflammation, they

are better able to hide in tissues, and humans experience fewer symptoms that might reveal their presence. Dr. Harn and his colleagues have demonstrated that the sugar molecule released by parasites may relieve a range of other serious inflammatory medical disorders. The glycan appears to serve as a powerful antirejection drug that may one day be used in patients who have received organ transplants. Moreover, it has been shown to block or even reverse the symptoms of multiple sclerosis in mice. Additionally, it may be used as a treatment for psoriasis, a disease that causes skin redness and irritation. More research is needed before this sugar molecule can be tested in humans; however, the investigators are hopeful that they can create effective treatments that provide all the advantages of parasitic worms without the worms themselves.

A.Suresh Kumar

Infrared Light Causes Organic Nanoparticles to Heat Up and Cook Cancer Cells

Novel organic nanoparticles that generate heat when exposed to infrared light effectively killed colorectal cancer cells in a cell-culture model system. Investigators at Wake Forest Baptist Medical Center (Winston-Salem, NC, USA) developed conjugated polymer nanoparticles (PNs) consisting of 2-ethylhexyl cyclopentadithiophene copolymerized with 2,1,3-benzothiadiazole (for nano-PCPDTBT) or 2,1,3-benzoselenadiazole (for nano-PCPDTBSe). The PNs were stable in aqueous media and showed no significant toxicity up to one mg/mL. Upon exposure to infrared light at 808 nm, the PNs generated temperatures above 50 degrees Celsius. Experiments were carried out to test the effect of the PNs on cultures of RKO and HCT116 colorectal cancer cells. Results revealed that exposure to infrared light for five minutes killed

more than 80% of the cells at nano-PCPDTBSe concentrations above 100 micrograms/mL, while at concentrations above 62 micrograms/mL for nano-PCPDTBT, more than 90% of cells were killed. The results of this study demonstrate how new medical advancements are being developed from materials science research. There is a lot more research that needs to be done so that these new nanoparticles can be used safely in patients, but the field of electrically-conductive polymers is broad and offers many opportunities to develop safe, organic nanoparticles for generating heat locally in a tissue.

T.Rajani

Fructose Effects on Brain Influence Overeating

A new study suggests that consuming fructose appears to cause changes in regional cerebral blood flow (CBF) that can lead to overeating. Researchers at Yale University used arterial spin labeling magnetic resonance imaging (MRI) to quantify regional CBF in 20 healthy normal-weight adult volunteers, both before and after drinking a 75-gram beverage of pure glucose or fructose. The main outcome measures were relative changes in hypothalamic regional CBF after ingestion. Secondary outcomes included whole-brain analyses to explore regional CBF changes, functional connectivity analysis to investigate correlations between the hypothalamus and other brain region responses, and hormone responses to fructose and glucose ingestion. The results showed that glucose ingestion increased functional connectivity between the hypothalamus and the thalamus and striatum, while fructose increased connectivity between the hypothalamus and thalamus, but not the striatum. Regional CBF within the hypothalamus, thalamus, insula, anterior cingulate, and striatum—the appetite and reward

regions— was reduced after glucose ingestion; in contrast, fructose reduced regional CBF in the thalamus, hippocampus, posterior cingulate cortex, fusiform, and visual cortex. Fructose ingestion produces smaller increases in circulating satiety hormones compared with glucose ingestion, and central administration of fructose provokes feeding in rodents, whereas centrally administered glucose promotes satiety. Thus, fructose possibly increases food-seeking behavior and increases food intake.

P. Siva Krishna

EDUCATION

PhD/Post Doctoral Programs

Admission to Ph.D. in Department of Zoology, University of Calcutta, Kolkata: Applications are invited for admission to Ph.D programmes in University of Calcutta, B. C. Road, Kolkata – 700 019, India in the Department of Zoology. The selection is made on the basis of interview only. Candidates with valid NET/GATE/M.Phil. or Equivalent Qualifications are not required to appear at the admission test but would need to qualify the interview. Date of Admission test: February 18, 2013. Date of Interview: February 25, 2013. Number of Vacancies for Ph.D. programme are 30. Candidates are requested to download the Ph.D. admission test application form from the University website. The filled in form is submitted to the Head of the Department (Zoology), 35, B. C. Road, Kolkata – 700 019 C.U, India.

Admission to Ph.D. in Biotechnology, South Asian University, New Delhi: Applications are invited for admission to Ph.D (Biotechnology) in South Asian University, Akbar Bhavan, Chanakyapuri, New Delhi – 110 021, India. Number of Vacancies for Ph.D. programme are

10. Candidates with M.Sc. degree in any branch of Biological Sciences/M.Tech (Biological sciences)/M.B.B.S./M.V.Sc./M.Pharma with a minimum of 55% marks or equivalent grade are eligible. An Entrance Test will be conducted on March 24, 2013. Candidates can apply online by connecting through the website or can send the filled application form regular post or courier by downloading and completing the application form from the website. Filled in application should reach to Director Admissions, South Asian University, Akbar Bhavan, Chanakyapuri, New Delhi- 110 021, India. Phones: +91-11-24122512—14. Email: admissions@sau.ac.in. on or before February 28, 2013. Date of Entrance test: March 24, 2013.

OPPORTUNITIES

National Centre for Cell Science, Pune, India.

Applications are invited from eligible candidates for Three Positions of Senior Research Fellow (SRF) and Three Positions of Junior Research Fellow (JRF) in various projects. Candidates with M.Sc or equivalent degree in any branch of Life Sciences with minimum of 55% marks are eligible. Preference will be given to candidates who had qualified CSIR-NET/GATE/UGC-LS examination. Eligible candidates may attend the walk in interview on February 7, 2013 (For JRF Positions) and February 8, 2013 (For SRF Positions) at Board Room, NCCS Complex, National Centre for Cell Science, Pune University campus, Behind Pune Vidyapeeth High School, Ganeshkhind, Pune-411007, India.

Central Institute of Post-Harvest Engineering and Technology, Ludhiana, Punjab, India.

Applications are invited from eligible candidates for one Research Associate (RA) position to work

in a research project under the National Fund for Basic, Strategic and Frontier Application Research in Agriculture (NFBSFARA) entitled “Development of Spectroscopic Methods for Detection and Quantification of Adulterants and Contaminants in Fruit Juices and Milk” at Central Institute of Post-Harvest Engineering and Technology, Ludhiana, Punjab. Candidates with Ph.D in Microbiology/ Analytical Chemistry/ Biochemistry/Food Science and Technology and relevant subjects or Candidates with M.Tech/ M.Sc. in any subject mentioned above with 60% marks and having two years experience in research /teaching/food industries are eligible. The application with detailed biodata should reach to Dr. S.N.Jha (Email ID: snjha_ciphet@yahoo.co.in), Principal Investigator, or Dr.Pranita Jaiswal (Email Id: pranitajaiswal@gmail.com), Co-PI, NF project, Central Institute of Post-Harvest Engineering and Technology, PO: PAU campus, Ludhiana -141004, Punjab, India through registered post or email and attend the walk in interview on 5th February 2013.

National Institute of Plant Genome Research, New Delhi, India.

Applications are invited from eligible candidates for the one Position of Research Associate (RA) and three Positions of Junior Research Fellow (JRF) in DBT-sub project-1 entitled “Chickpea genome sequence analysis and its alignment to genetic map of Next Generation Challenge Programme on Chickpea Genomics” under the supervision of Dr. Mukesh Jain, Scientist, NIPGR. For the post of RA candidates with PhD in Life Sciences, Biotechnology, Bioinformatics, Molecular Biology or any other related field are eligible. Candidates having experience in the area of advanced molecular biology, genomics, transcriptomics, microarray data analysis will be given preference.

For the post of JRF candidates with M.Sc degree in Life Sciences, Biotechnology, Bioinformatics, Molecular Biology or any other related field are eligible. Candidates having experience in the area of advanced molecular biology, next generation sequencing, data analysis and molecular markers analysis will be given preference. Only hard copy of the application in the given format should reach to Dr. Mukesh Jain, Staff Scientist - III, National Institute of Plant Genome Research, Aruna Asaf Ali Marg, P.O. Box No. 10531, New Delhi - 110067, India on or before February 2, 2013.

Gujarat Ecological Education & Research (GEER) Foundation, Gandhinagar, Gujarat, India. Applications are invited from eligible candidates for the Two Positions of Research Associate (RA) and Five Positions of Junior Research Fellow (JRF) to work in World Bank funded India Integrated Coastal Zone Management (ICZM) Project at Gujarat Ecological Education & Research (GEER) Foundation, Gandhinagar, Gujarat. For the post of RA candidates with PhD in Life Sciences or related field and having Minimum one Year of experience as SRF are eligible. For the post of JRF candidates with M.Sc degree in Life Sciences or any other related field are eligible. Interested and eligible candidates may send their application in a prescribed form (available on official website: www.geerfoundation.gujarat.gov.in) with latest Curriculum-Vitae, covering letter, photocopies of mark sheets, credentials & age proof to The Director, GEER Foundation, Indroda Nature Park, P.O.Sector-7, Gandhinagar, 382 007, Gujarat, India.

SEMINARS/WORKSHOPS/ CONFERENCES

International conference on Biotechnology in Human Welfare, Warangal, India: An International Conference on Biotechnology in Human Welfare was going to held on February 7th - 9th, 2013 at Kakatiya University, Warangal organized by Department of Biotechnology, Kakatiya University, Vidyanarayapuri, Warangal – 506009, Andhra Pradesh, India. Abstract can be submitted online through E-mail: icbtkuwgl@yahoo.com. For further details contact: Prof.Dr.A.Sadanandam, Head & Organizing Secretary, Department of Biotechnology, Kakatiya University, Vidyanarayapuri, Warangal – 506009, Andhra Pradesh, India. Off: +91(0)870-2439600. Fax: +91(0)870-2438800. Resi: +91(0)870-2571049. Mobi: +91(0)9849146811. Email: nandamas@rediffmail.com, nandamas@gmail.com, icbtkuwgl@yahoo.com.

National Seminar on Computer Aided Drug Design, Tirupati, India: A 4th National Seminar on Computer Aided Drug Design was going to held on February 15th - 16th, 2013 at Sri Padmavati Auditorium & Bioinformatics center, Sri Venkateswara Institute of Medical Sciences University organized by SVIMS Bioinformatics Centre, Department of Bioinformatics, Sri Venkateswara Institute of Medical Sciences University, Tirupati, Andhra Pradesh, India. Abstract can be submitted through E-mail: svims.btisnet@nic.in on or before February 5th, 2013. For further details contact: Dr. A. UmaMaheswari, Co-ordinator of BIF, Bioinformatics Centre, SVIMS University, Tirupati, Tamil Nadu, India. E-mail: svims.btisnet@nic.in. Phone No: +918772287727. Website: <http://svimsbic.org>.

National Conference on Recent Advances in Molecular and Immuno Diagnostics, Hyderabad, India: A National Conference on Recent Advances in Molecular and Immuno Diagnostics was going to held on February 22nd - 23rd, 2013 at Gandhi Medical College Alumni Auditorium, Musheerabad, Hyderabad organized by Aurora's Degree and PG College, Chikkadpally, Hyderabad-500020, India and Bioworld Research Technologies. Abstract can be submitted through E-mail: cmid2013@adc.edu.in or srksuripeddi@gmail.com on or January 1st, 2013. For further details contact: Dr. A. Ravi Kiran, Convener, Head, Department of Biochemistry, Aurora's Degree and PG College, Chikkadpally, Hyderabad-500020, India. Tel: 04027662668. Website: www.adc.edu.in.

National Seminar on Nanobiomaterials (NSN-2013), Coimbatore, India: A National Seminar on Nanobiomaterials (NSN-2013) was going to held on February 14th - 15th, 2013 at Anna University Regional Centre, Coimbatore organized by Biotechnology Centre, Department of Biotechnology and Nanotechnology, Anna University Regional Centre, Coimbatore - 641047, India. For further details contact: Dr. Renuka Devi, Organizing Secretary, Biotechnology Centre, Department of Biotechnology and Nanotechnology, Anna University Regional Centre, Coimbatore - 641047, India. Email: autcbebiotech@gmail.com.



ALLIANCE INSTITUTE OF ADVANCED PHARMACEUTICAL AND HEALTH SCIENCES

#604A, Aditya Trade Centre, Ameerpet,
Hyderabad – 500 038, India
Phone: 040-66663326 / 23730072, Website:
www.allianceinstitute.org

About Alliance

Alliance, located conveniently in the heart of Hyderabad, trains industry-ready graduates by bridging education with industry needs in pharmaceutical sciences. Alliance's visionary management built state of the art facilities and laboratories to provide quality education meeting national and international standards.

Collaboration with JNTUH, India

Alliance is having collaboration with **Jawaharlal Nehru Technological University, Hyderabad (JNTUH)**, which is a premier institution with academic and research-oriented programs, offered through the constituent and affiliated colleges. Alliance's syllabi, academic regulations and course structure are **approved by the JNTUH. JNTUH awards the degrees after fulfilling the degree requirements.**

Collaboration with University of the Pacific, USA

University of the Pacific, ranks in the top 100 among the 3000 national universities in the United States. Alliance has entered into research collaboration with Thomas J Long School of Pharmacy and Health Sciences, University of the Pacific.

Alliance students have an option to do research work at the University of the Pacific to fulfill requirements for MS degree in India. Pacific faculty teaches Alliance students via live online classes. Pacific is also interested to offer admissions to Alliance students based on their performance at Alliance.

Programs offered

- * MS in Industrial Pharmaceutics
- * MS in Pharmaceutical Analysis & Quality Control
- * MS in Drug Development & Regulatory Affairs

For admissions, application forms and additional information visit online at
www.jntuh.ac.in/alliance or www.allianceinstitute.org.

Registered with Registrar of News Papers for India
Regn. No. APENG/2008/28877

Association of Biotechnology and Pharmacy

(Regn. No. 28OF 2007)

Executive Council

Hon. President

Prof. B. Suresh

President, Pharmacy Council of India
New Delhi

President Elect

Prof. K. Chinnaswamy

Chairman, IPA Education Division and
EC Member Pharmacy Council of India
New Delhi

Vice-Presidents

Prof. M. Vijayalakshmi

Guntur

Prof. T. K. Ravi

Coimbatore

General Secretary

Prof. K. R. S. Sambasiva Rao

Guntur

Regional Secretary, Southern Region

Prof. T. V. Narayana

Bangalore

Treasurer

Dr. P. Sudhakar

Guntur

Advisory Board

Prof. C. K. Kokate, Belgaum

Prof. B. K. Gupta, Kolkata

Prof. Y. Madhusudhana Rao, Warangal

Prof. M. D. Karwekar, Bangalore

Prof. K. P. R. Chowdary, Vizag

Dr. V. S.V. Rao Vadlamudi, Hyderabad

Executive Members

Prof. V. Ravichandran, Chennai

Prof. Gabhe, Mumbai

Prof. Unnikrishna Phanicker, Trivandrum

Prof. R. Nagaraju, Tirupathi

Prof. S. Jaipal Reddy, Hyderabad

Prof. C. S. V. Ramachandra Rao, Vijayawada

Dr. C. Gopala Krishna, Guntur

Dr. K. Ammani, Guntur

J. Ramesh Babu, Guntur

Prof. G. Vidyasagar, Kutch

Prof. T. Somasekhar, Bangalore

Prof. S. Vidyadhara, Guntur

Prof. K. S. R. G. Prasad, Tirupathi

Prof. G. Devala Rao, Vijayawada

Prof. B. Jayakar, Salem

Prof. S. C. Marihal, Goa

M. B. R. Prasad, Vijayawada

Dr. M. Subba Rao, Nuzividu

Prof. Y. Rajendra Prasad, Vizag

Prof. P. M. Gaikwad, Ahamednagar

Printed, Published and owned by Association of Bio-Technology and Pharmacy # 6-69-64 : 6/19, Brodipet, Guntur - 522 002, Andhra Pradesh, India. Printed at : Don Bosco Tech. School Press, Ring Road, Guntur - 522 007. A.P., India Published at : Association of Bio-Technology and Pharmacy # 6-69-64 : 6/19, Brodipet, Guntur - 522 002, Andhra Pradesh, India. Editors : Prof. K.R.S. Sambasiva Rao, Prof. Karnam S. Murthy